



PARIS 2017



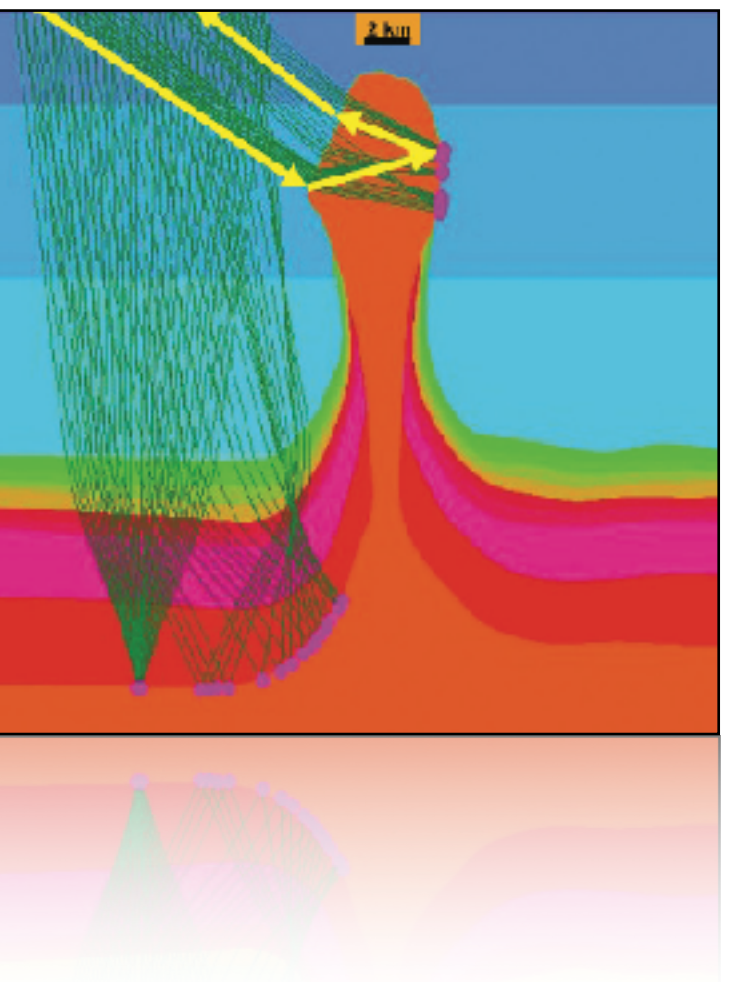
Variance-based salt body reconstruction

O. Ovcharenko, V. Kazei, D. Peter, T. Alkhalifah

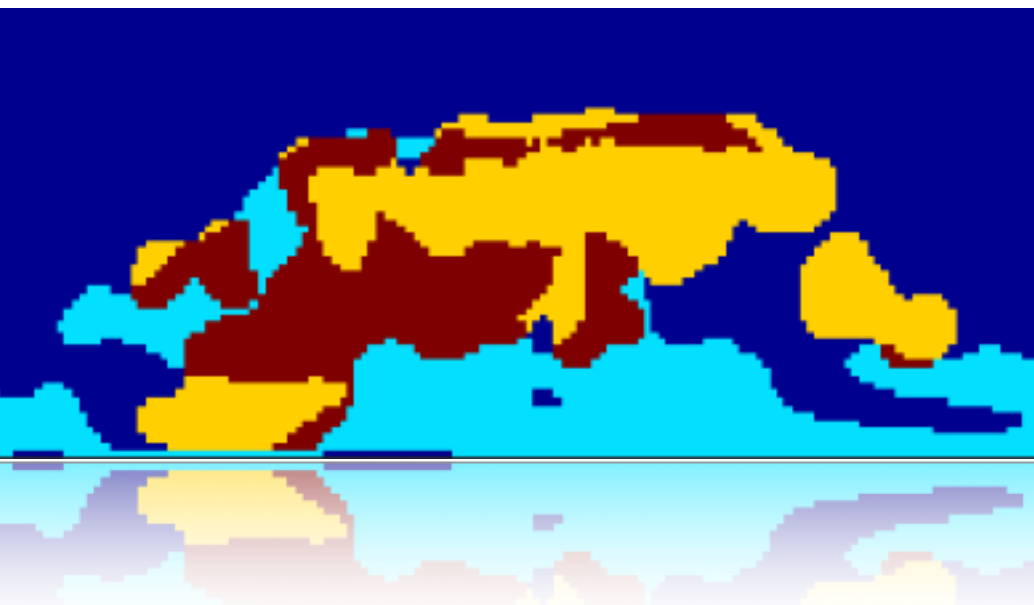
June 14, 2017

Outline

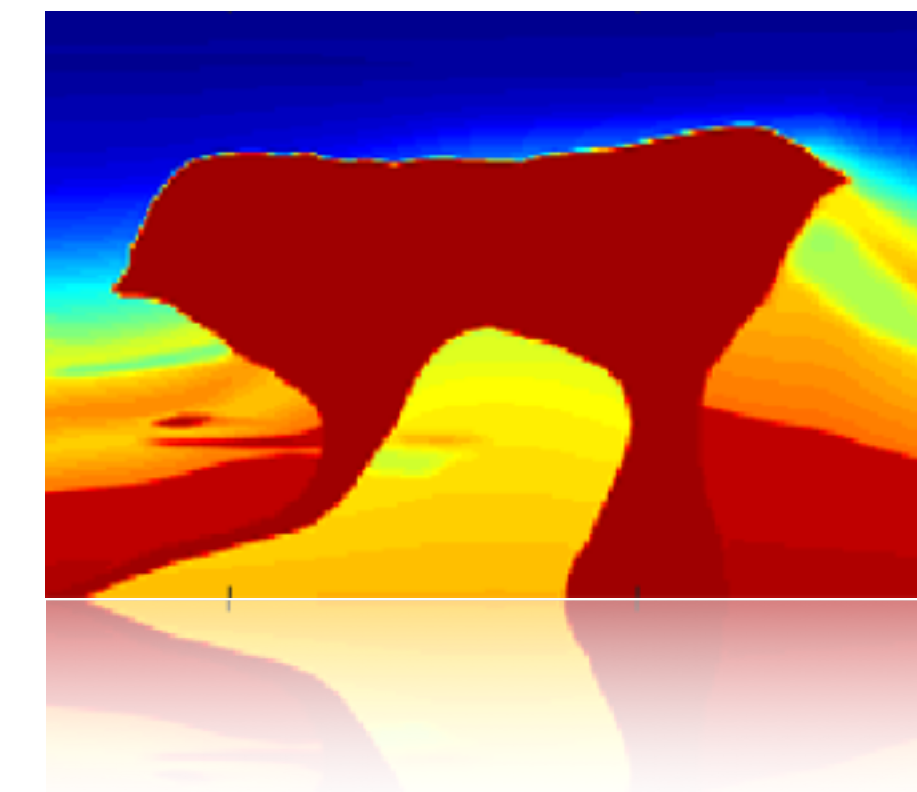
Motivation



Salt flooding technique

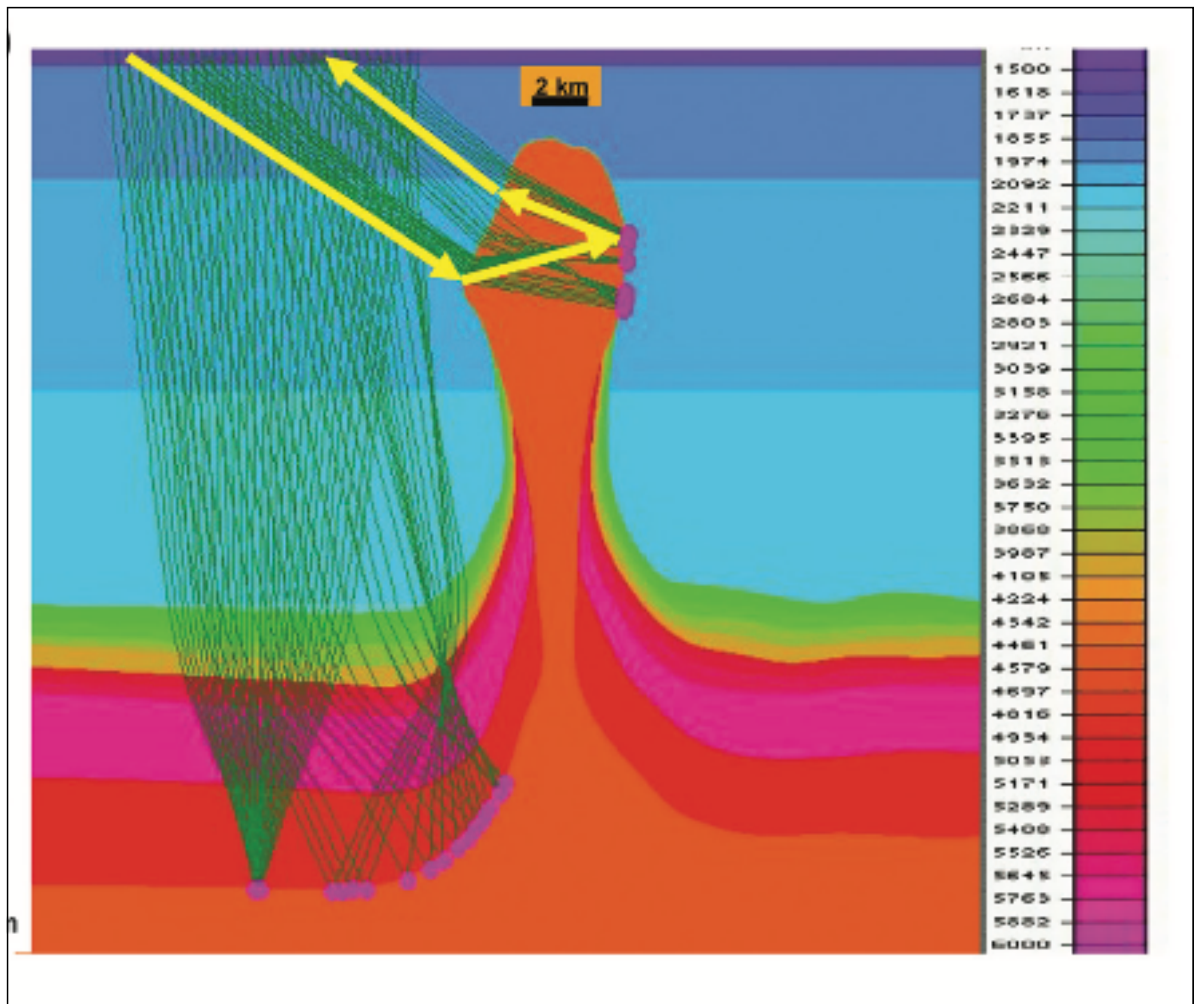


BP2004 model results



Motivation

- Hydrocarbons below salt bodies
- Seismic imaging challenged by high-velocity contrasts
- Complex geometries, steep flanks
- Multipulses
- Illumination issues



(Jones et al., 2014)

Motivation

“Top-to-bottom” manual approach

- Robust
- Interpreter-biased
- Time consuming

Introduction

Seismic interpretation and modeling is an integration of geological, geophysical and engineering data. In depth imaging, expertise from both geophysical processing and geological interpretation are becoming key factors in bringing out high quality imaging products. However, in depth imaging processing practice we could sometimes detect the knowledge gaps between seismic processing, geological and interpretation skills for the salt velocity modeling. Two problems - exclusive geophysical interpretation and insufficient geological interpretation - are the direct results of the gap.

The first problem, exclusive geophysical interpretation which means geophysical reflection is the only concern for interpretation, is usually caused by lack of geologic data or without knowledge of regional geology and salt tectonics. Because salt is one of the most impressive geological features shown in the seismic data in the Gulf of Mexico, it is easy to believe that salt should always be homogeneous and salt boundaries should always have strong reflections in seismic sections. This philosophy for interpreting salt worked well when exploration was focused on shallow and less complex areas. However, since exploration moved to deep and complex area this method has become outdated. In these more complex areas, salts can be deformed by many geological events and consequently are not homogeneous. Additionally acoustic impedances of salt and sediments can be very close and consequently reflections from salt boundaries can be very weak.

The second problem, insufficient geological interpretation which means geological data are the only concern for

Salt model building process

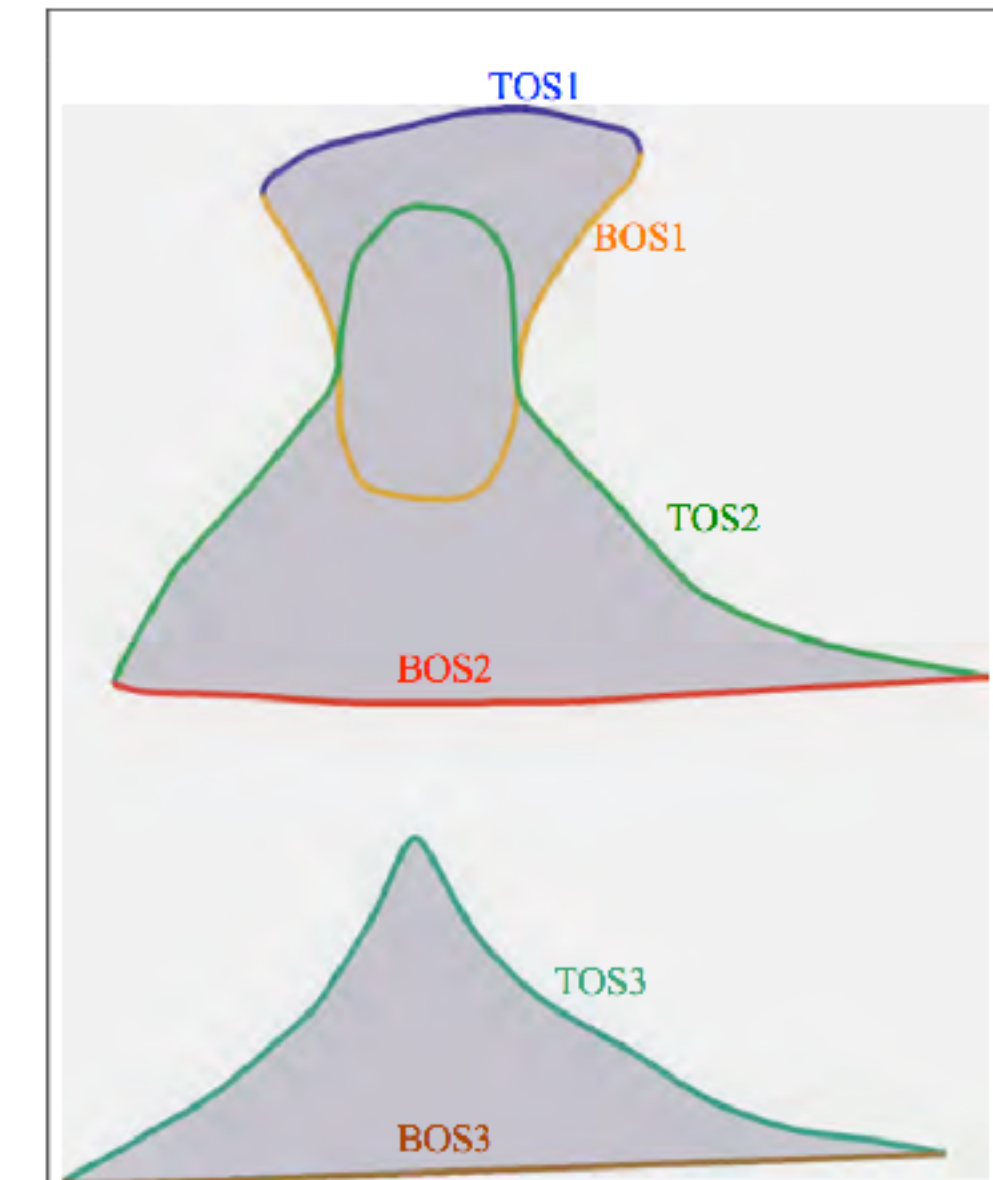


Figure 1: Schematic salt model building process.

(Zhang et al., 2009)

Motivation

Constrained optimization

- Automatic
- A priori model assumptions
- Computationally expensive

2 through 6. These figures visually demonstrate that this strategy leads to a controlled building of the velocity model as the hinge-loss constraints are gradually relaxed.

Results

The first model we present is the central part of the BP 2004 velocity model (Billette and Brandsberg-Dahl, 2005). FWI without TV or asymmetric TV constraints clearly fails to converge to a global minimum — compare Figures 2b and 2c — because the starting model shown in Figure 2a does not contain accurate low wavenumbers, which causes convergence to a local minimum. When TV and asymmetric TV constraints constrain the inversion, the inversion scheme converges to the much-improved solution shown in Figure 2d.

The salt body in Figure 3 is remarkably well recovered with the proposed method, which we expect to produce good results provided that: (1) the combination of (relaxed) constraints eliminate the adverse effects of local minima incurred during the previous FWI cycle; (2) sharp reflectors are introduced that are of the correct sign; (3) progress is made during the previous FWI cycle; and (4) the “fine scales” of the previous FWI cycle contribute to the “coarse scales” of the next cycle.

We also applied this approach to a portion of the SEAM model (Fehler and

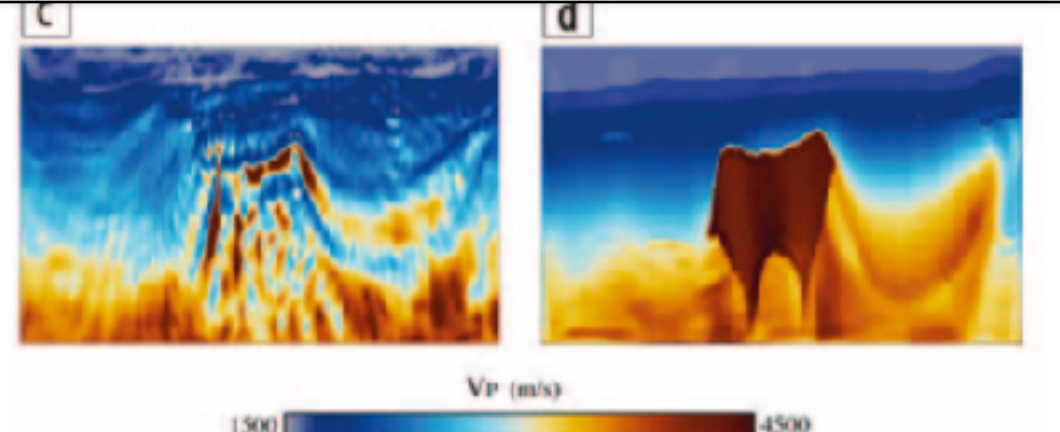


Figure 2. (a) Starting model; (b) true model; (c) FWI final model; (d) FWI + TV and asymmetric TV constraints final model.

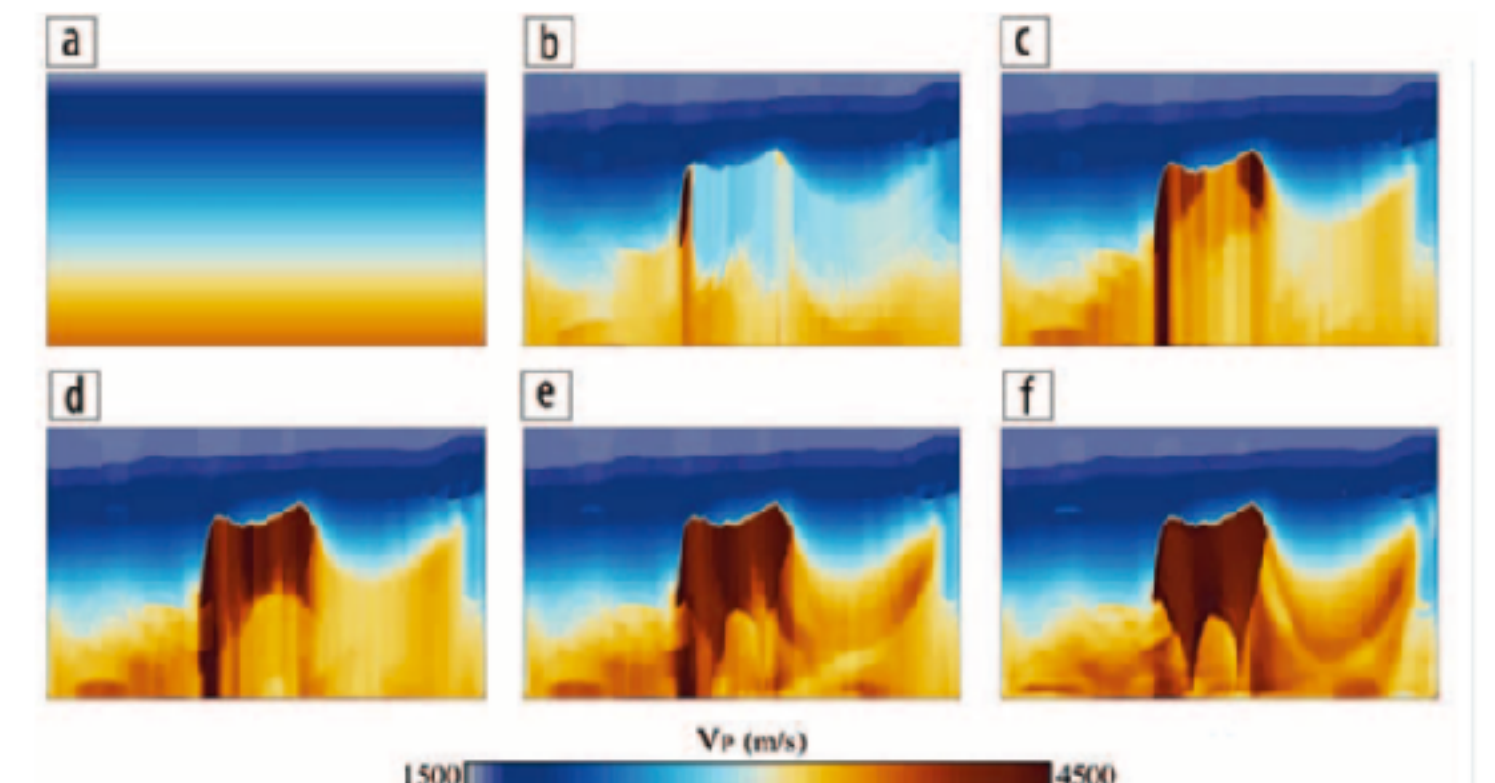


Figure 3. Snapshots for (a) the starting, and (b–f) the recovered velocity models, with one-sided TV continuation where the value of ξ/ξ_{true} is equal to (b) 0.01, (c) 0.1, (d) 0.2, (e) 0.5, and (f) 0.9.

(Esser et al., 2016)

Motivation

Gradient conditioning

- Less iterations
- Limited domain of convergence

THE SCATTERING ANGLE WAVENUMBER CONTINUATION

The scattering angle filter, as described above, offers an opportunity to control the wavenumbers we inject into the model from the gradients. It is not a direct control, such as a simple filter, it is, however, tied to the background velocity providing more

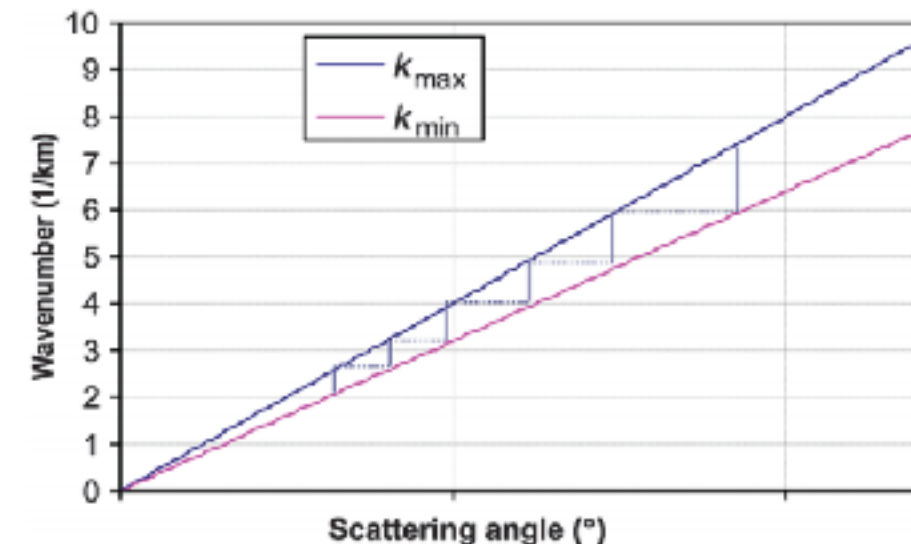


Figure 6. A schematic plot depicting the progress in scattering angle from high to low to allow for a proper wavenumber continuation.

velocity inversion tend to favor a top-to-bottom approach, having higher resolution in the shallow part provided by scattering angle

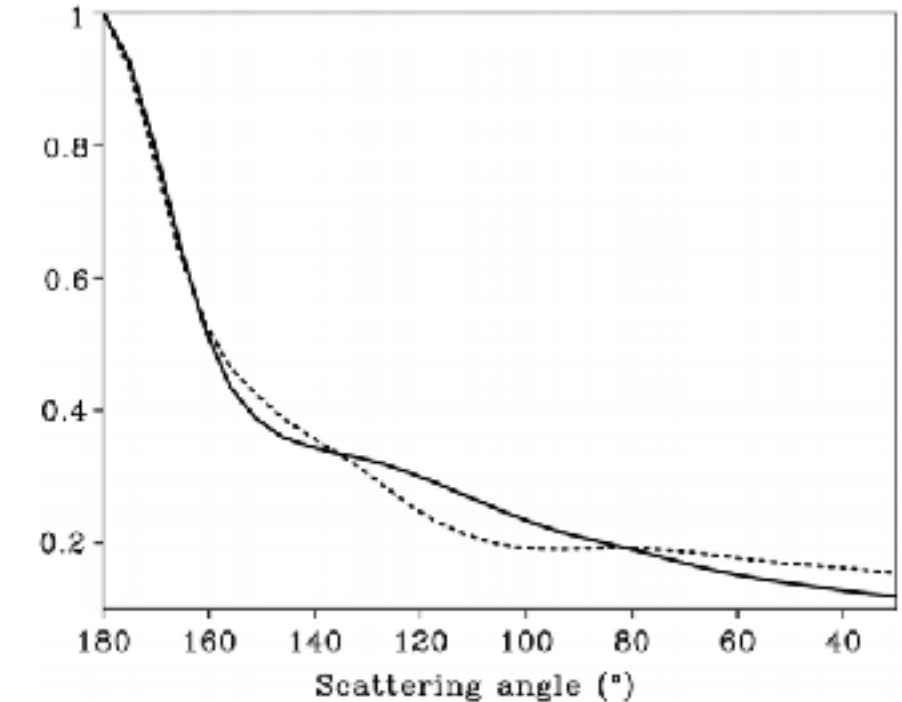


Figure 7. The objective function as a function of scattering angle for a continuation in terms of scattering angle from diving waves (180°) to reflections (solid curve) compared with a continuation in terms of wavenumber filtering from low to high mapped to scattering angle for comparison (dashed curve).

(Alkhalifah, 2016)

Motivation

Many challenges in salt body imaging using FWI

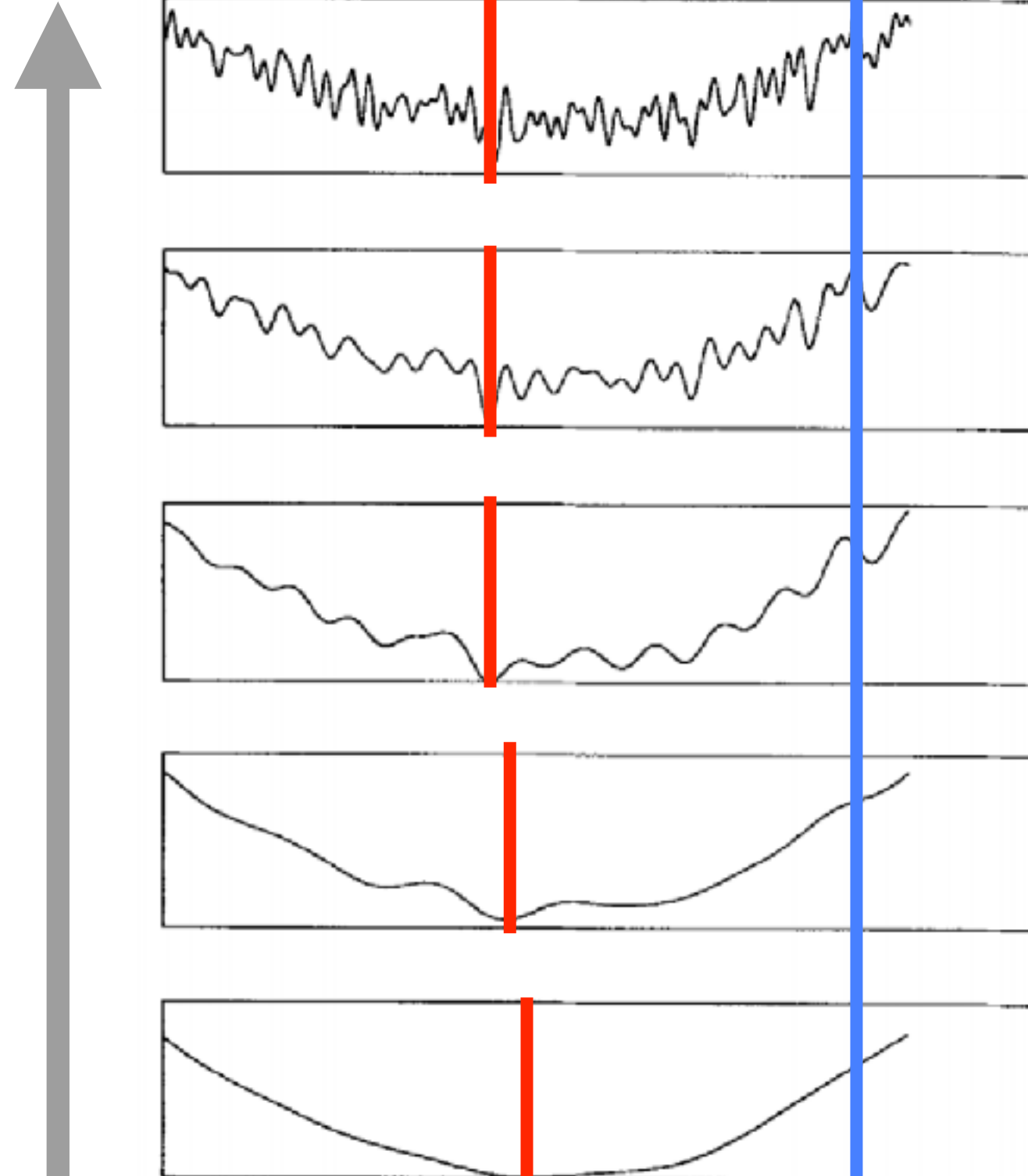
We don't have:

- Accurate starting model
- Low-frequency data
- Long-offset data
- ...

How to overcome these difficulties?

Multiscale

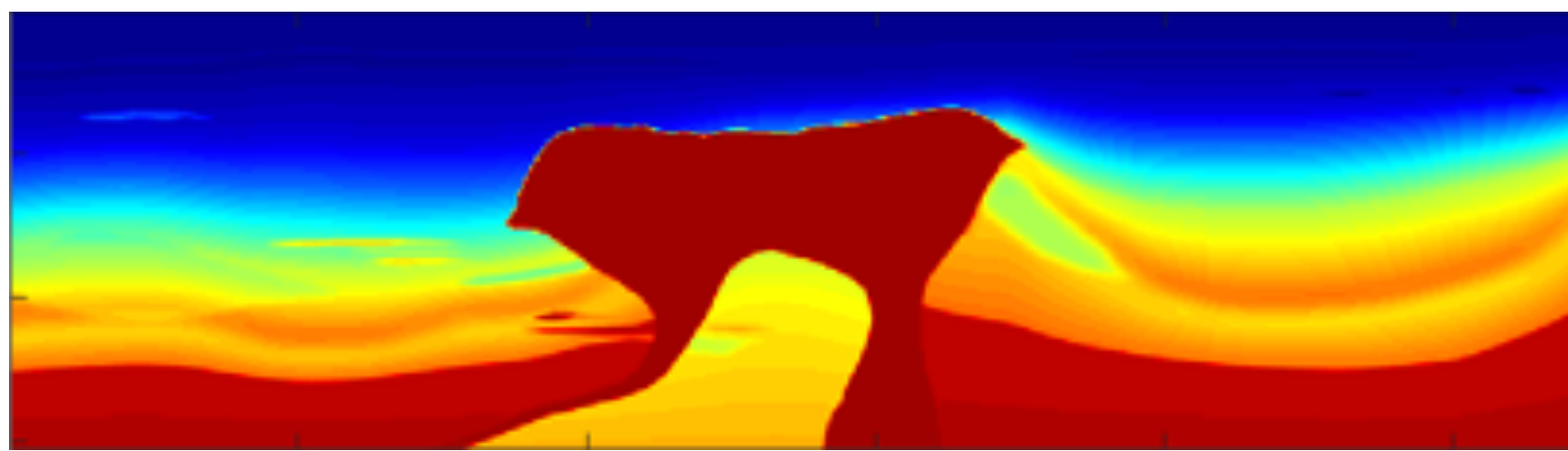
Global-minimum



(Bunks, 1995)

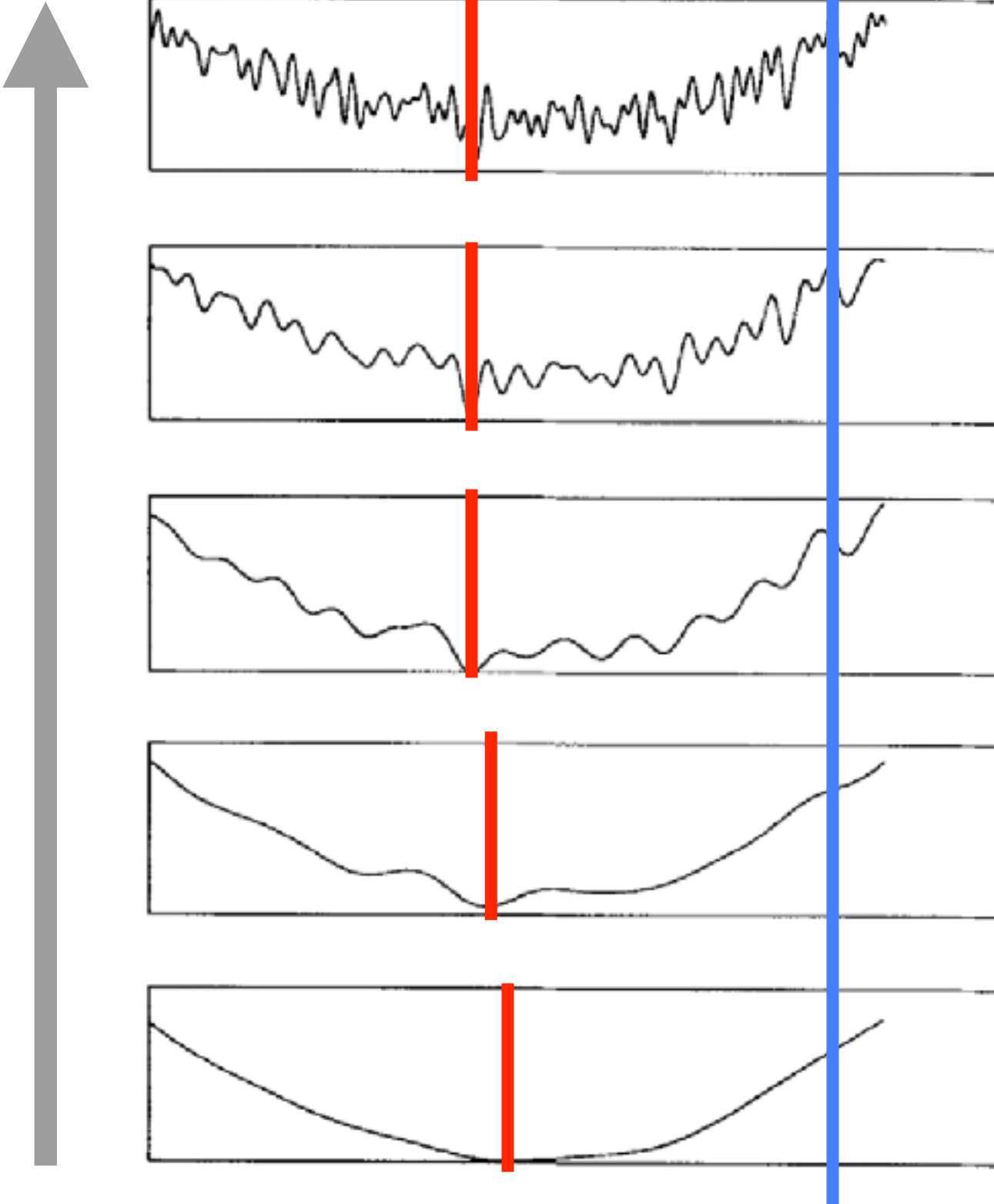
High

Low

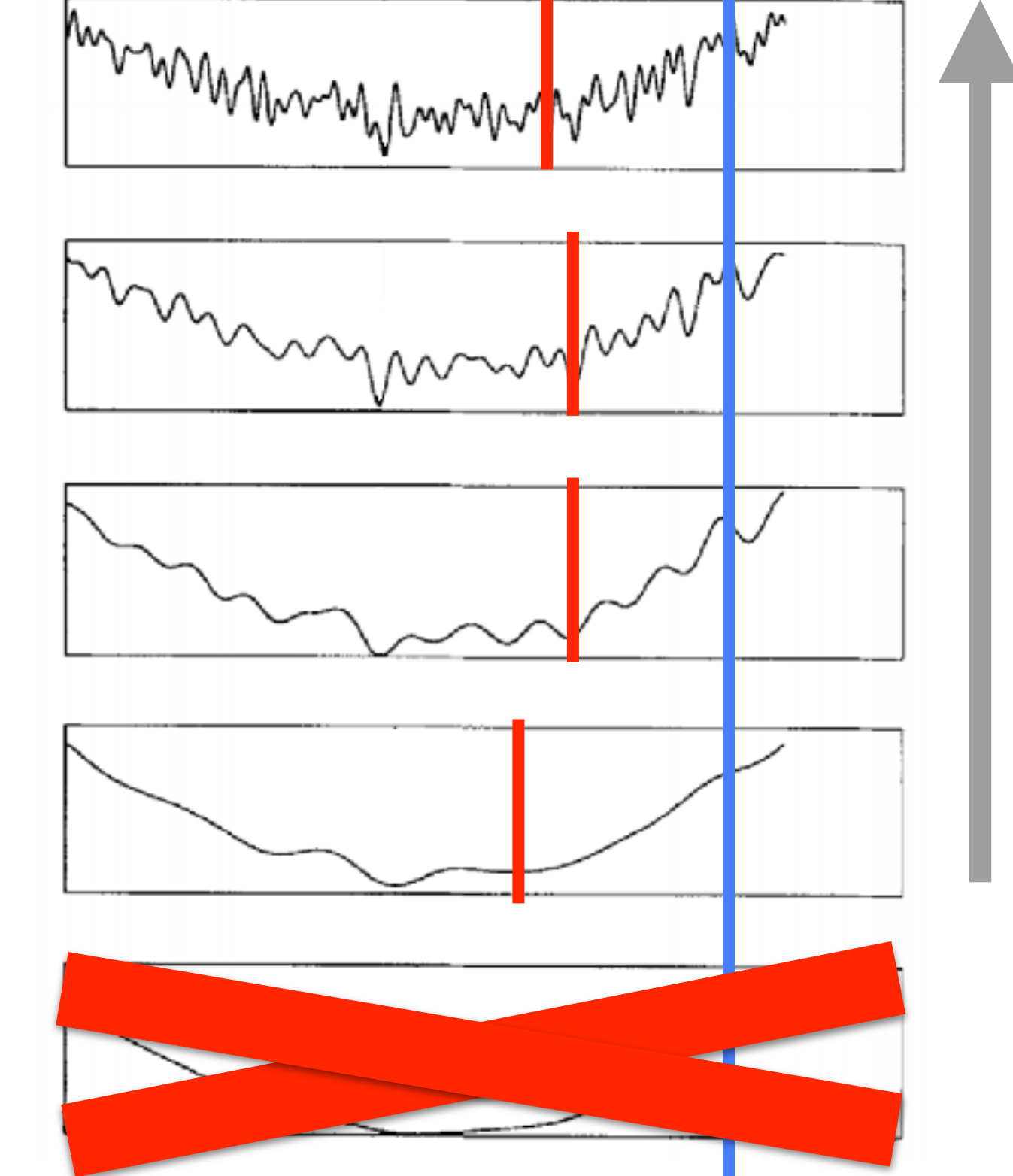


Multiscale

Global-minimum

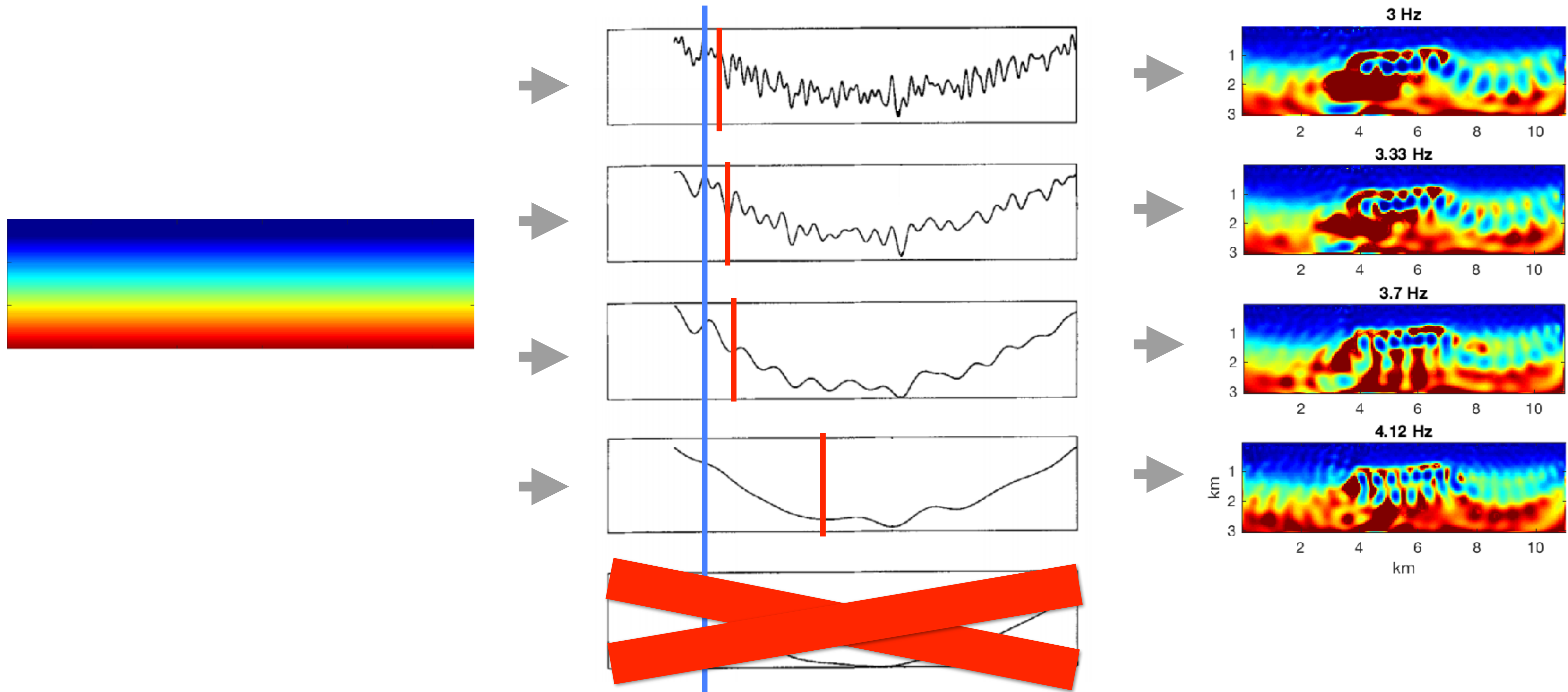


Local-minimum



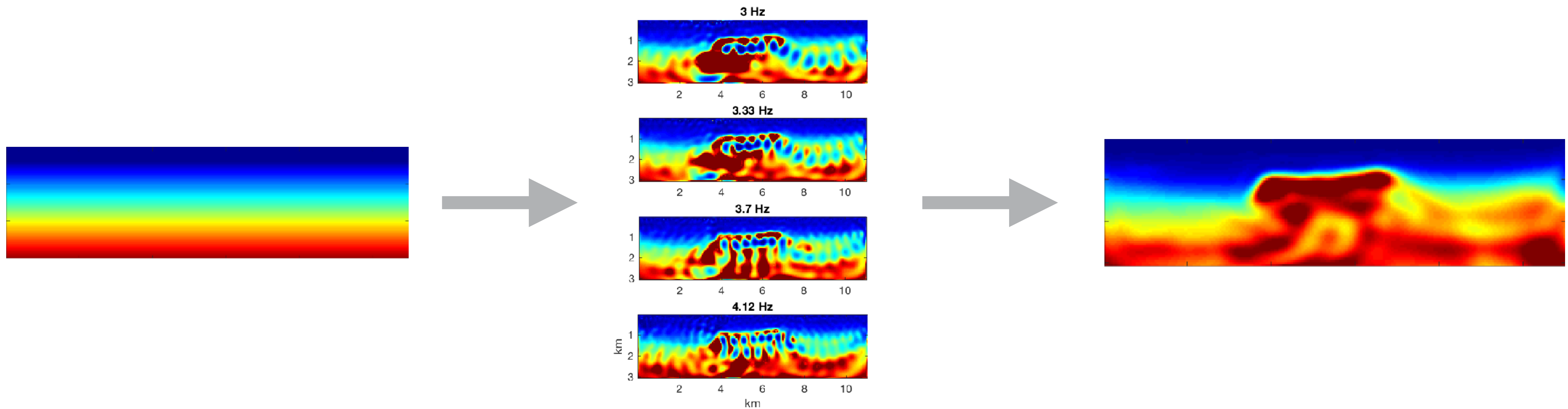
Multiscale strategy needs low-frequency data to find global minimum

Local minima at different frequencies



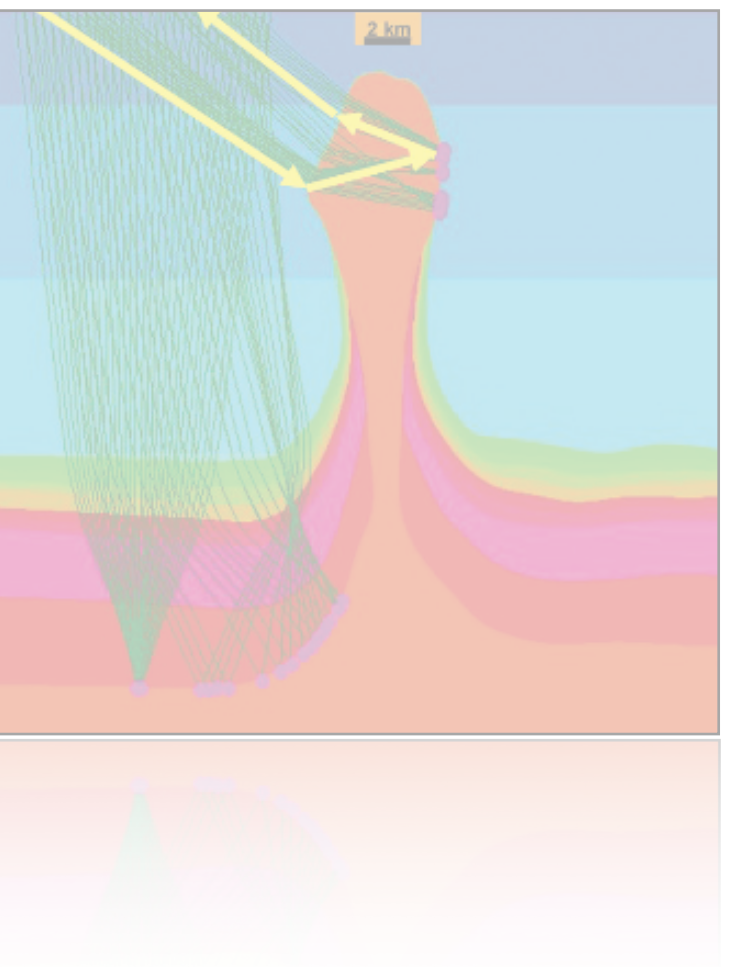
The proposed idea

Use variance between inversion results at different frequencies to build a better initial model for FWI

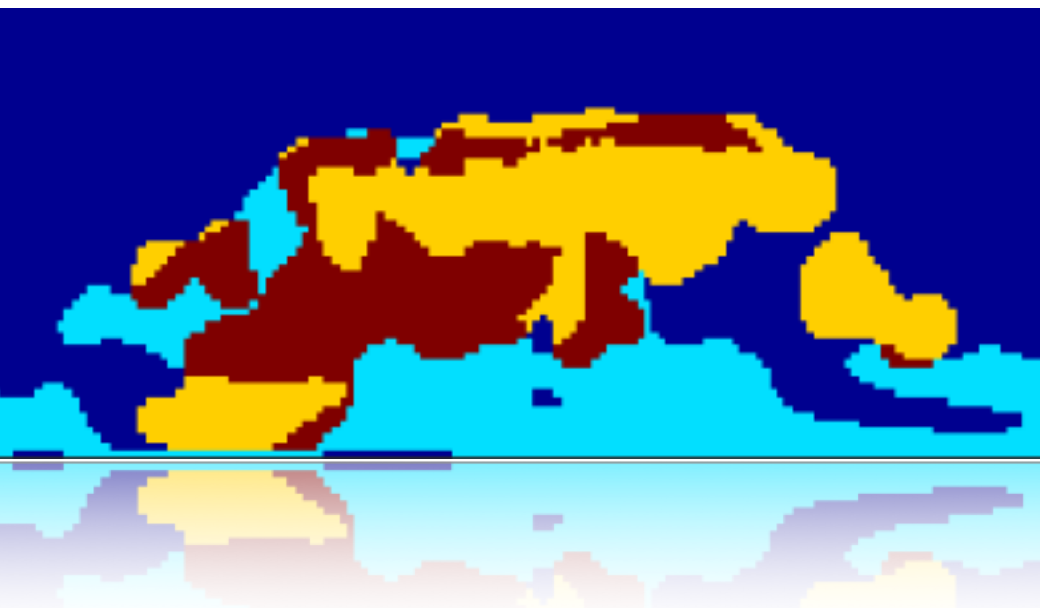


Outline

Motivation



Salt flooding technique



BP2004 model results

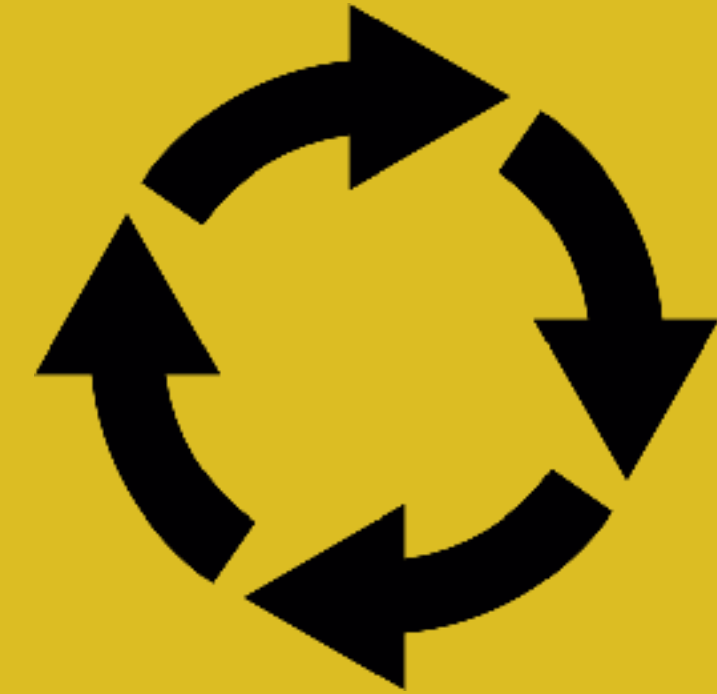


Variance-based salt flooding - Workflow

0. Updates from different frequencies

1. Average updates
2. Variance map and mask
3. Variance-based flooding

4. *FWI starting from “flooded” model

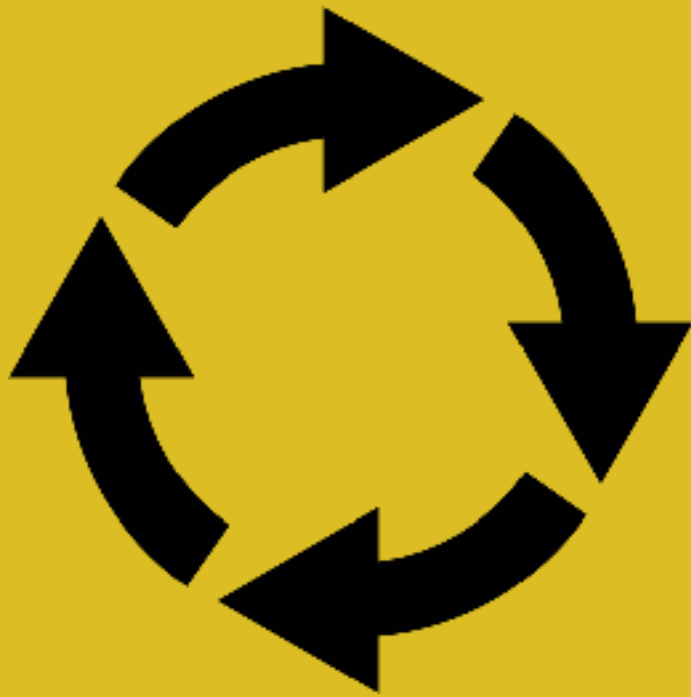


Variance-based salt flooding - Workflow

0. Updates from different frequencies

1. Average updates
2. Variance map and mask
3. Variance-based flooding

4. *FWI starting from “flooded” model

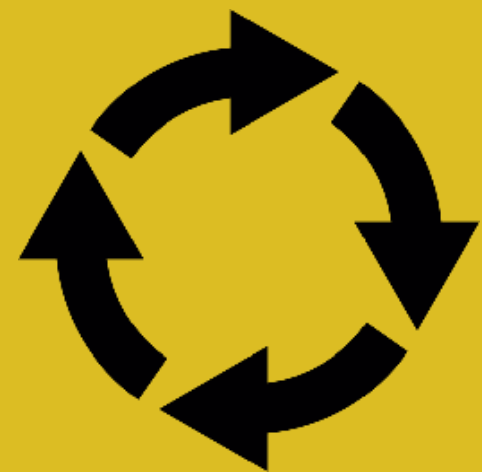


0. Modeling

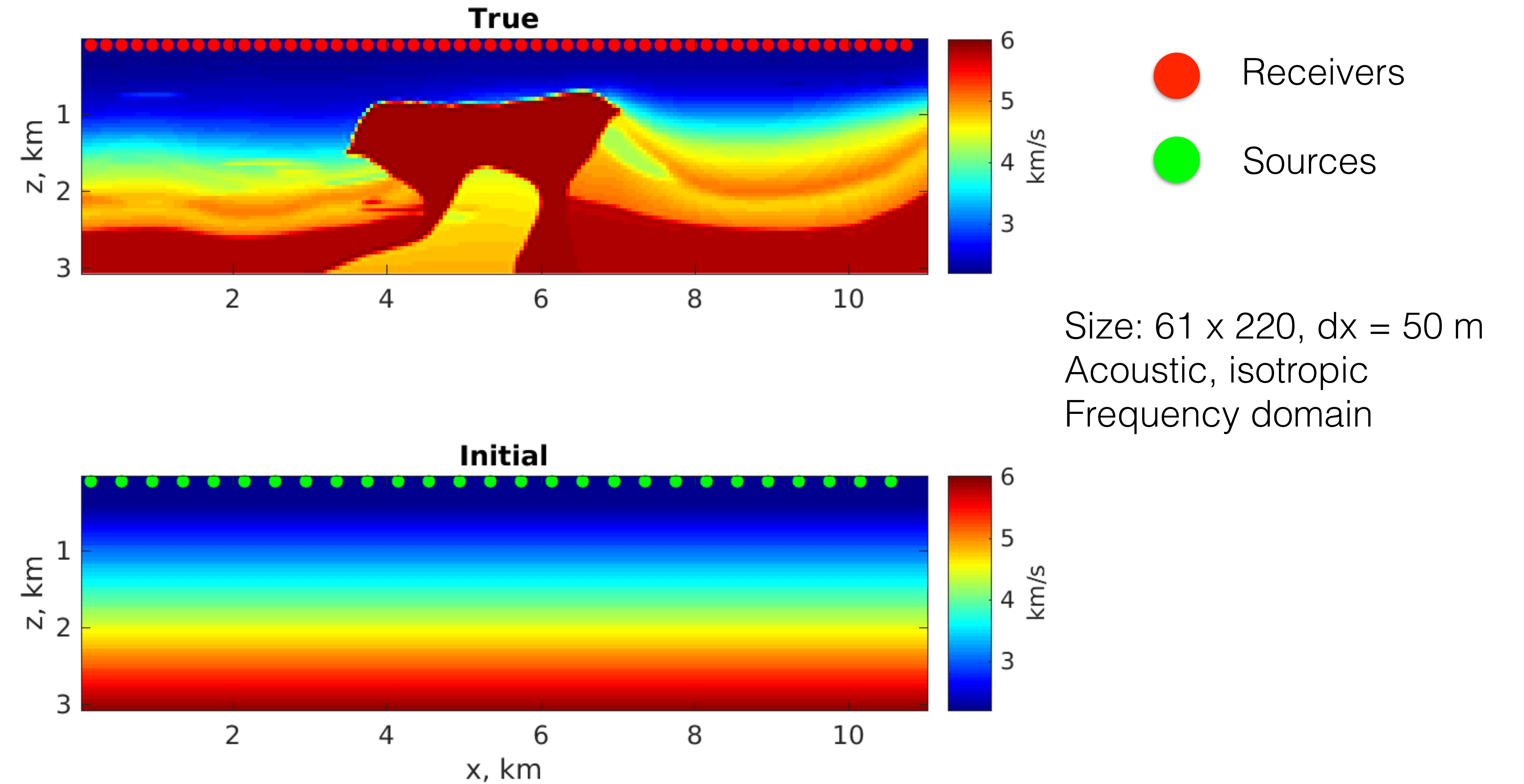
1. Averaging

2. Variance

3. Flooding



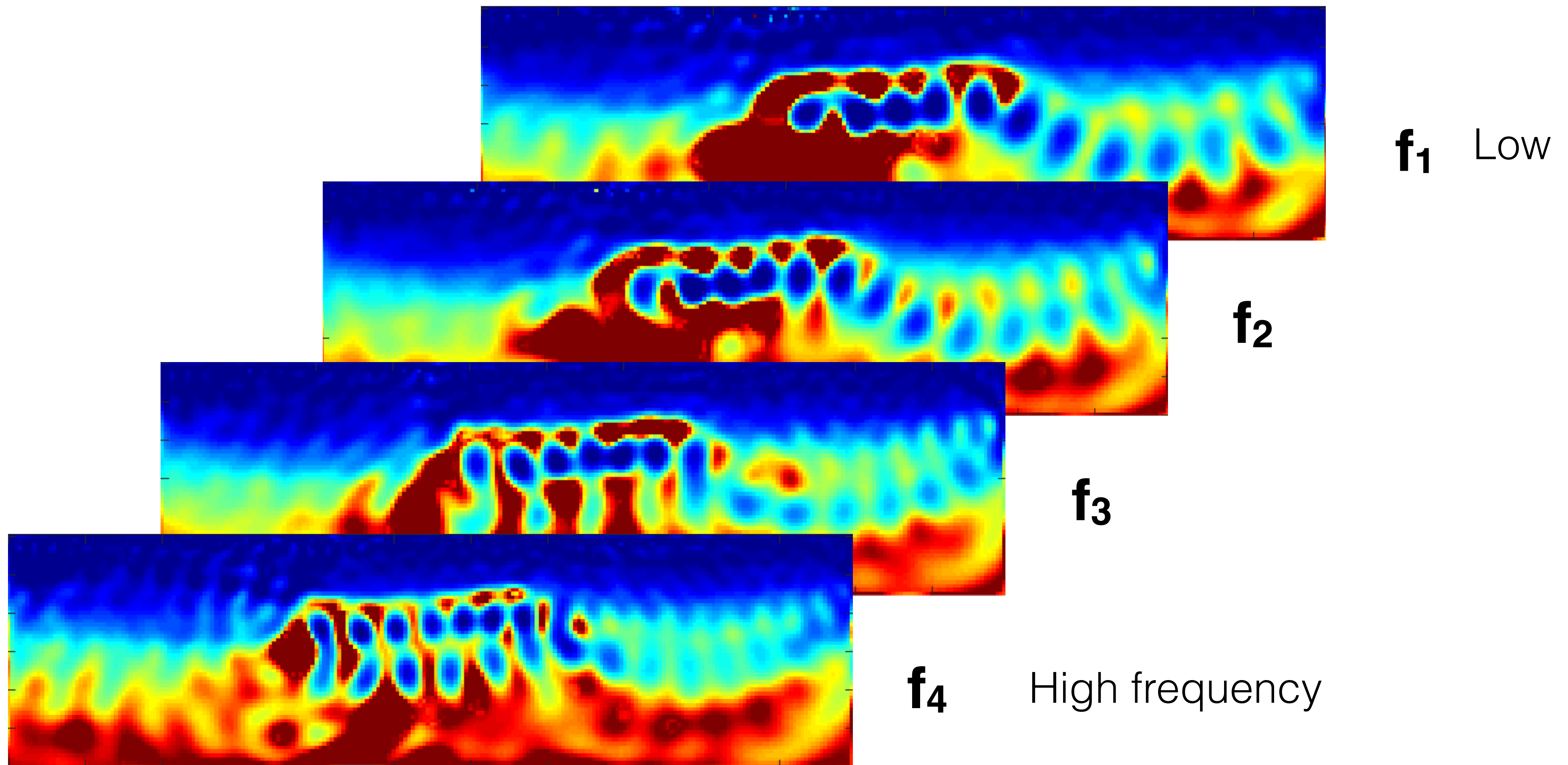
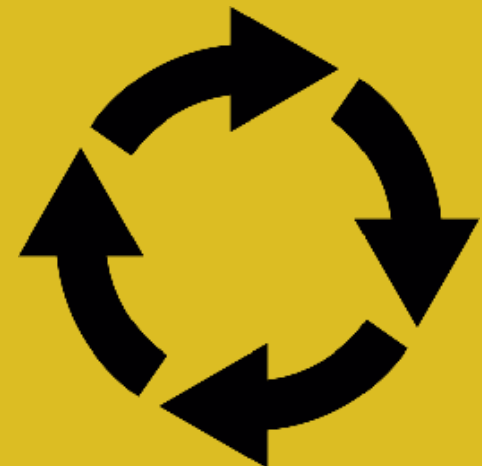
Model updates from different frequencies



Model updates from different frequencies

0. Modeling

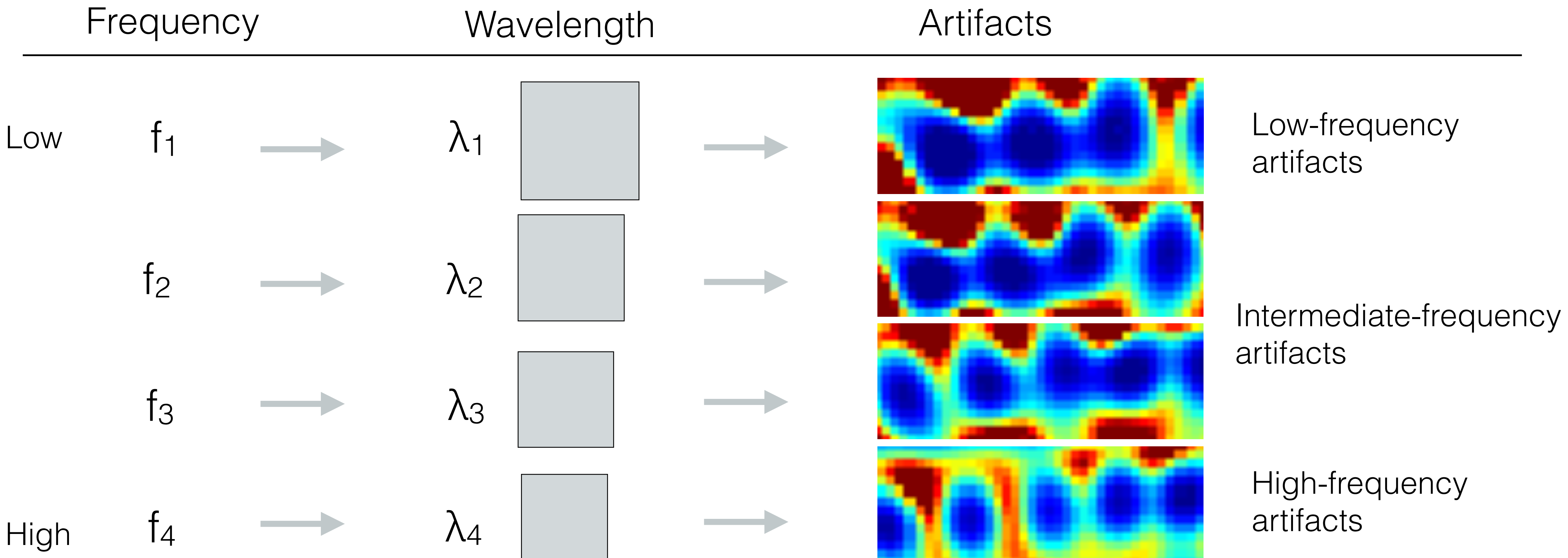
1. Averaging
2. Variance
3. Flooding



Selection of frequencies

Size of cycle-skipping artifacts proportional to wavelength λ

$$f_2 = \frac{\lambda_1}{\lambda_2} f_1$$

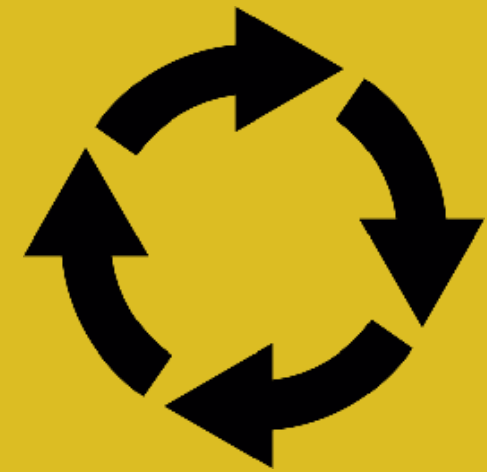


0. Modeling

1. Averaging

2. Variance

3. Flooding

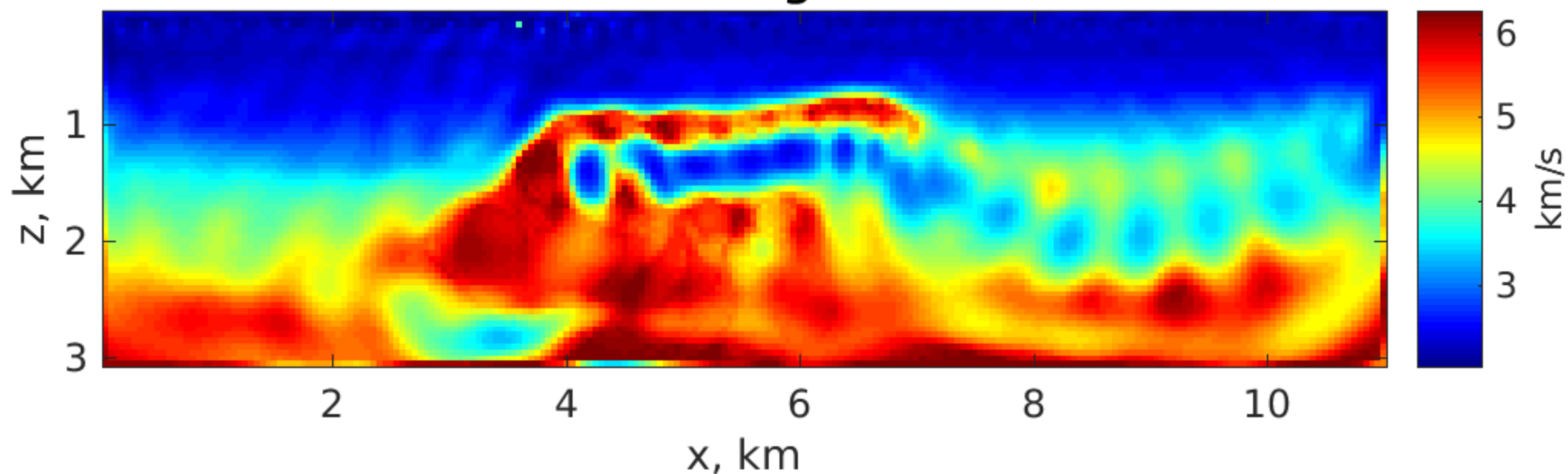


Weighted average

$$\mathbf{M}_b = \frac{\sum_{k=1}^N \mathbf{M}_k w_k}{\sum_{i=1}^N w_i} \quad \text{using weights}$$

$$w_k = \frac{1}{f_k}$$

Average



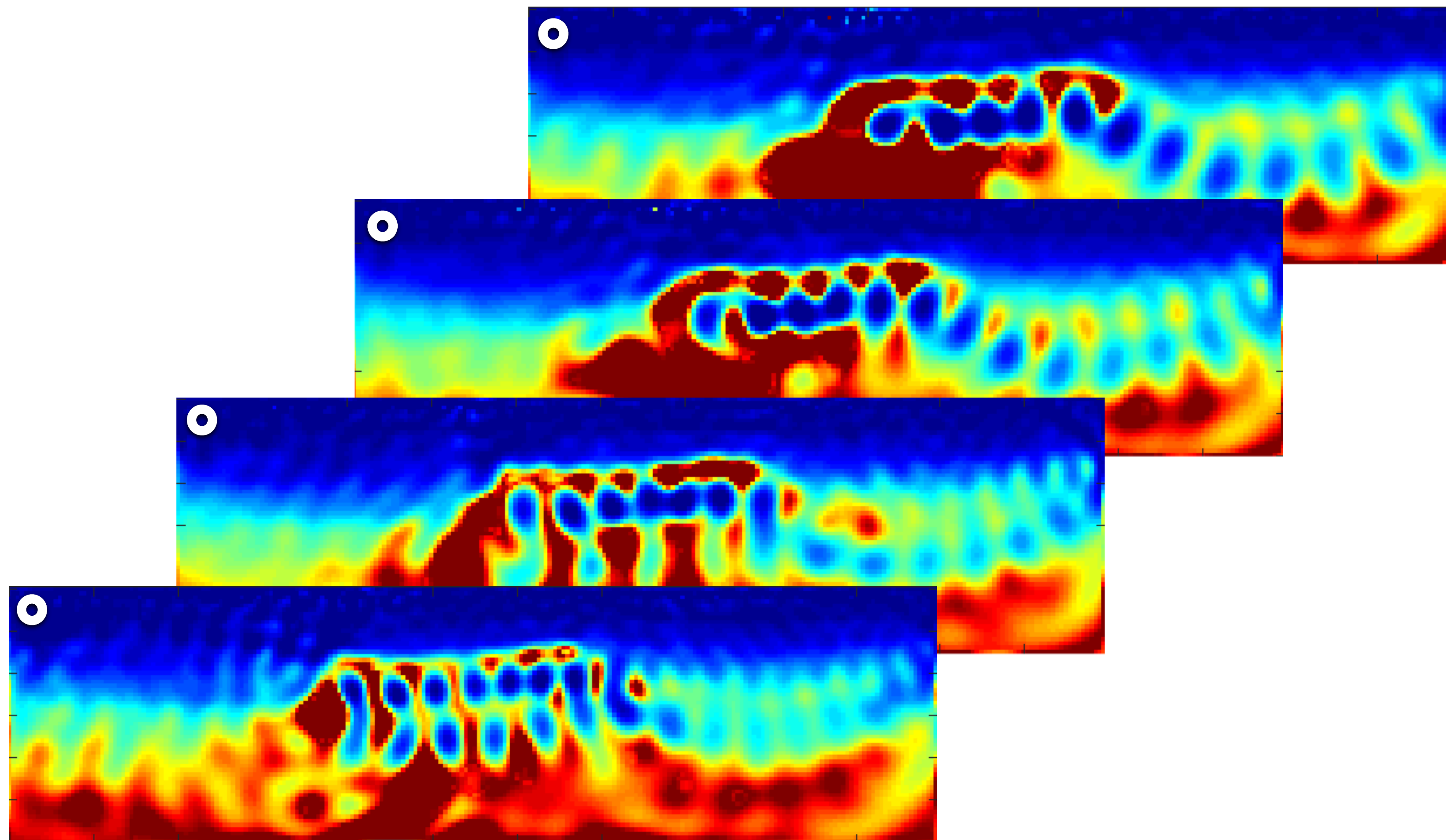
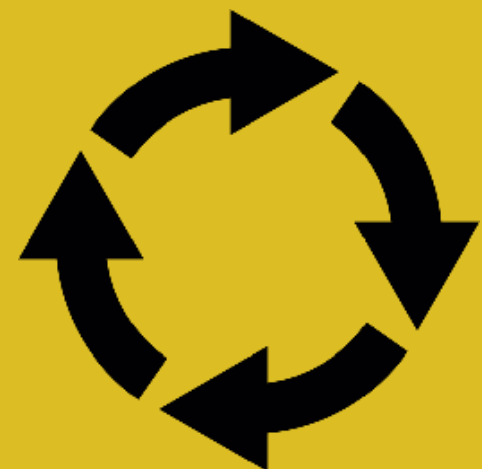
Variance between updates

0. Modeling

1. Averaging

2. Variance

3. Flooding



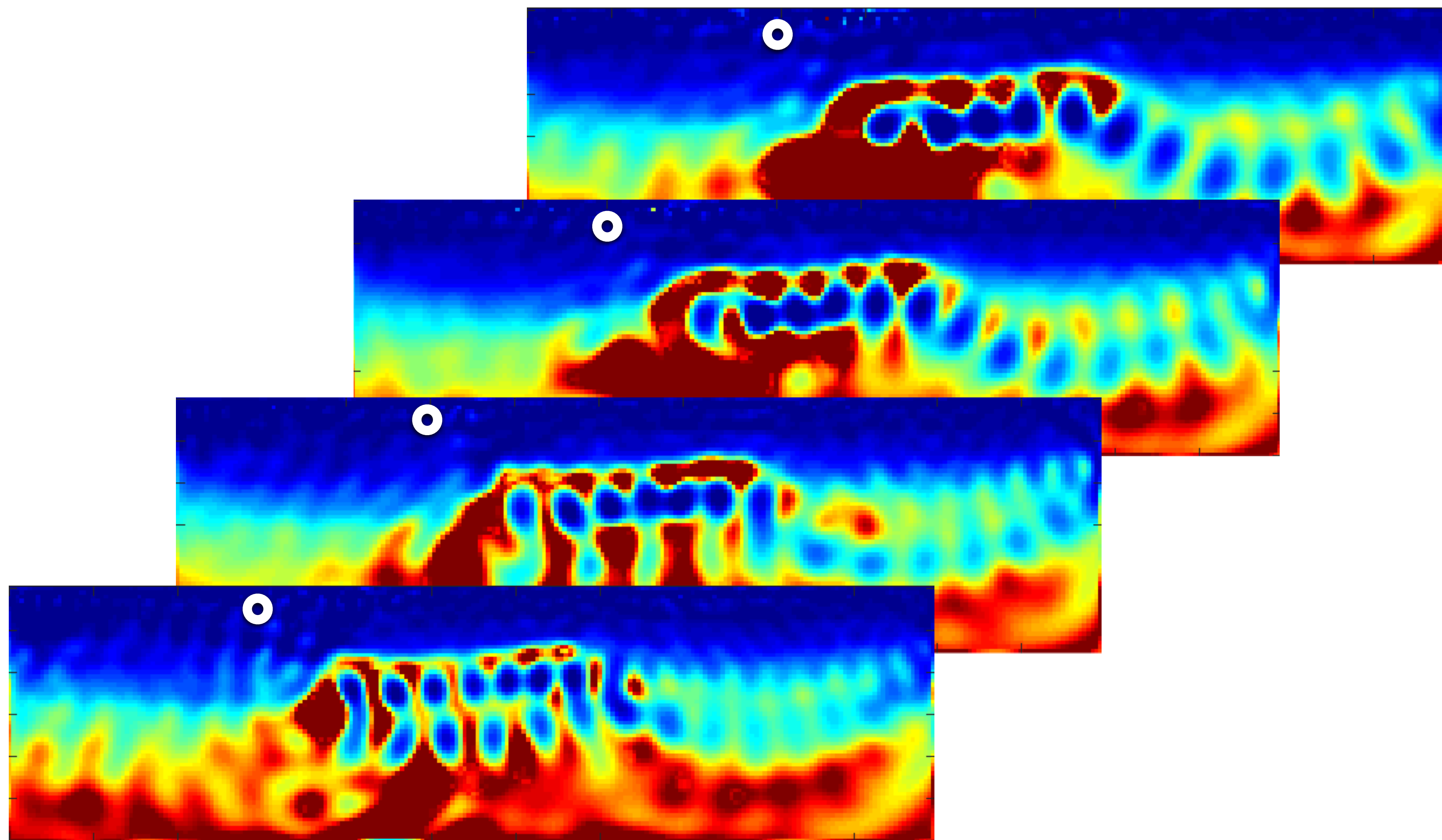
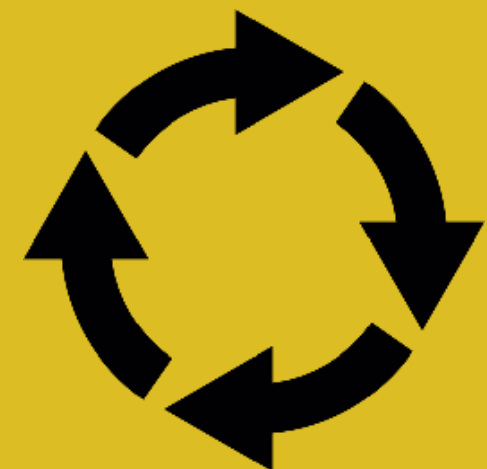
Variance between updates

0. Modeling

1. Averaging

2. Variance

3. Flooding



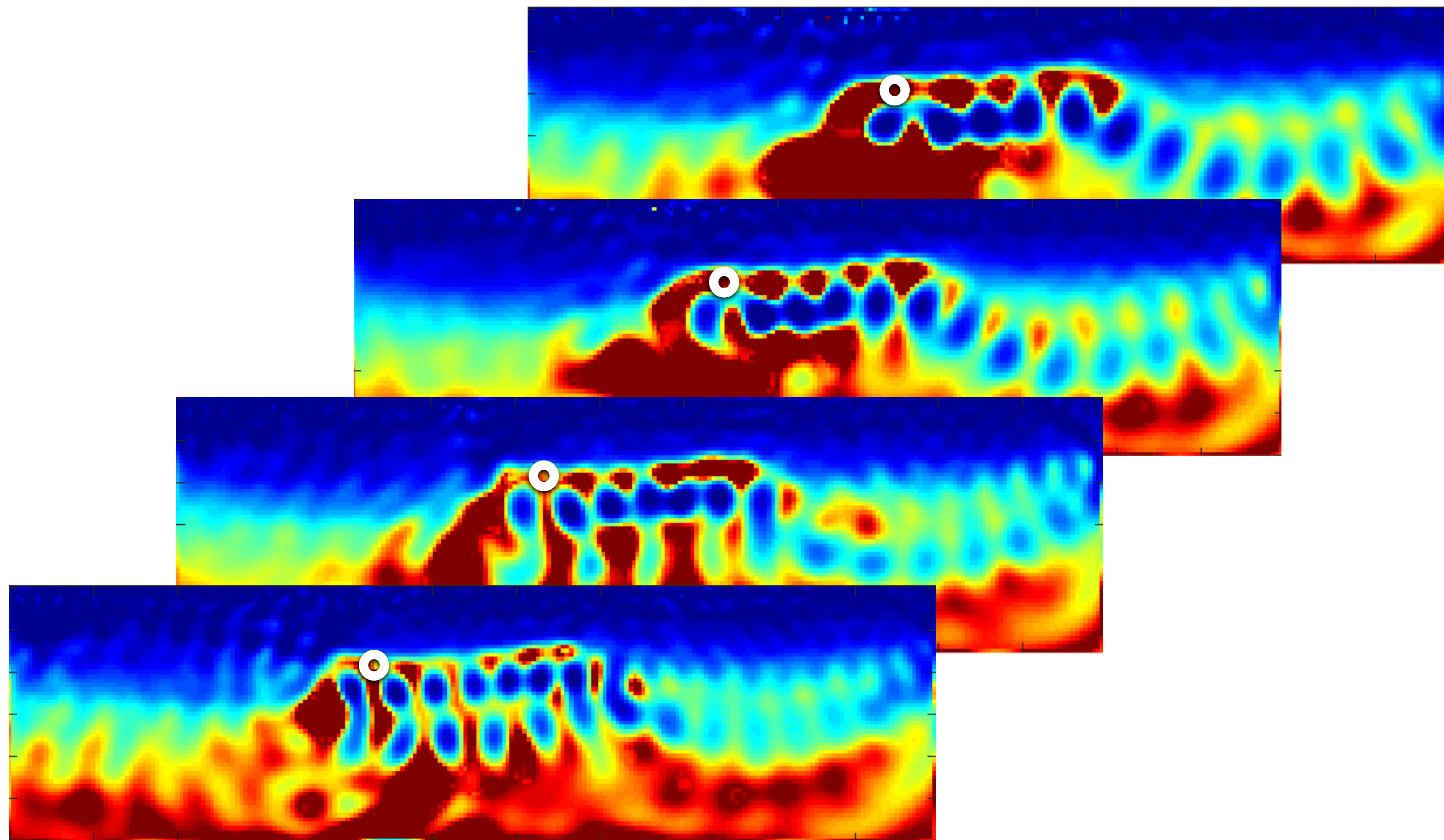
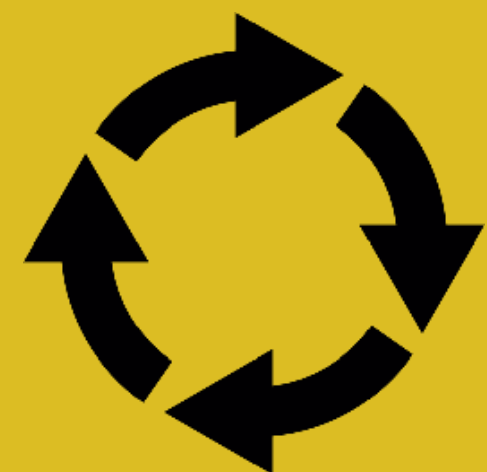
Variance between updates

0. Modeling

1. Averaging

2. Variance

3. Flooding

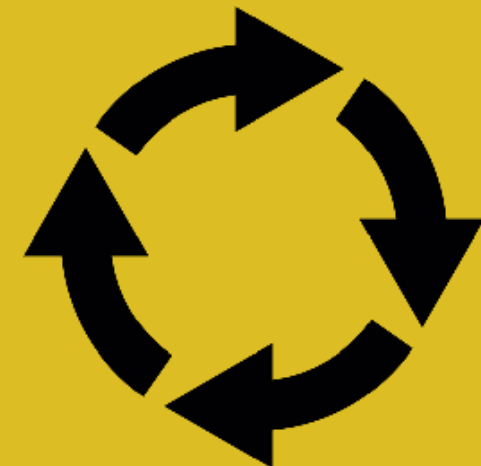


0. Modeling

1. Averaging

2. Variance

3. Flooding



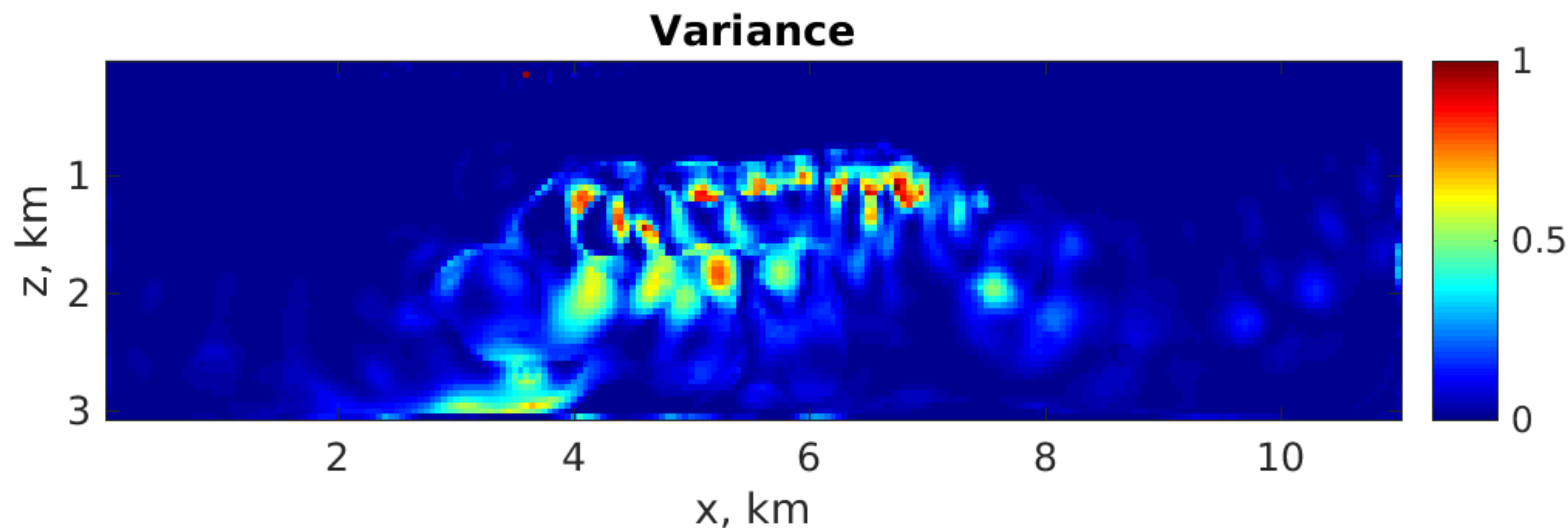
Variance

Weighted variance

$$\mathbf{V} = \frac{\sum_{k=1}^N w_k (\mathbf{M}_k - \mathbf{M}_b)^2}{\sum_{i=1}^N w_i}$$

using weights

$$w_k = \frac{1}{f_k}$$

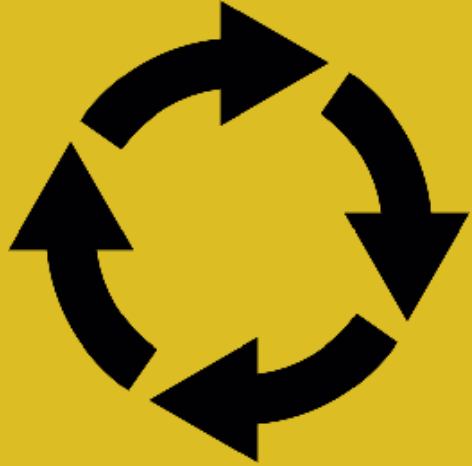


0. Modeling

1. Averaging

2. Variance

3. Flooding

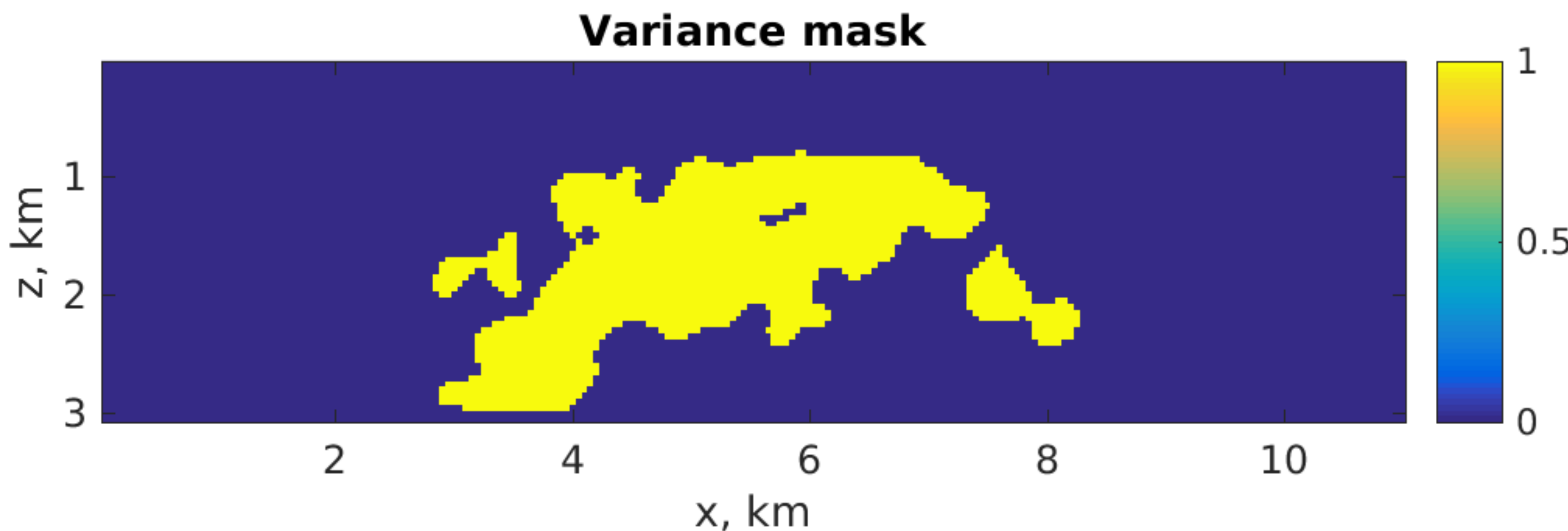


Variance mask

Floating variance threshold

$$\epsilon \sim \frac{V_{max}}{V_{avg}}$$

ϵ_0	Initial threshold
V_{max}	Maximum variance
V_{avg}	Average variance



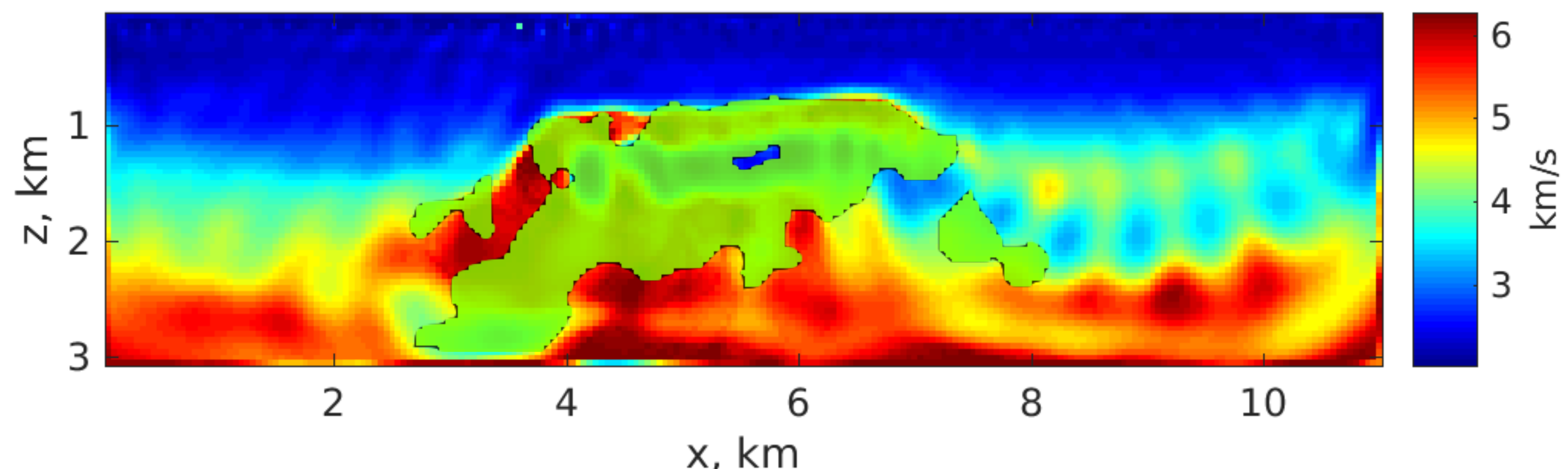
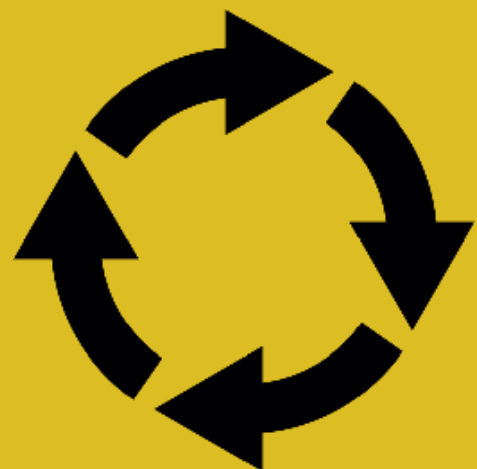
Variance mask and model overlap

0. Modeling

1. Averaging

2. Variance

3. Flooding



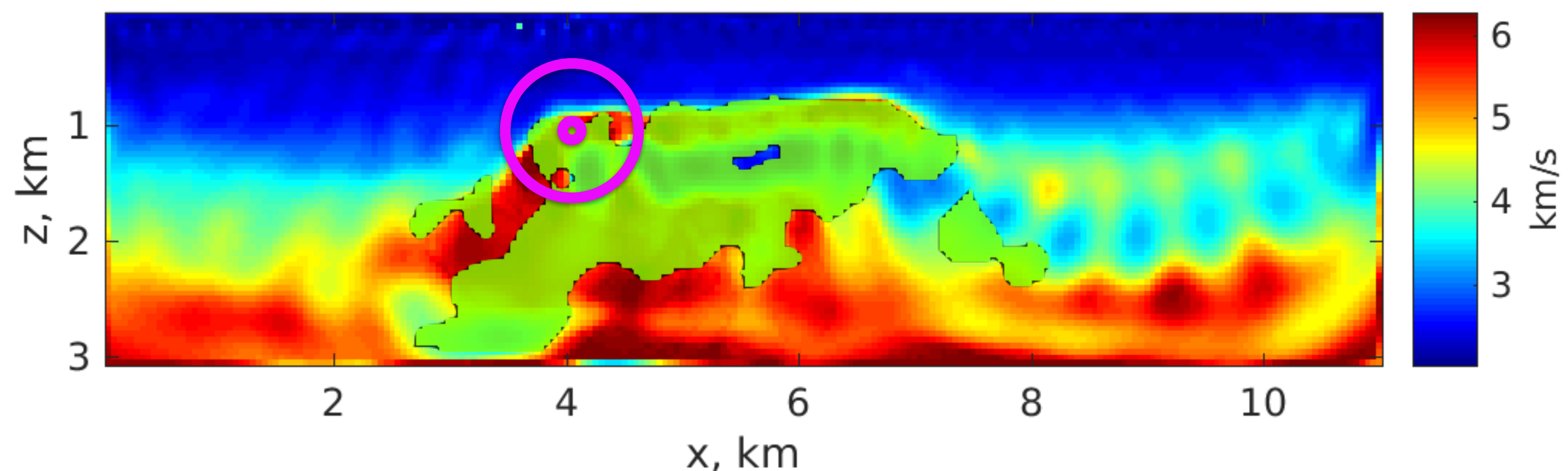
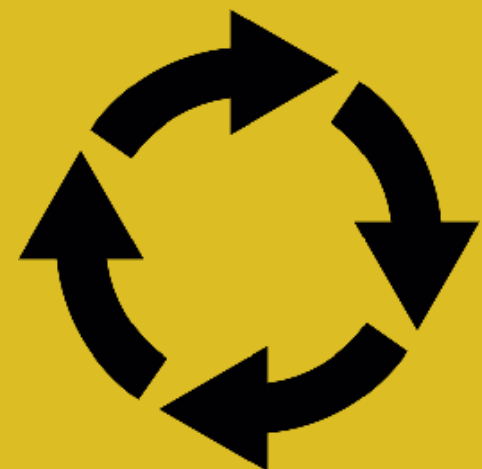
Variance mask and model overlap

0. Modeling

1. Averaging

2. Variance

3. Flooding



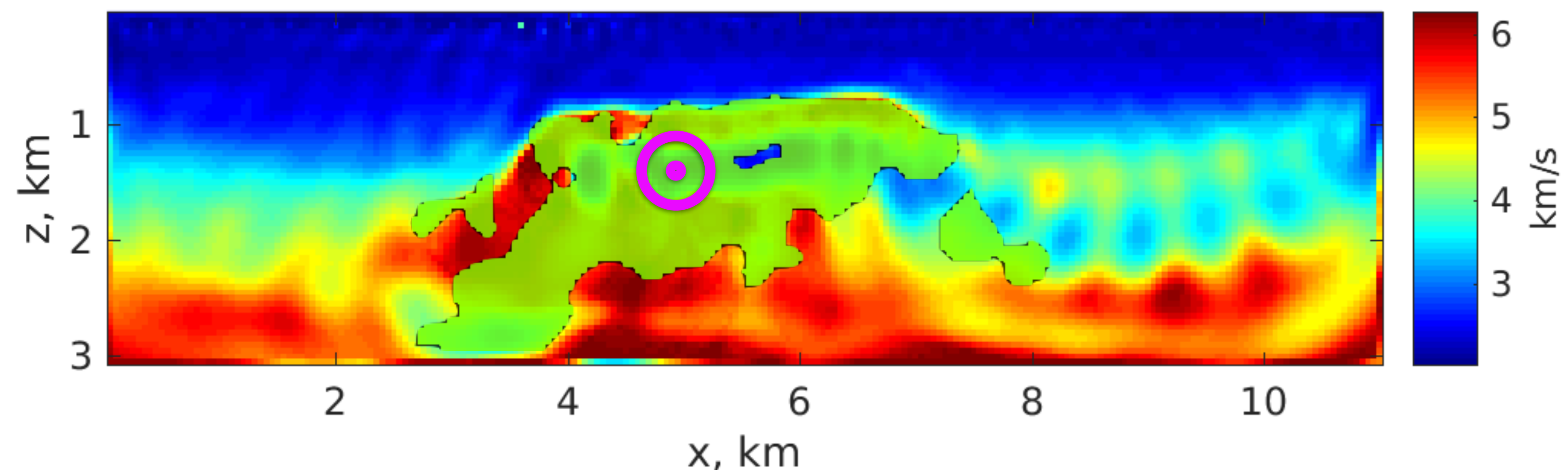
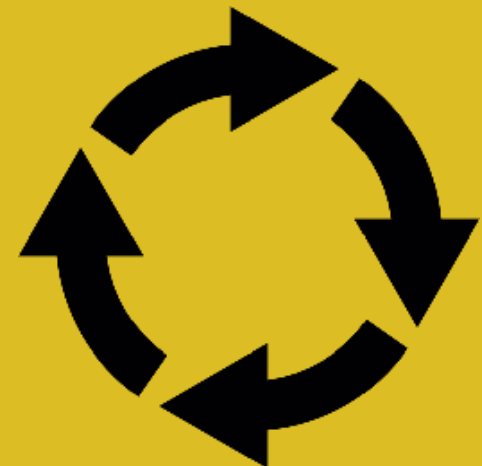
Variance mask and model overlap

0. Modeling

1. Averaging

2. Variance

3. Flooding



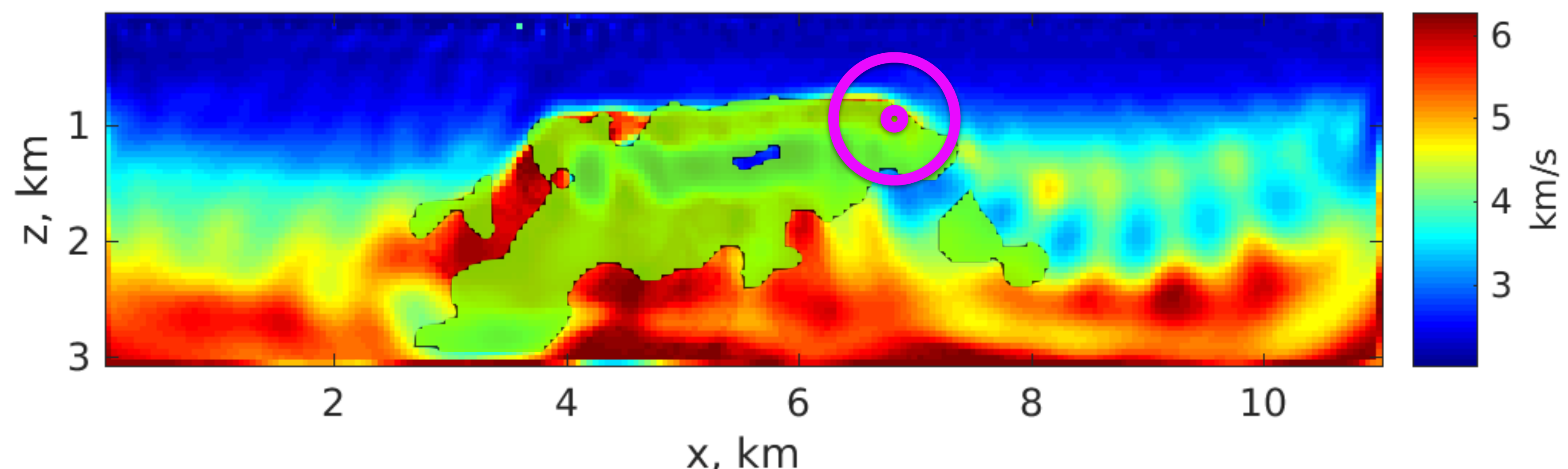
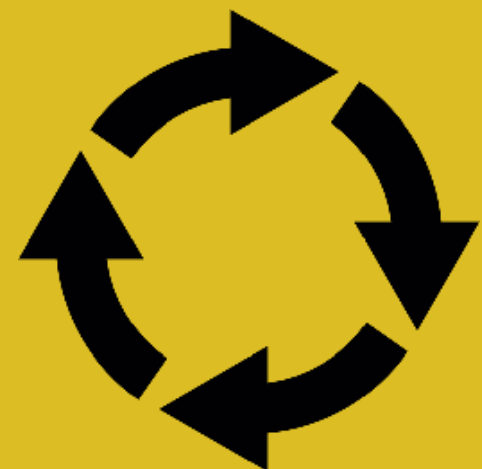
Variance mask and model overlap

0. Modeling

1. Averaging

2. Variance

3. Flooding



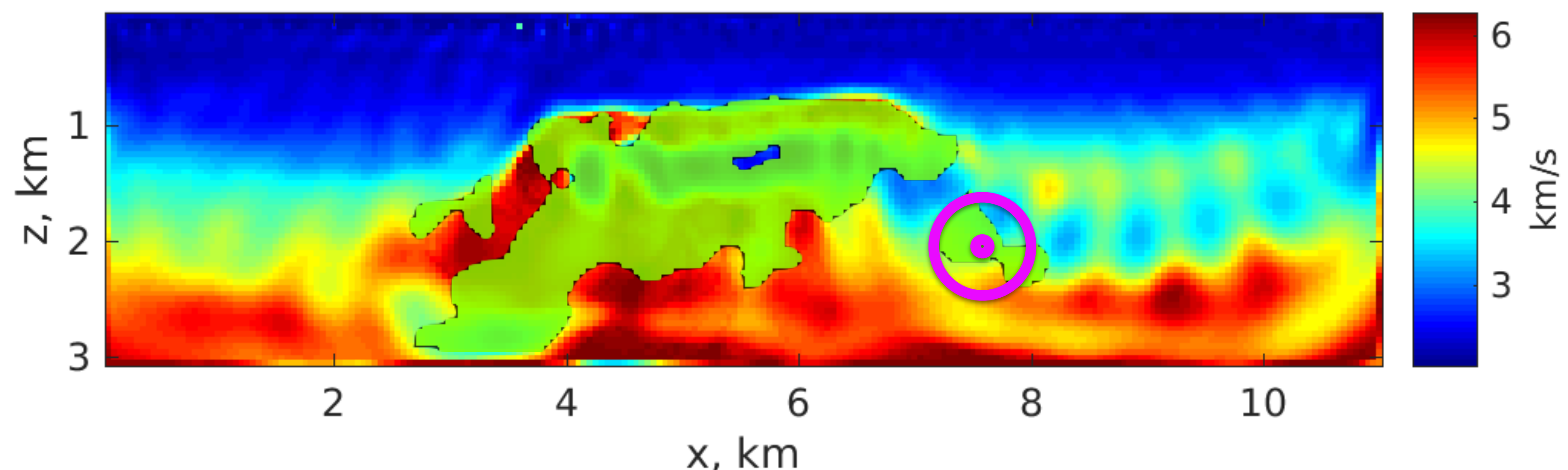
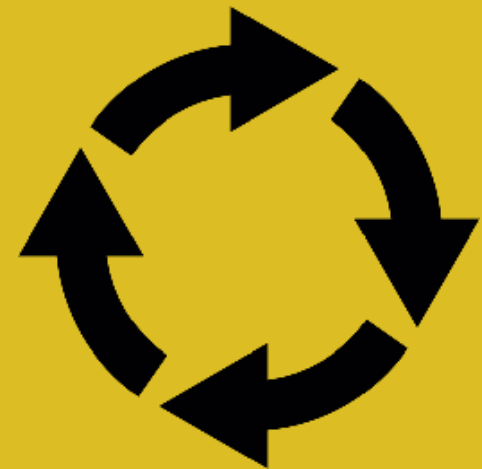
Variance mask and model overlap

0. Modeling

1. Averaging

2. Variance

3. Flooding



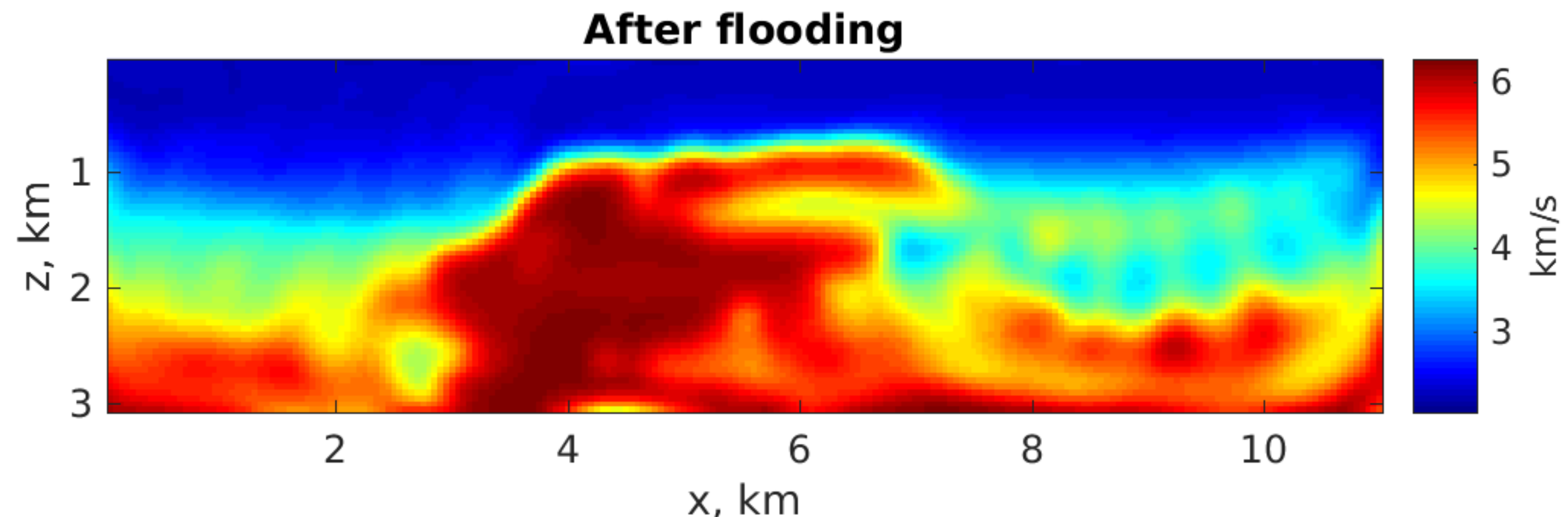
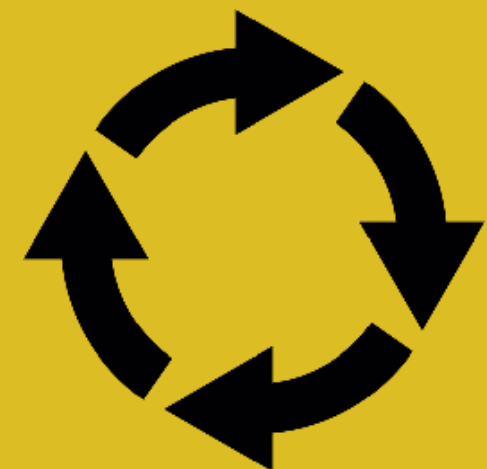
Variance mask and model overlap

0. Modeling

1. Averaging

2. Variance

3. Flooding



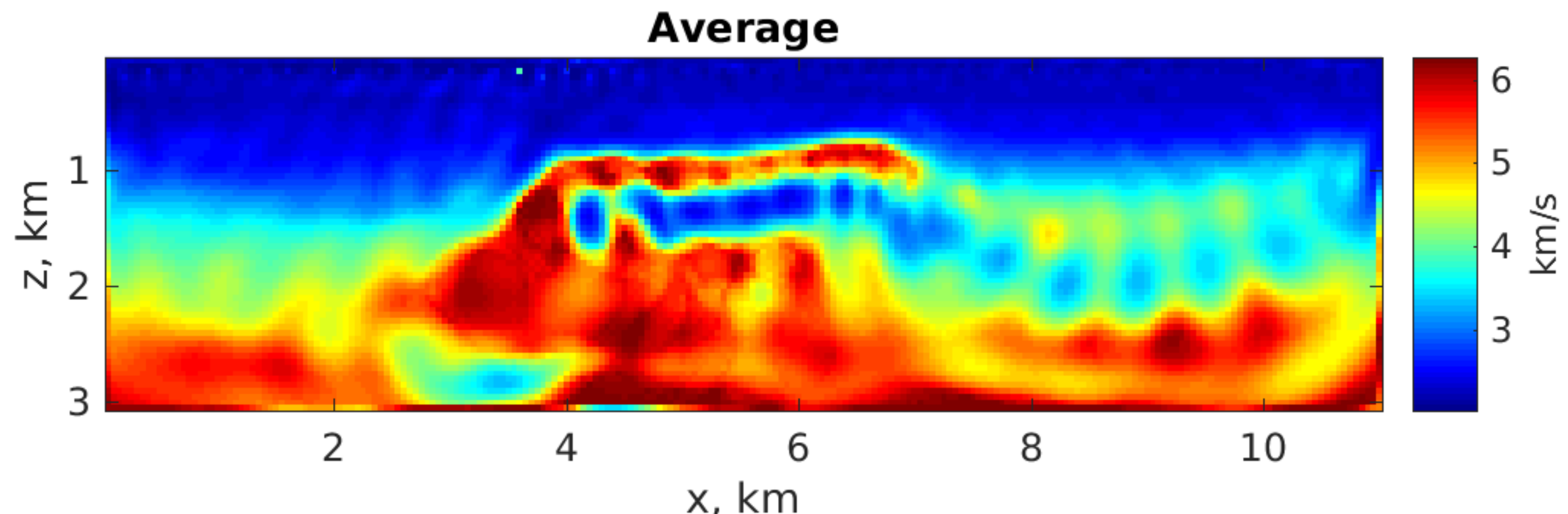
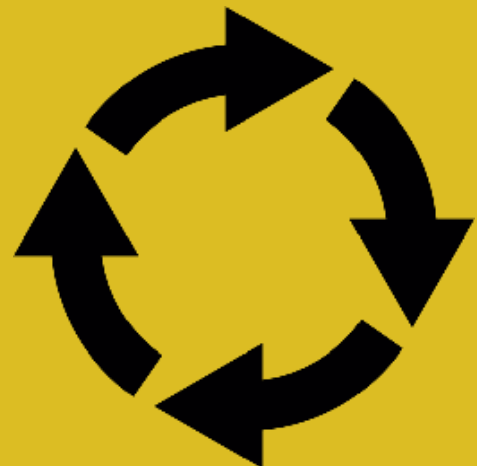
Variance mask and model overlap

0. Modeling

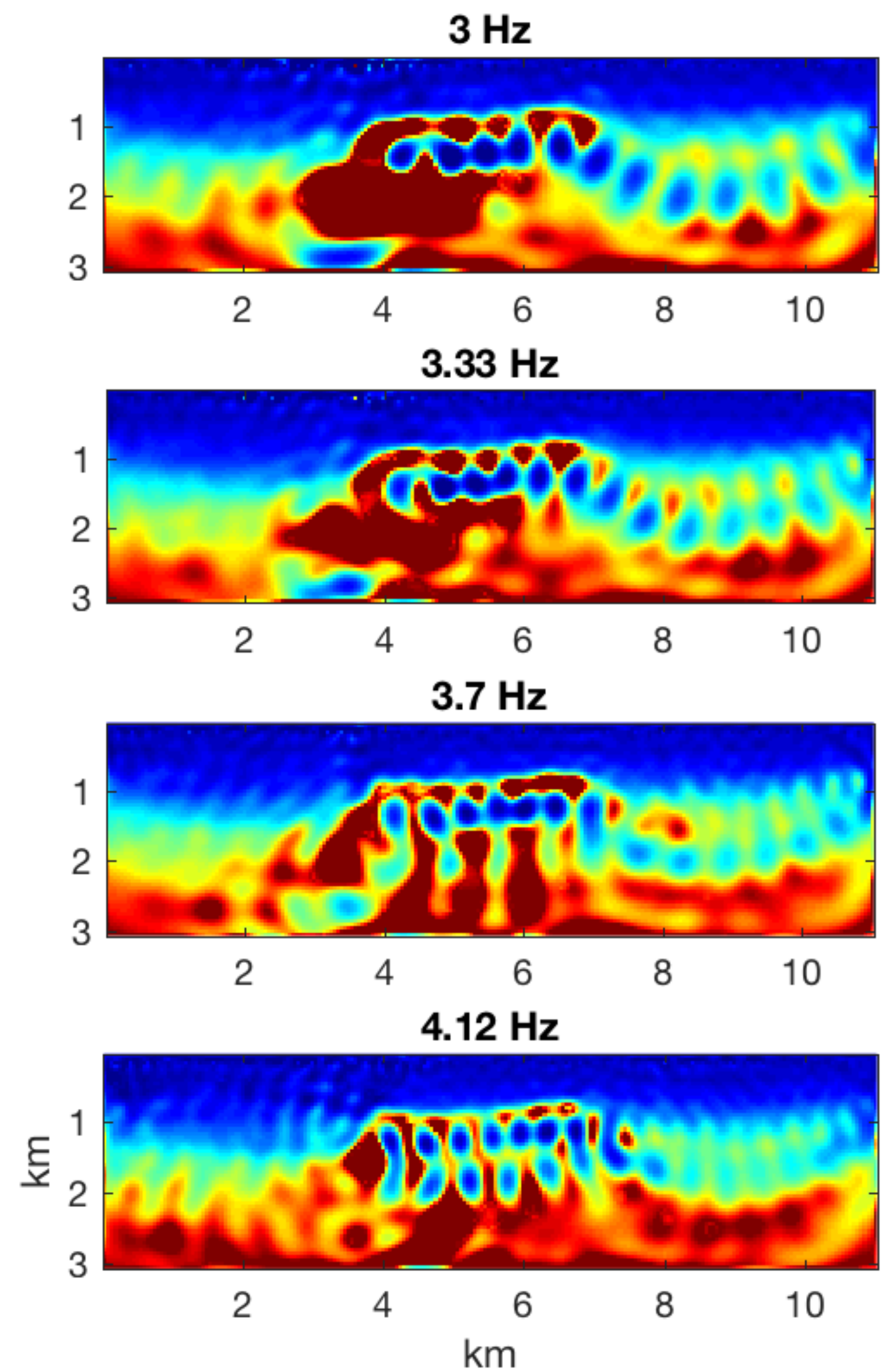
1. Averaging

2. Variance

3. Flooding



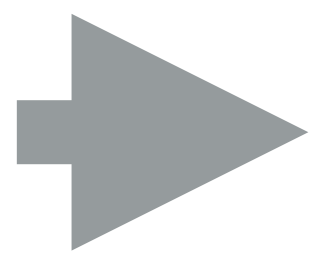
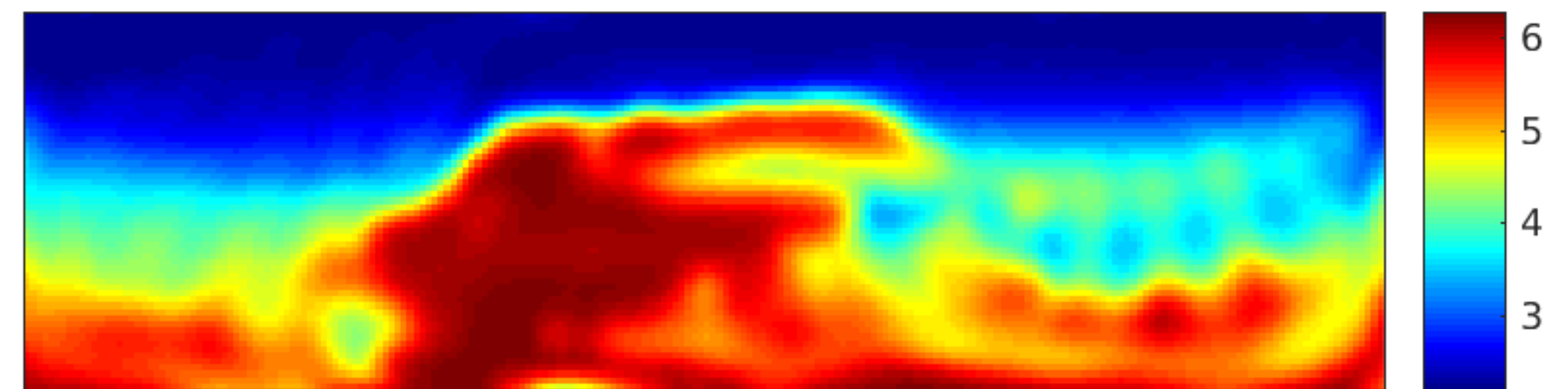
Input



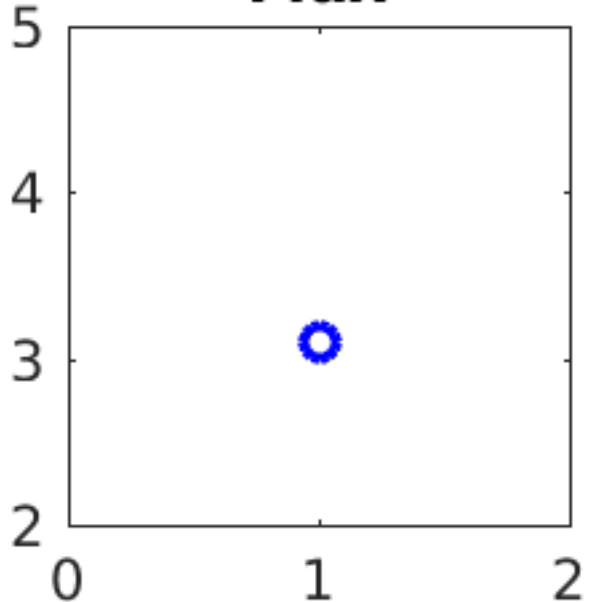
Masks



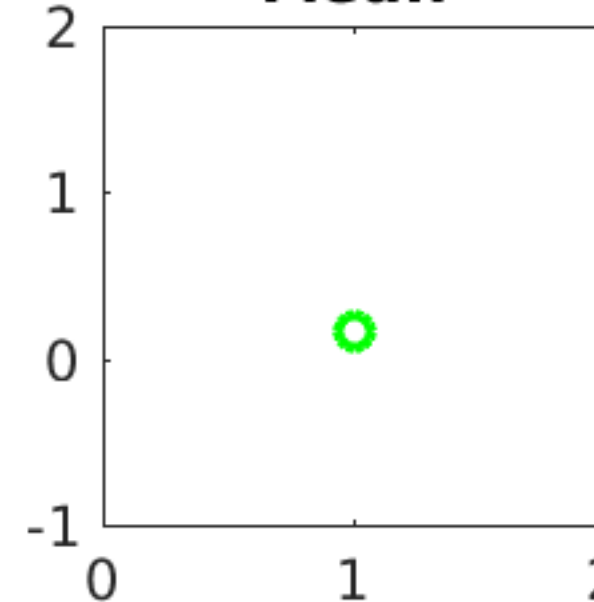
Result



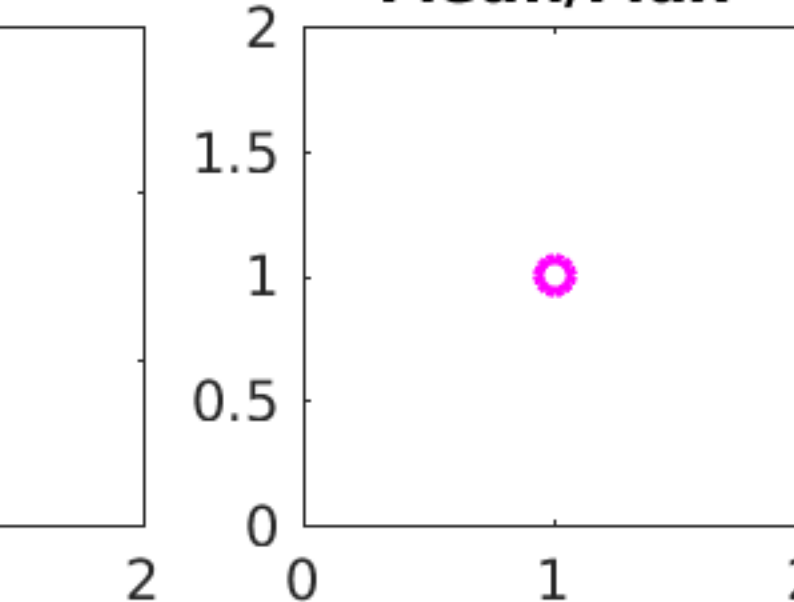
Max



Mean



Mean/Max



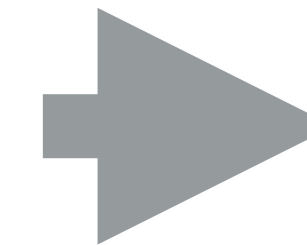
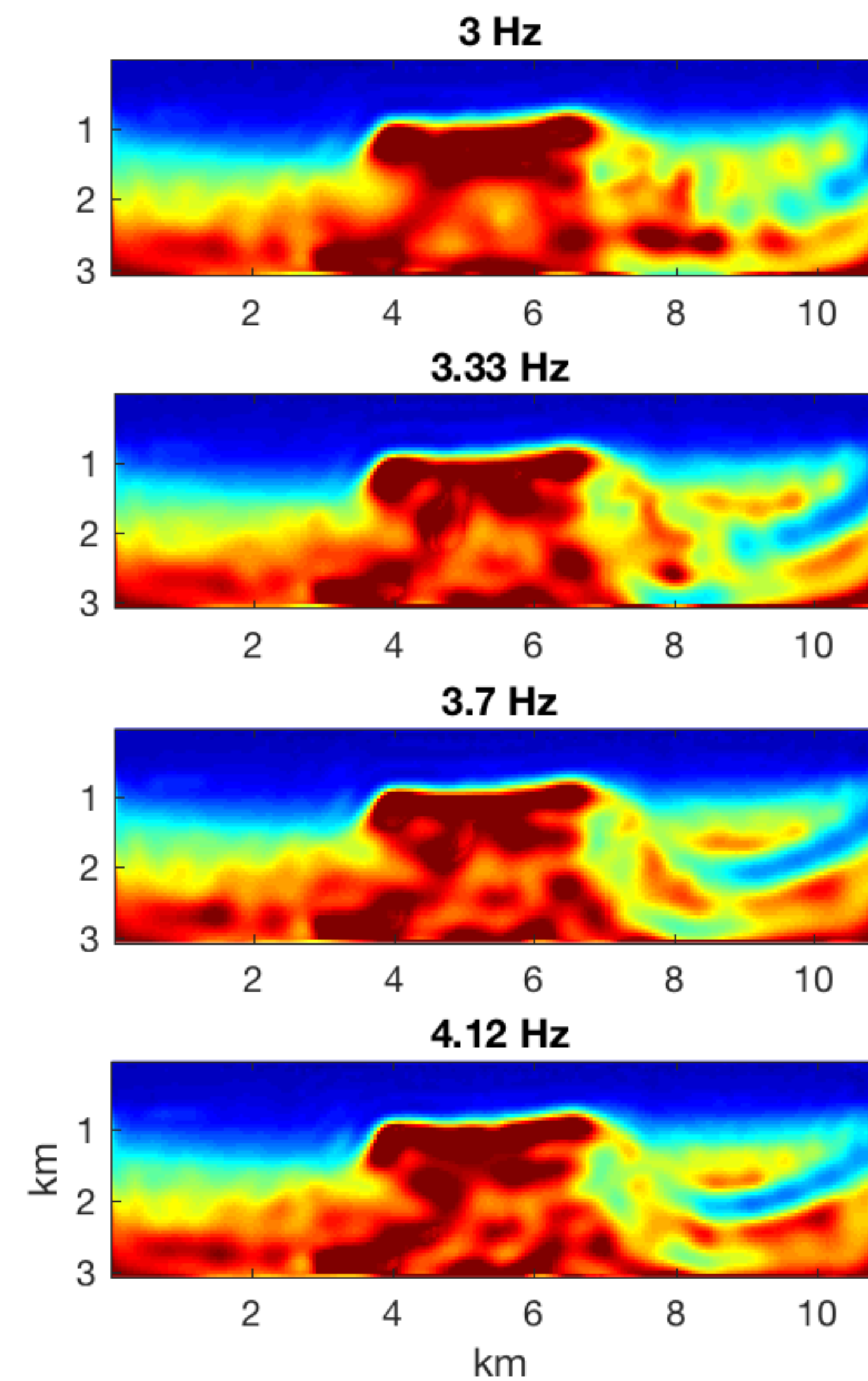
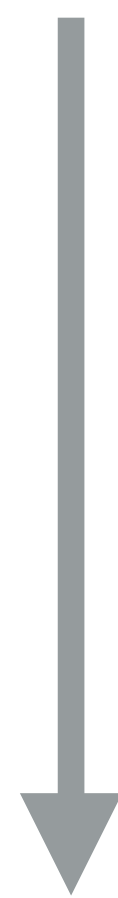
Flooding 1

Var > 0.2

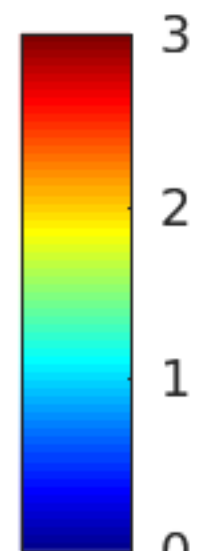
Max = 3.1

Mean = 0.17

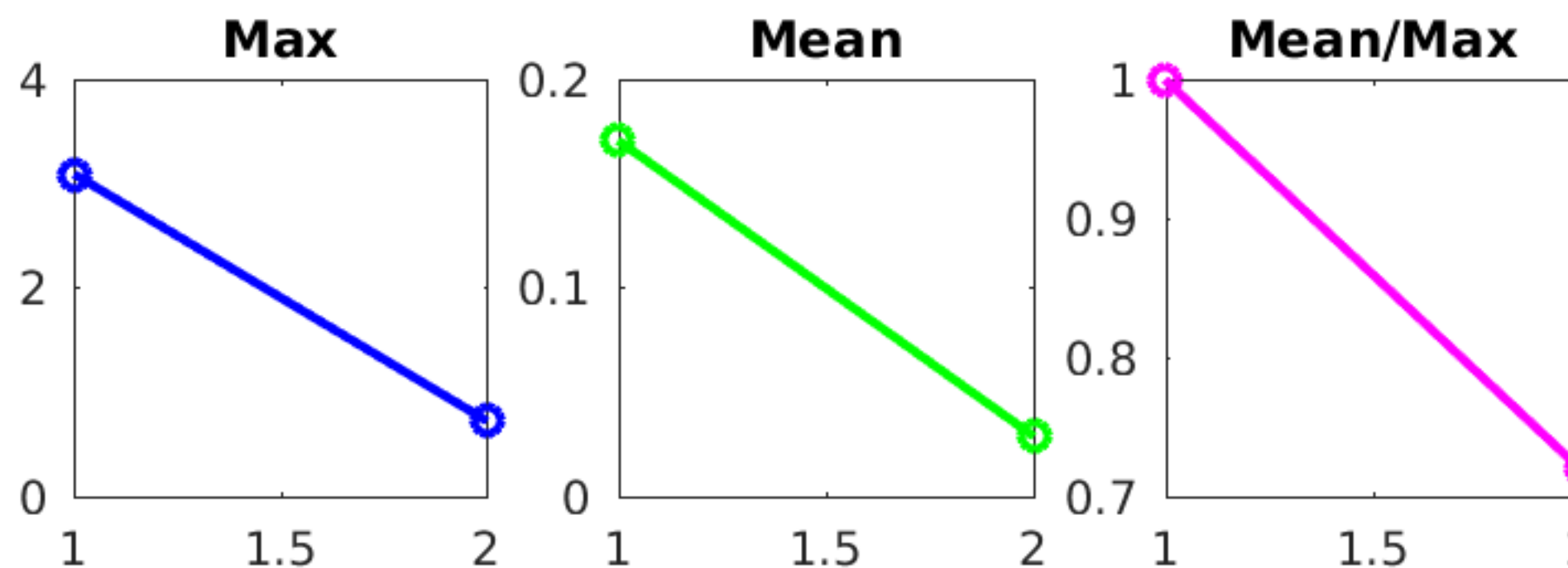
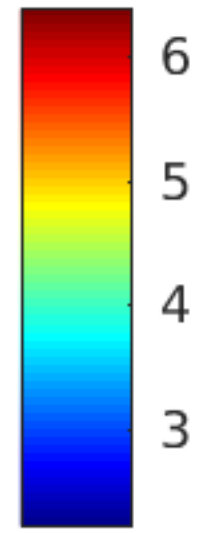
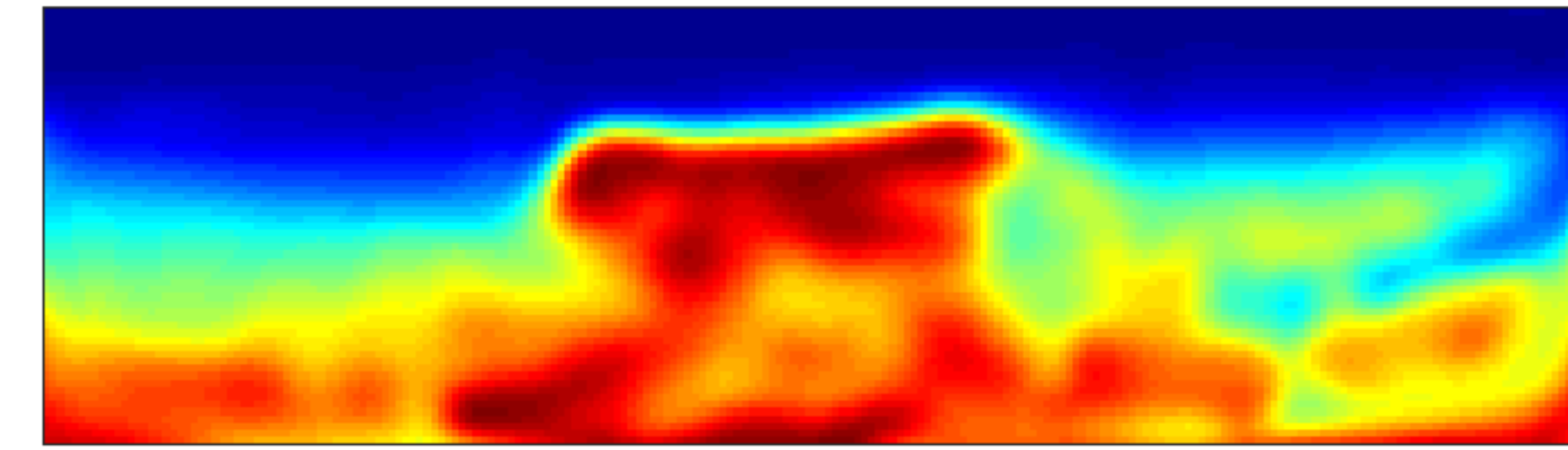
Input



Masks



Result



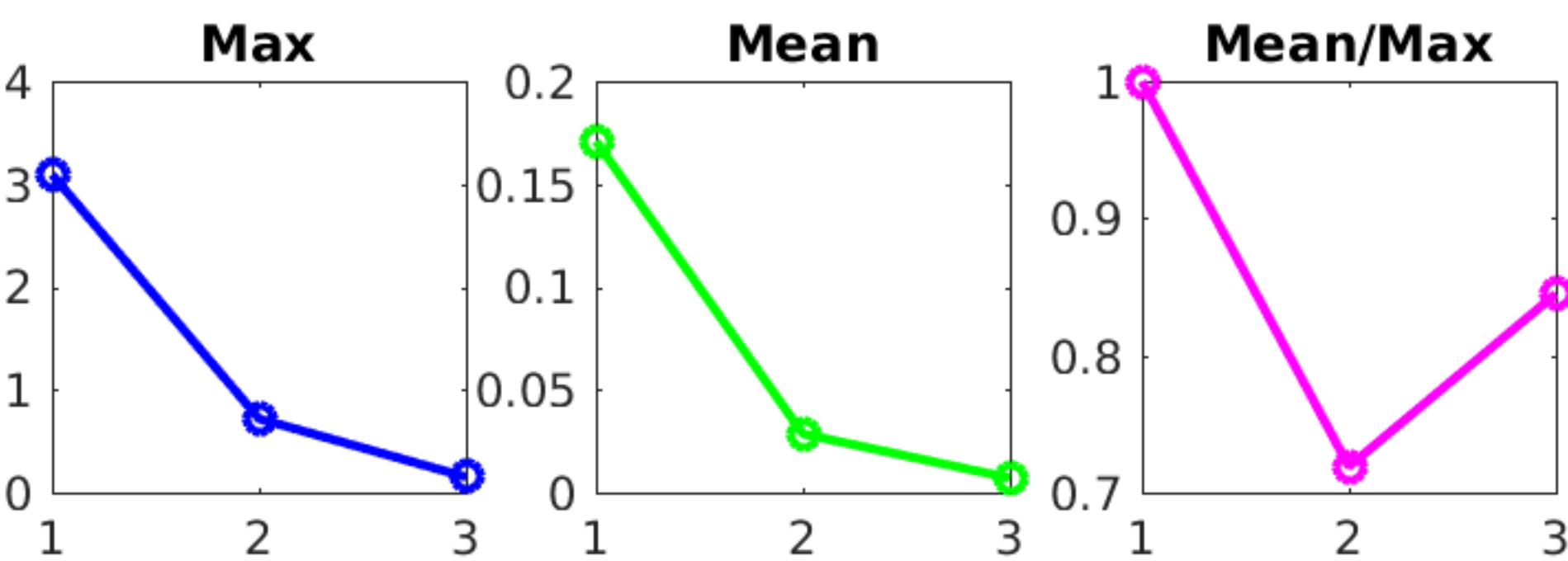
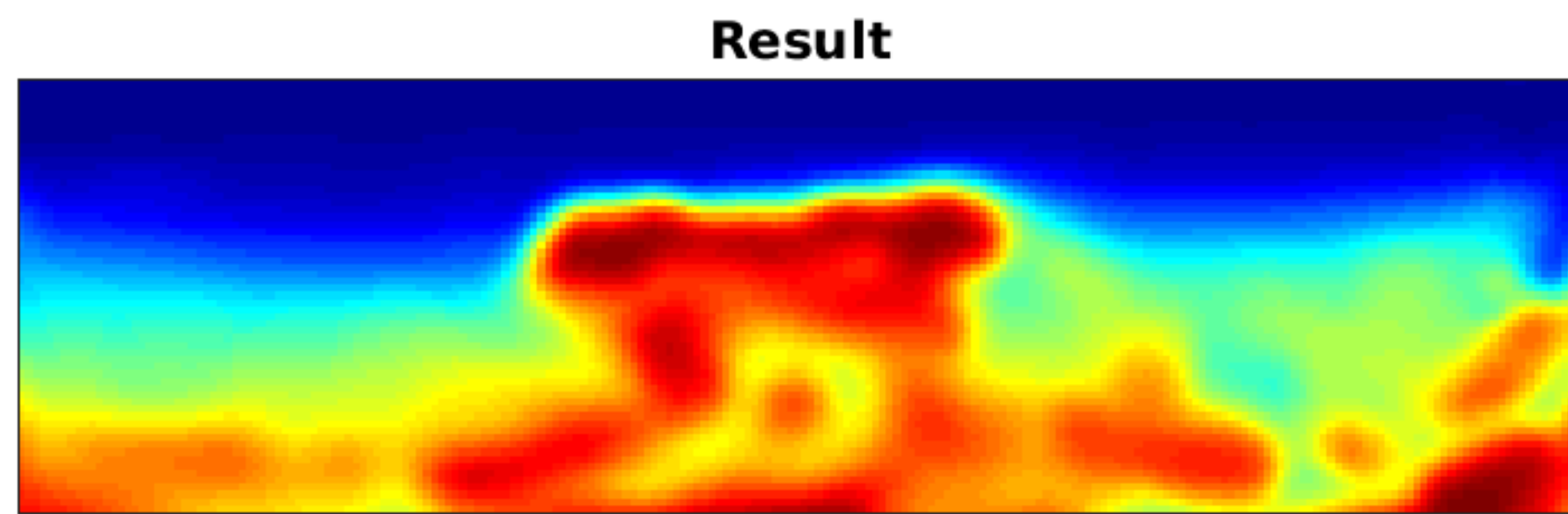
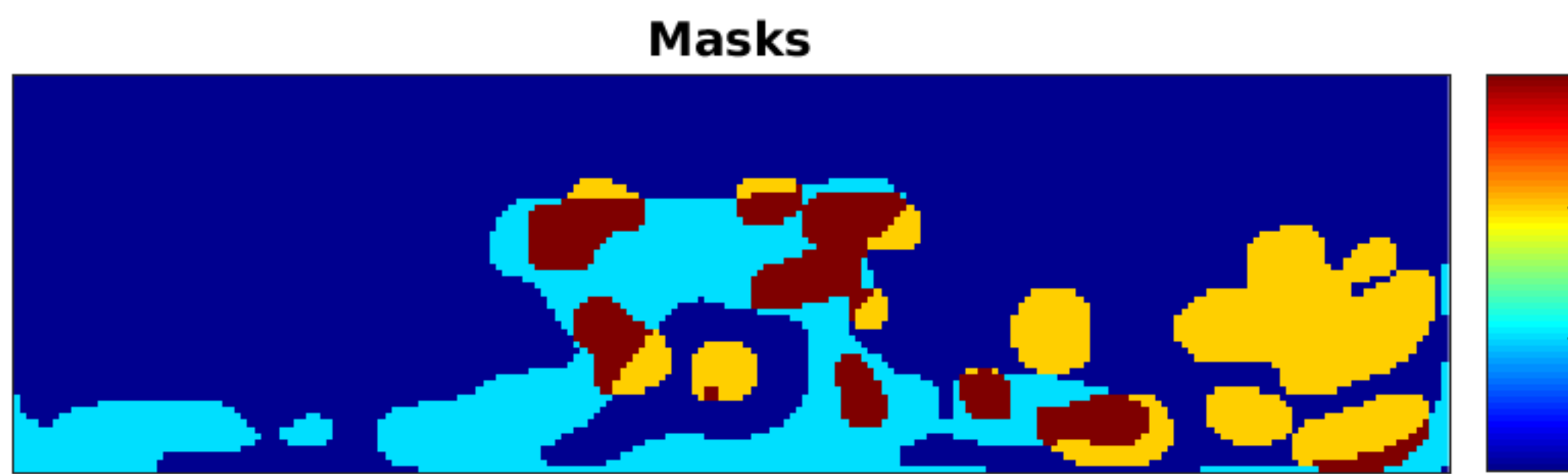
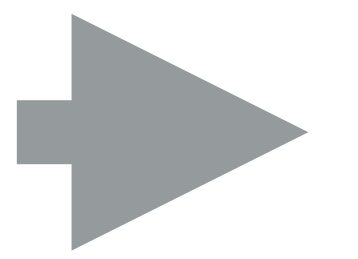
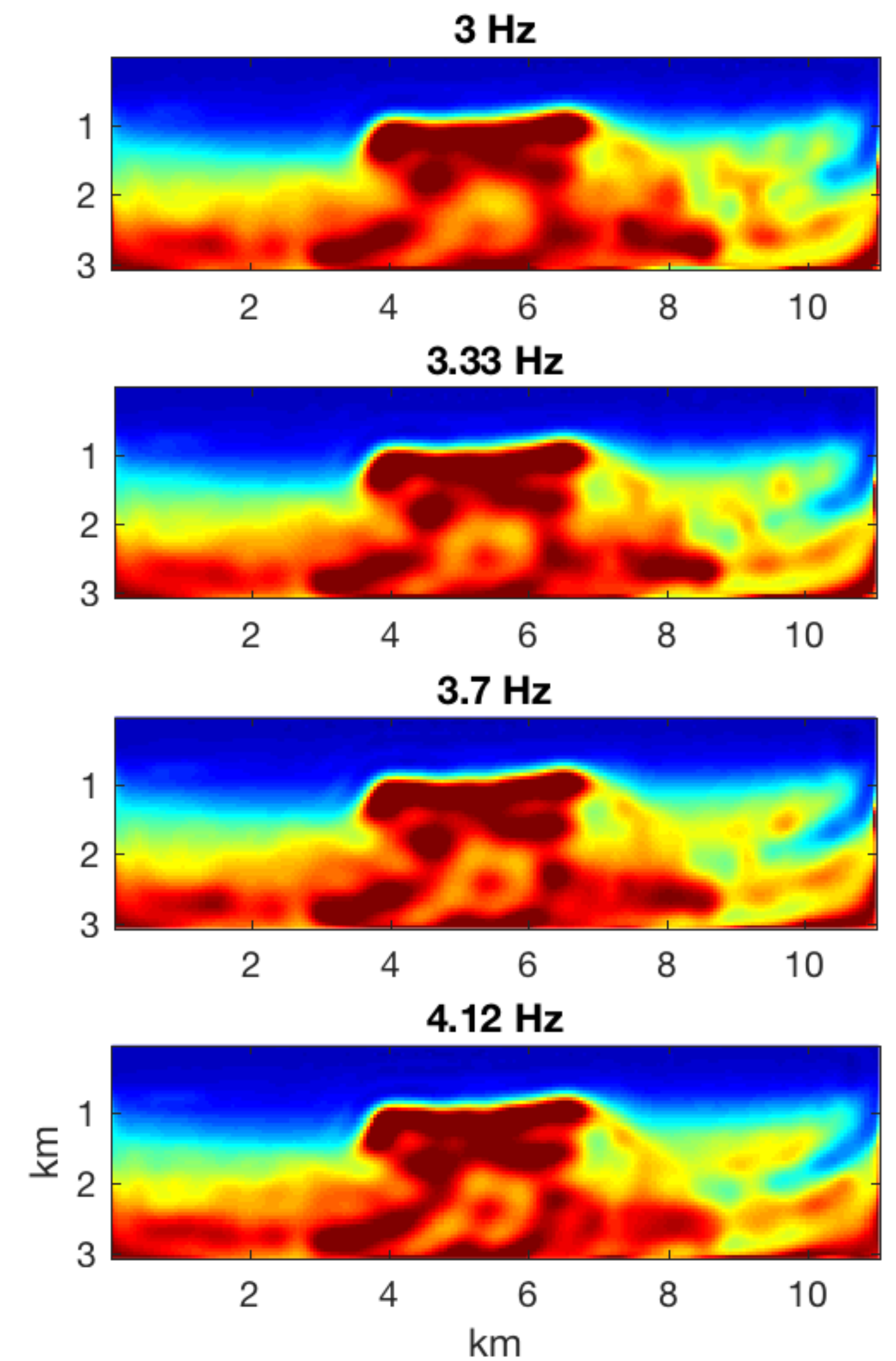
Flooding 2

Var > 0.28

Max = 0.72

Mean = 0.029

Input



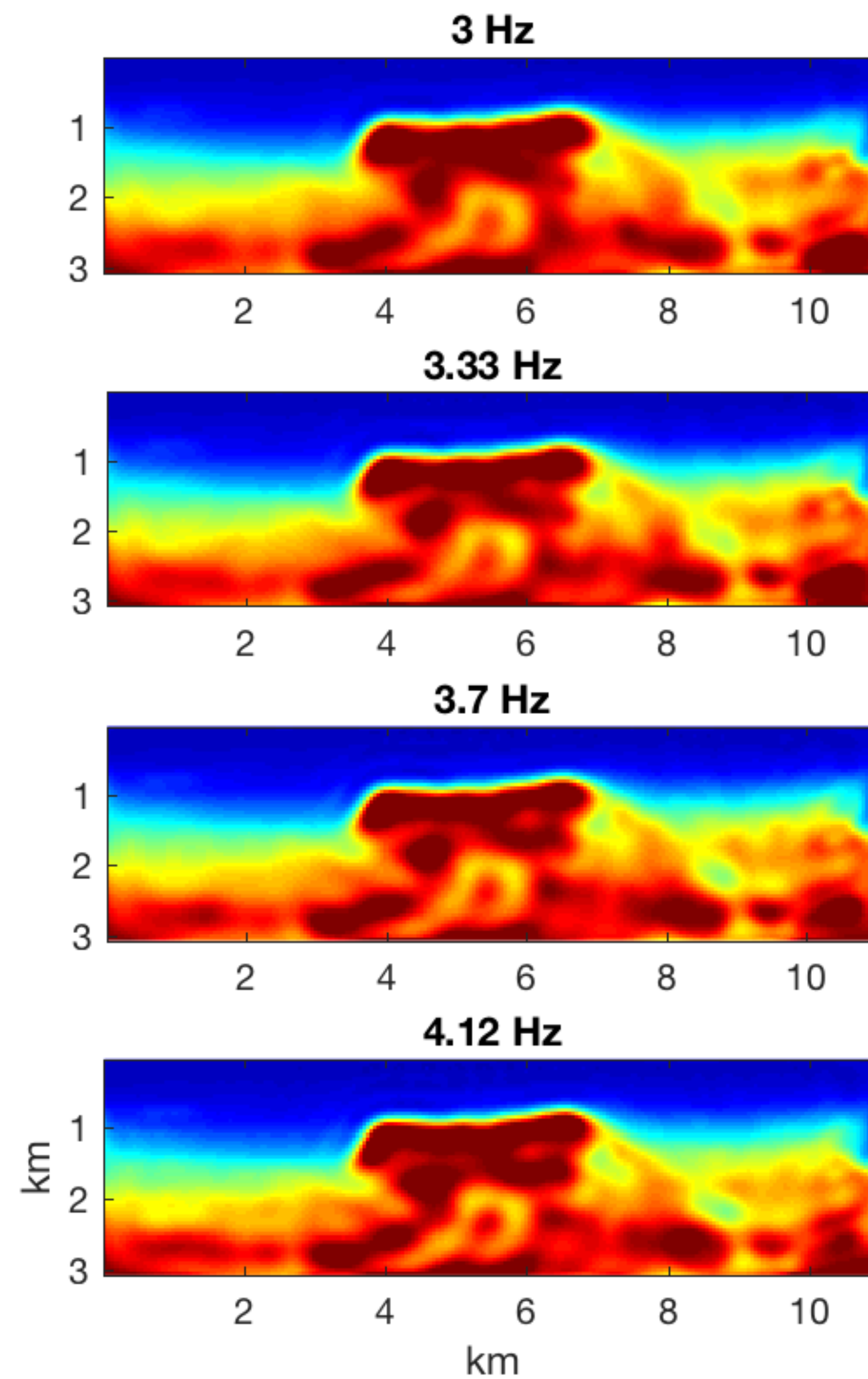
Flooding 3

Var > 0.24

Max = 0.15

Mean = 0.0071

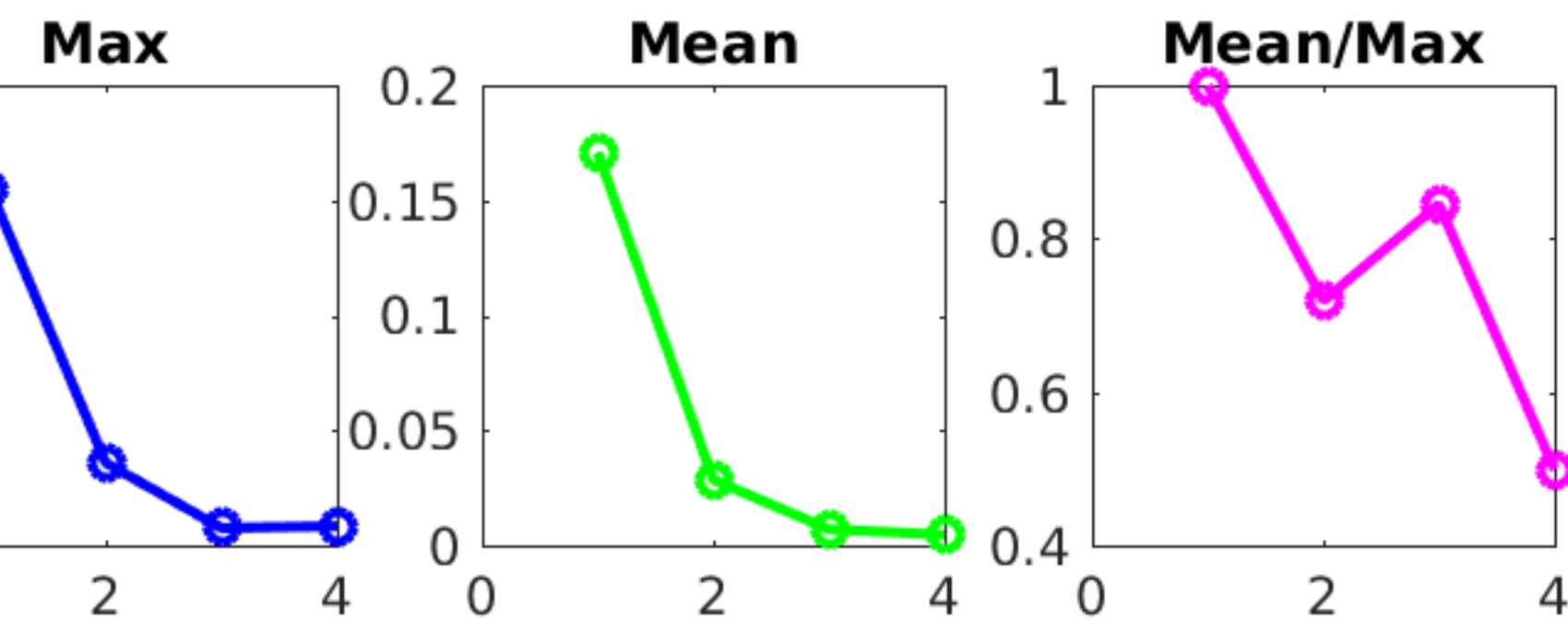
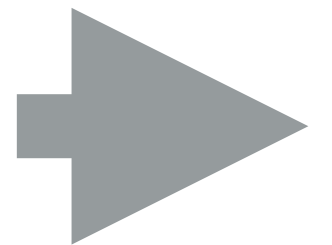
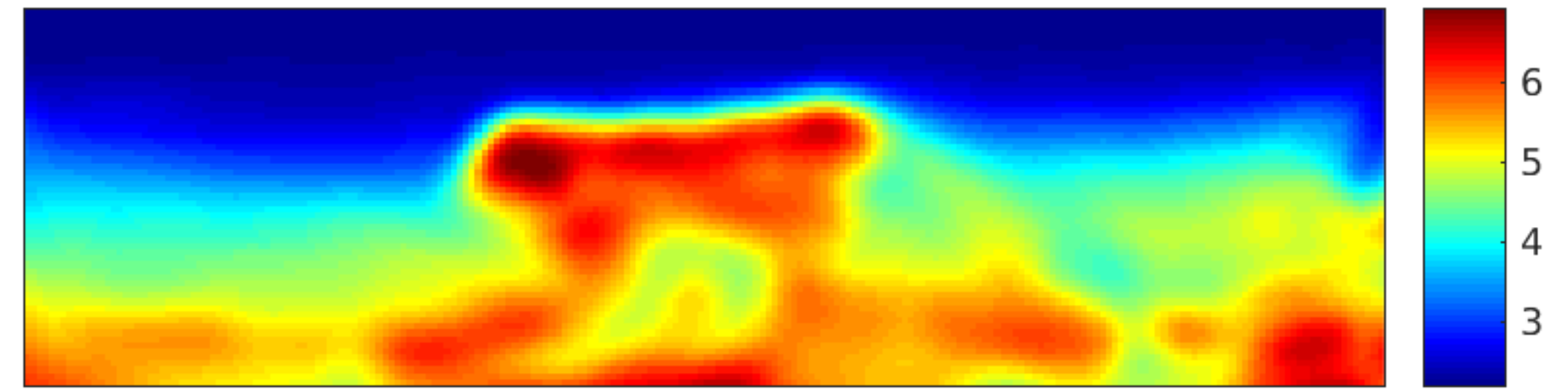
Input



Masks



Result



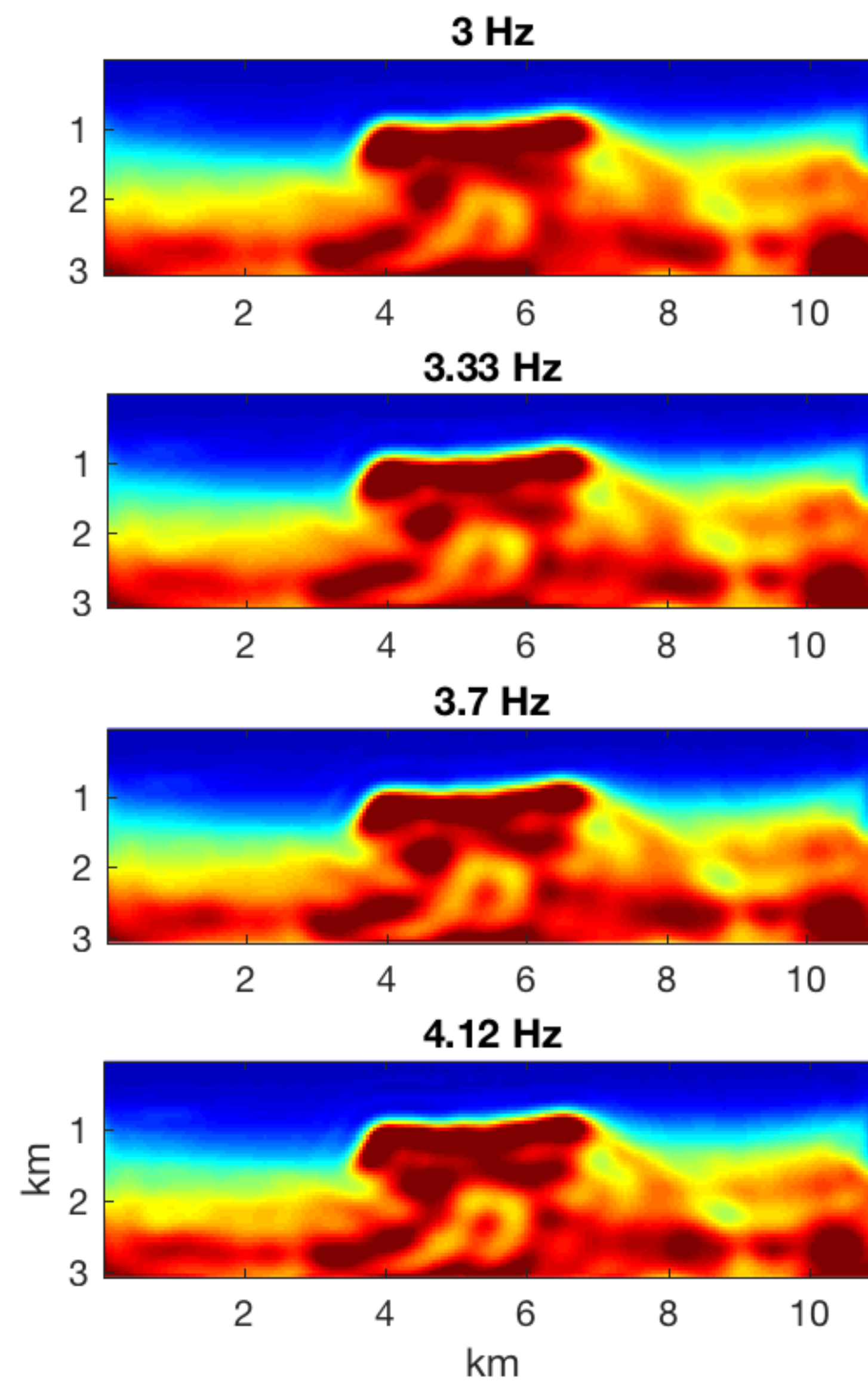
Flooding 4

Var > 0.4

Max = 0.17

Mean = 0.0046

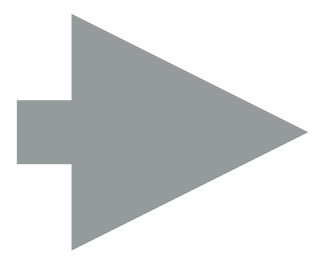
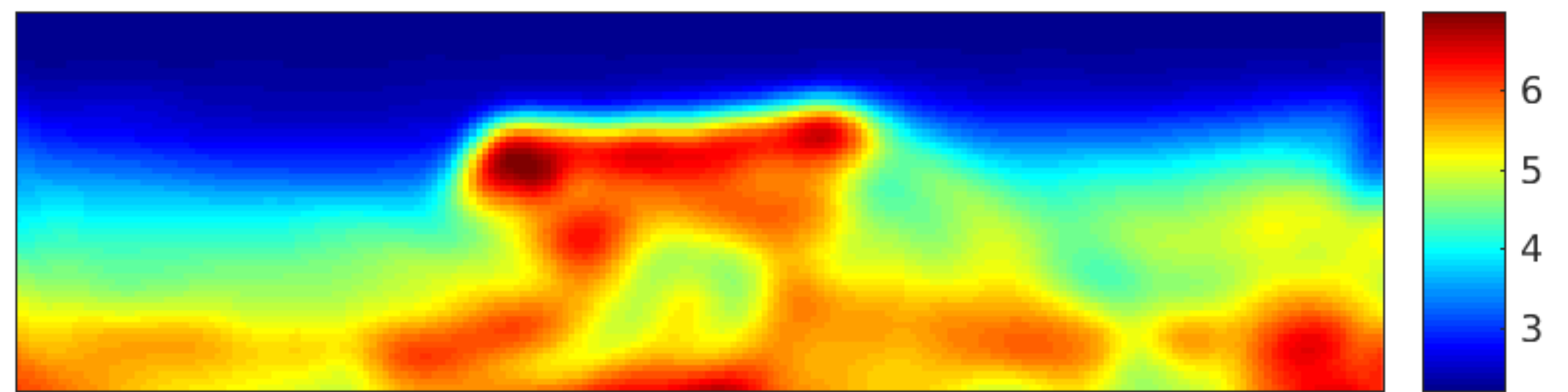
Input



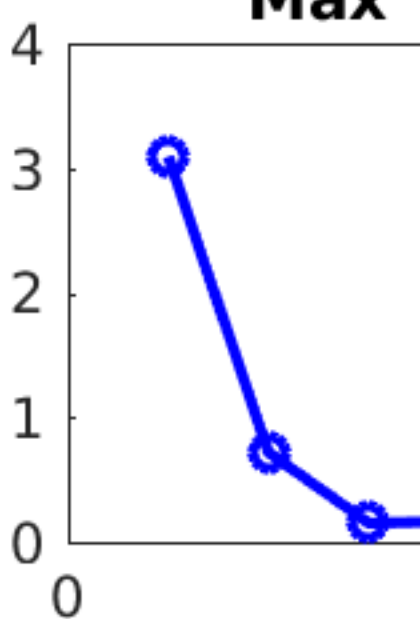
Masks



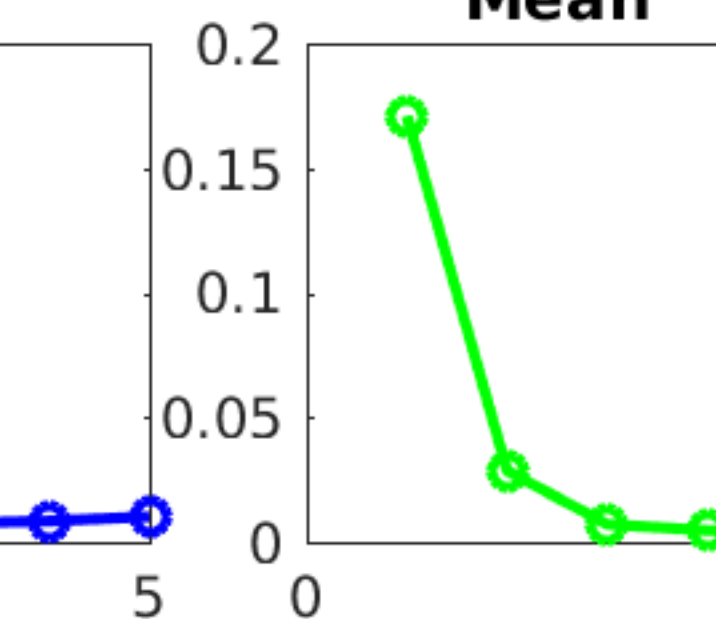
Result



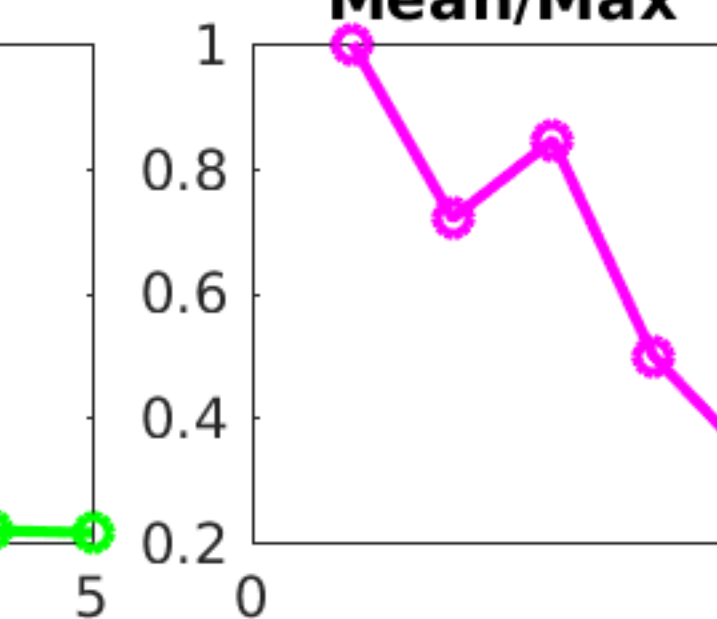
Max



Mean



Mean/Max



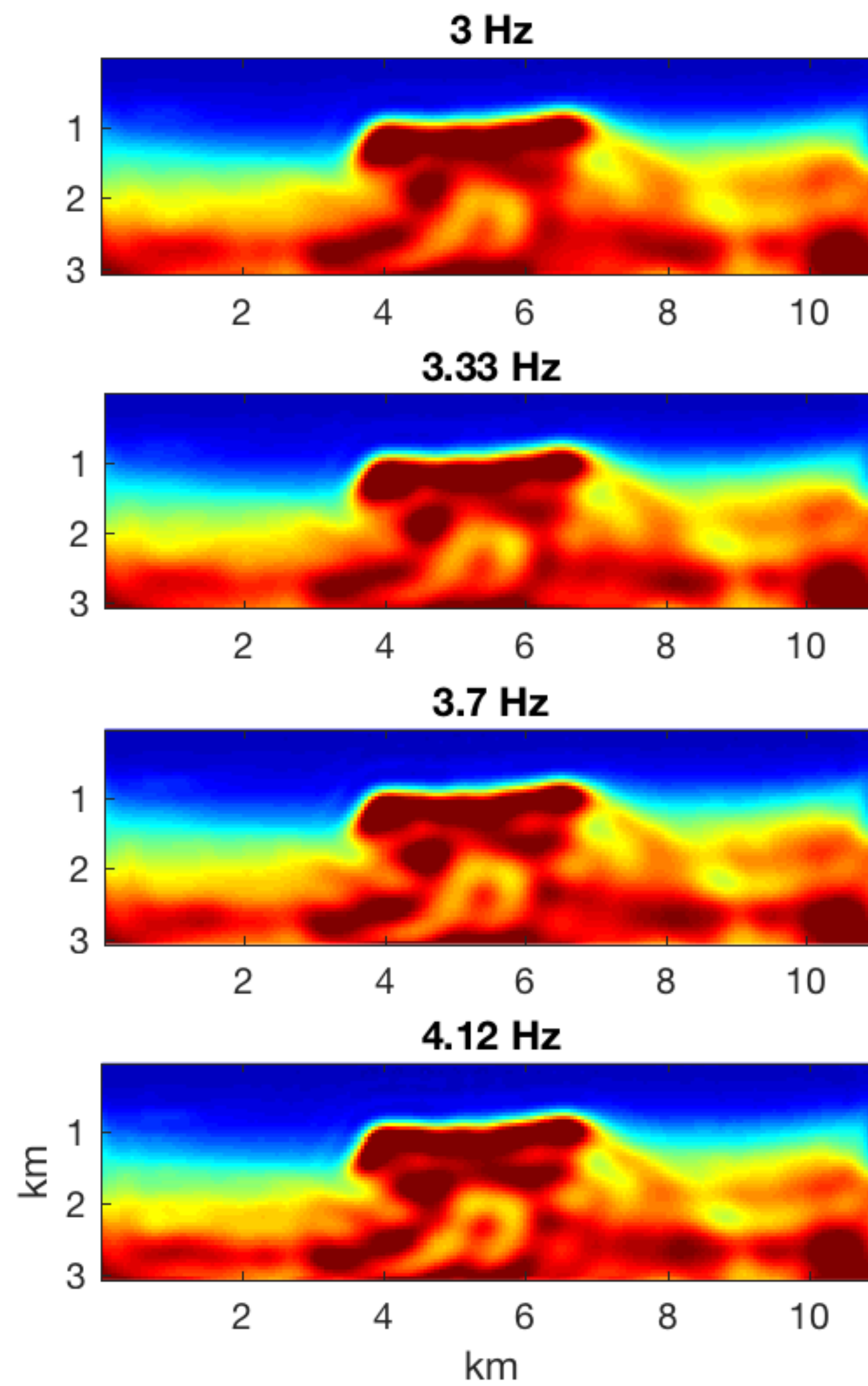
Flooding 5

Var > 0.61

Max = 0.2

Mean = 0.0037

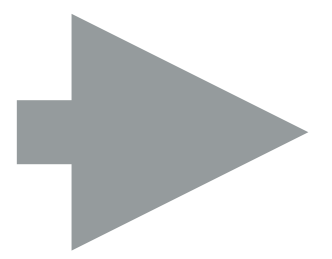
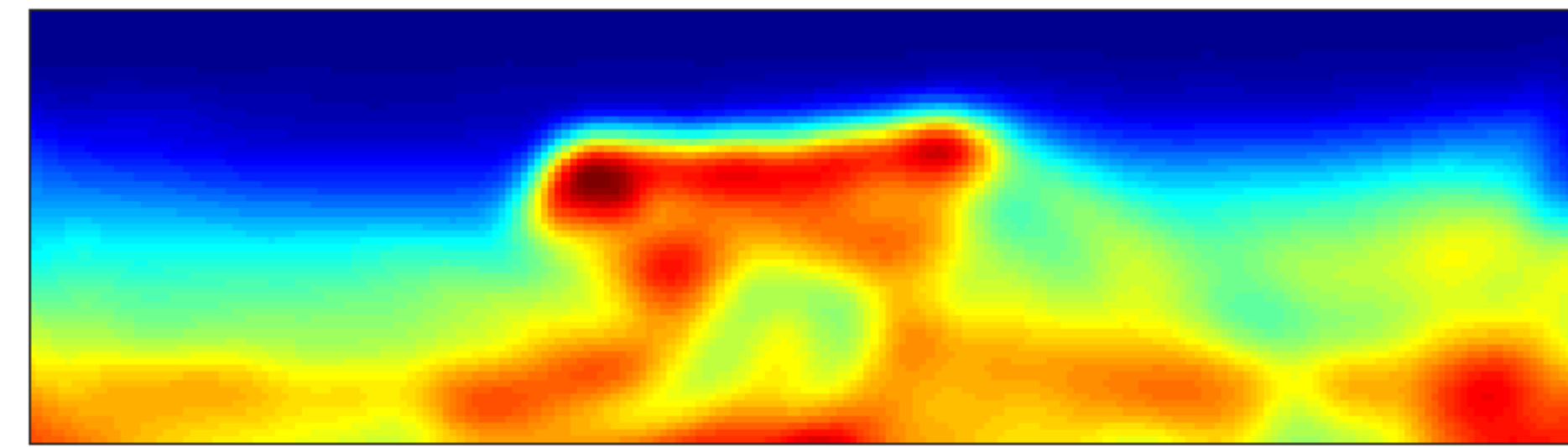
Input



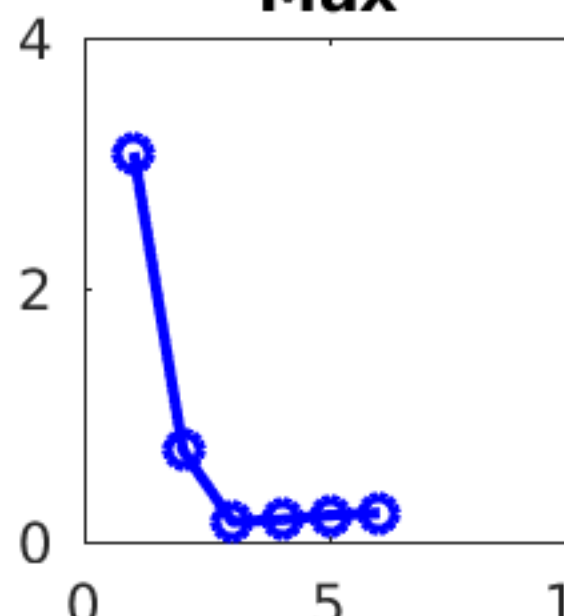
Masks



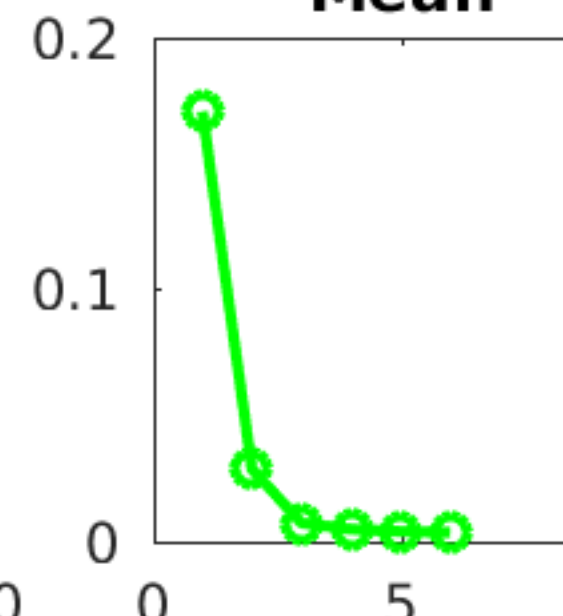
Result



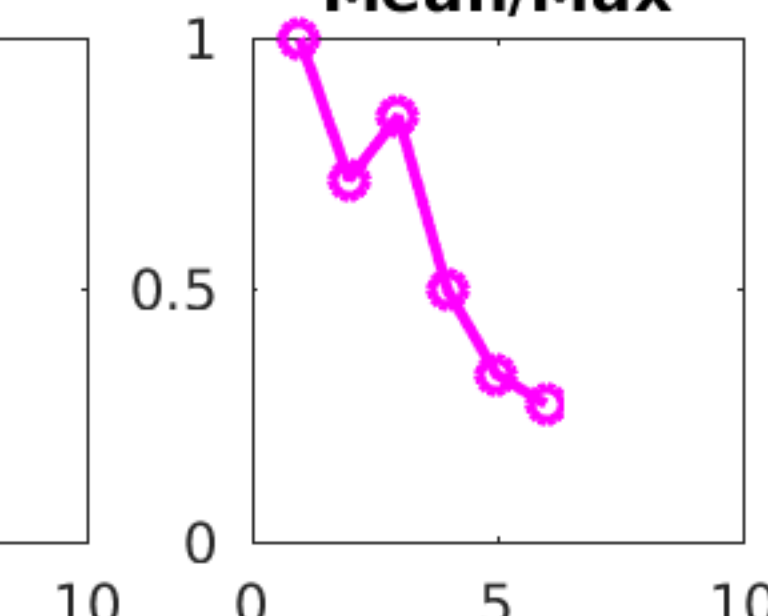
Max



Mean



Mean/Max



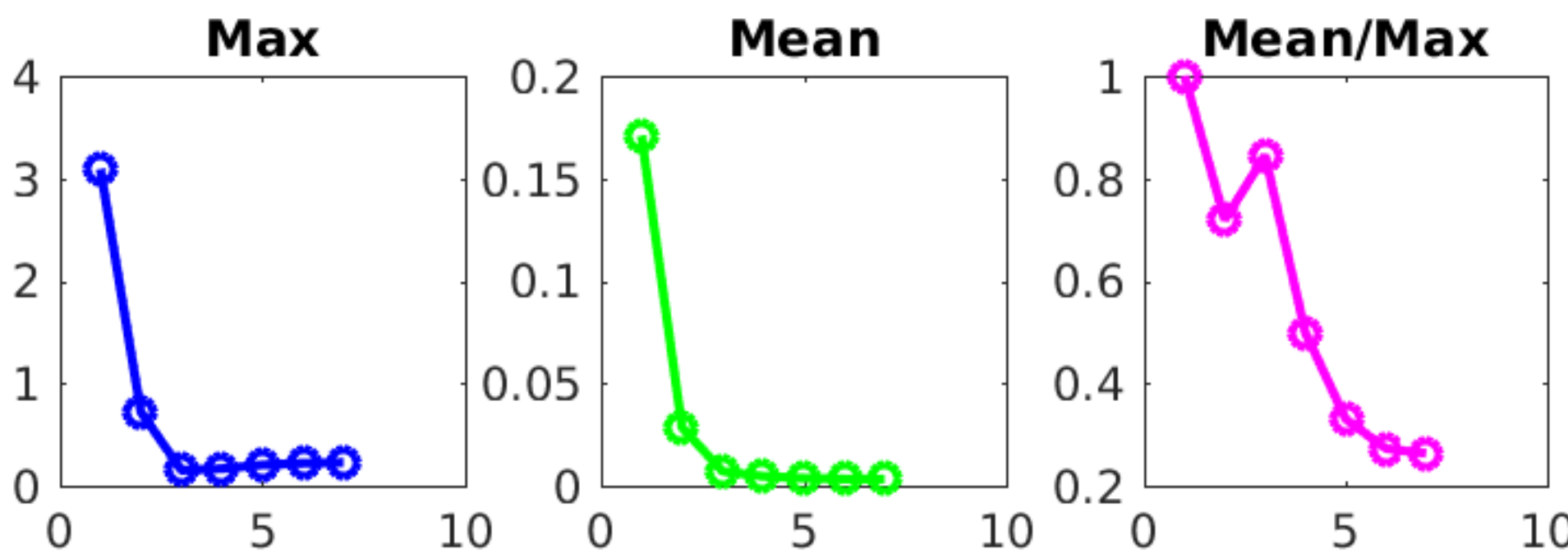
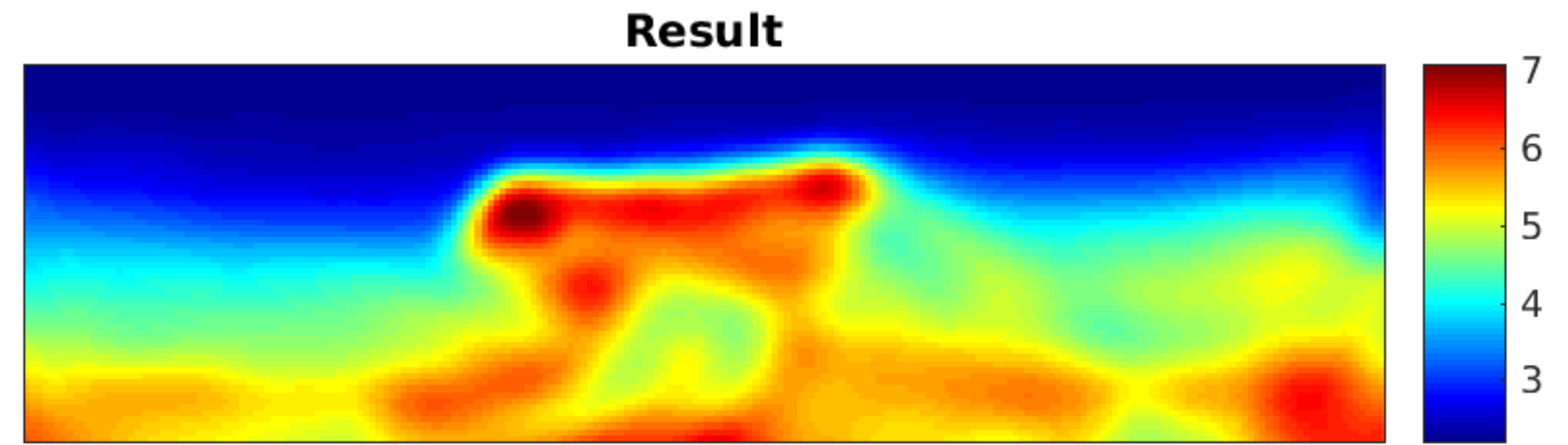
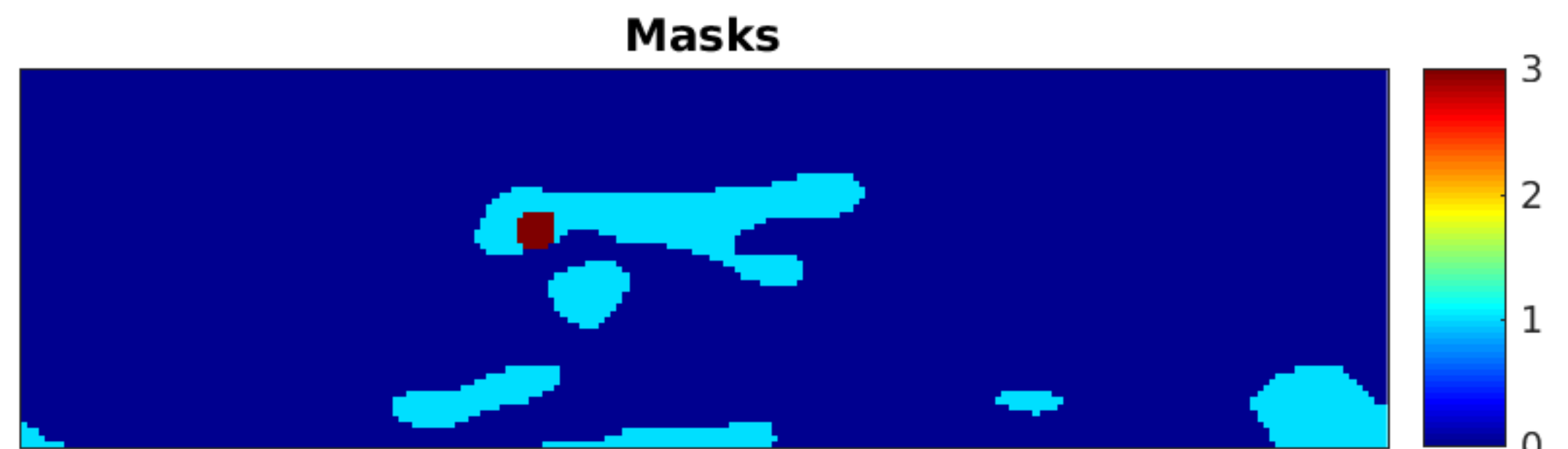
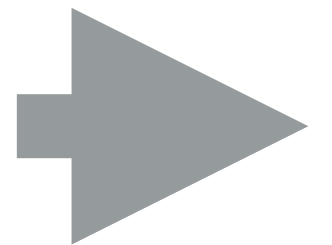
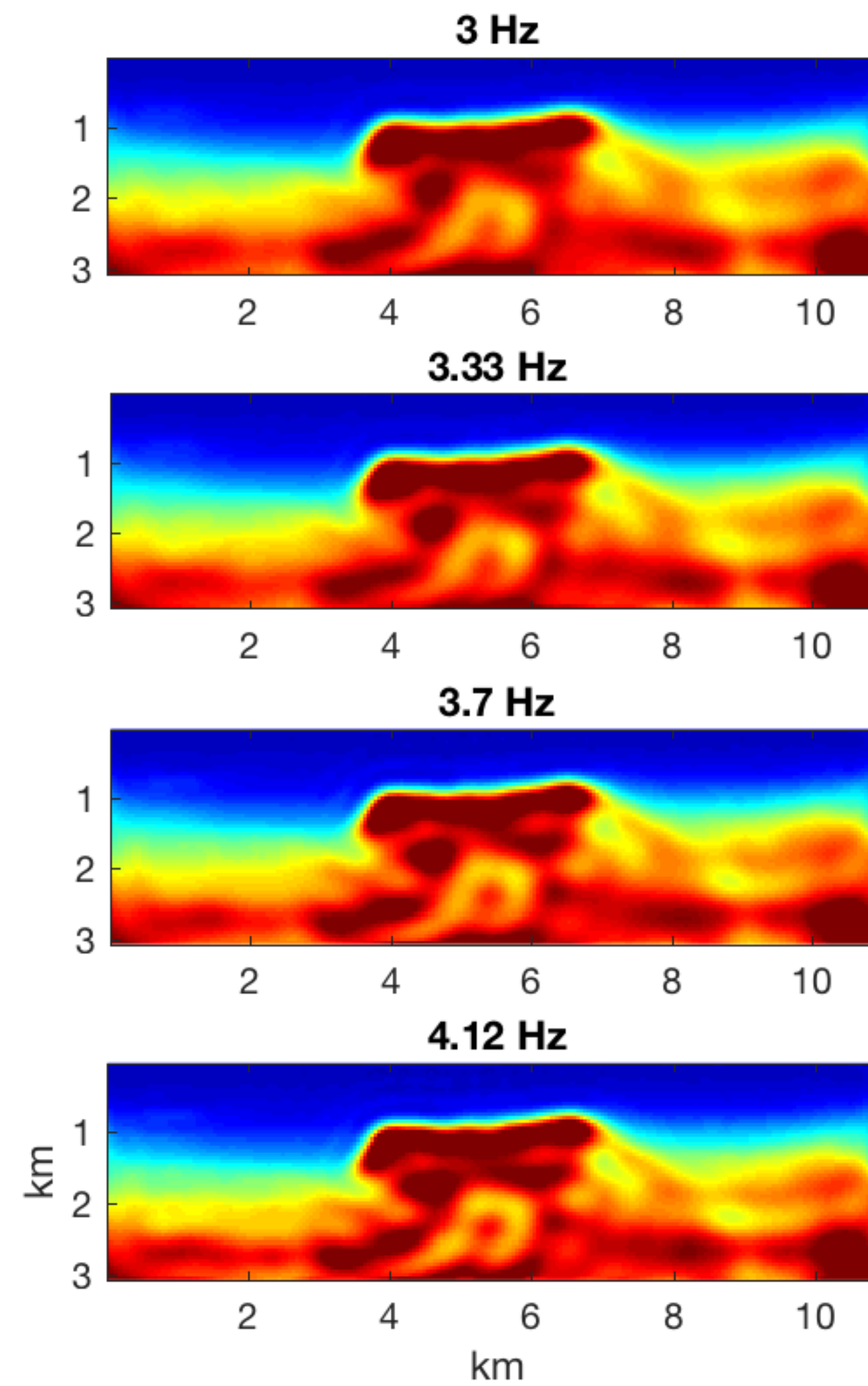
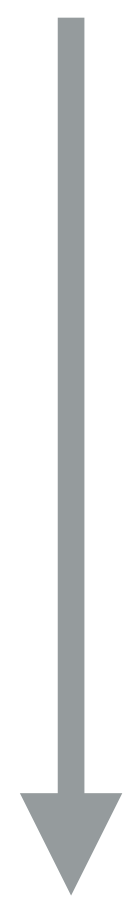
Flooding 6

Var > 0.73

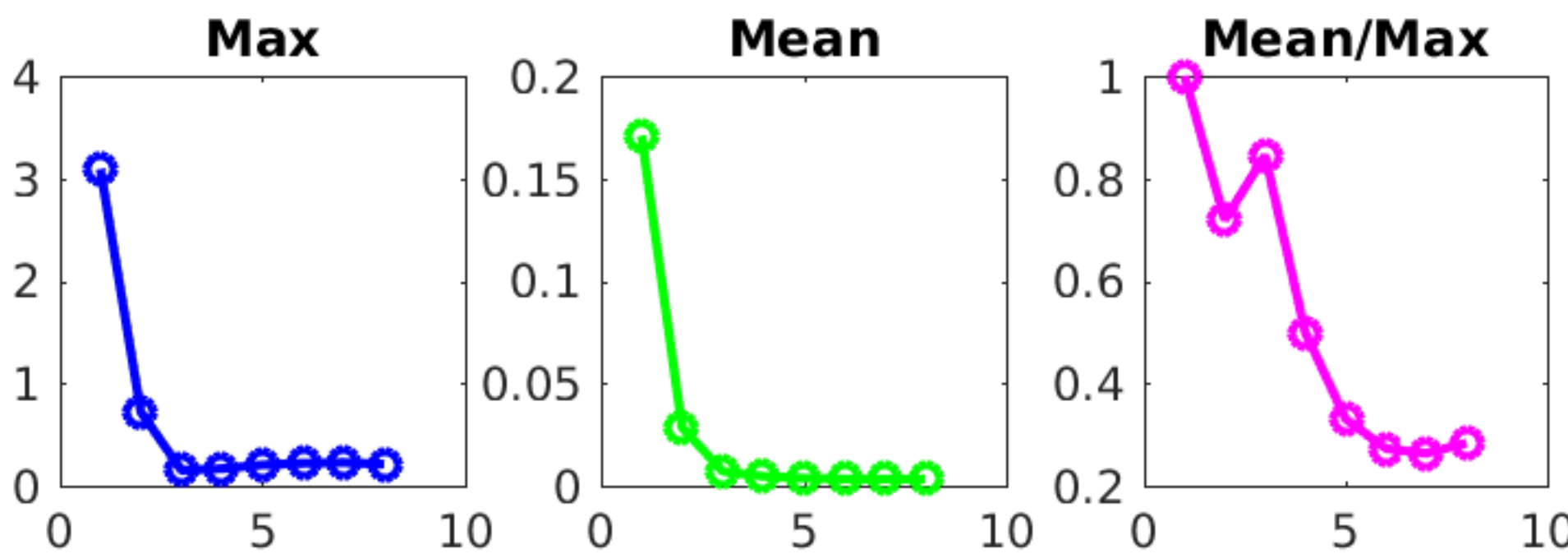
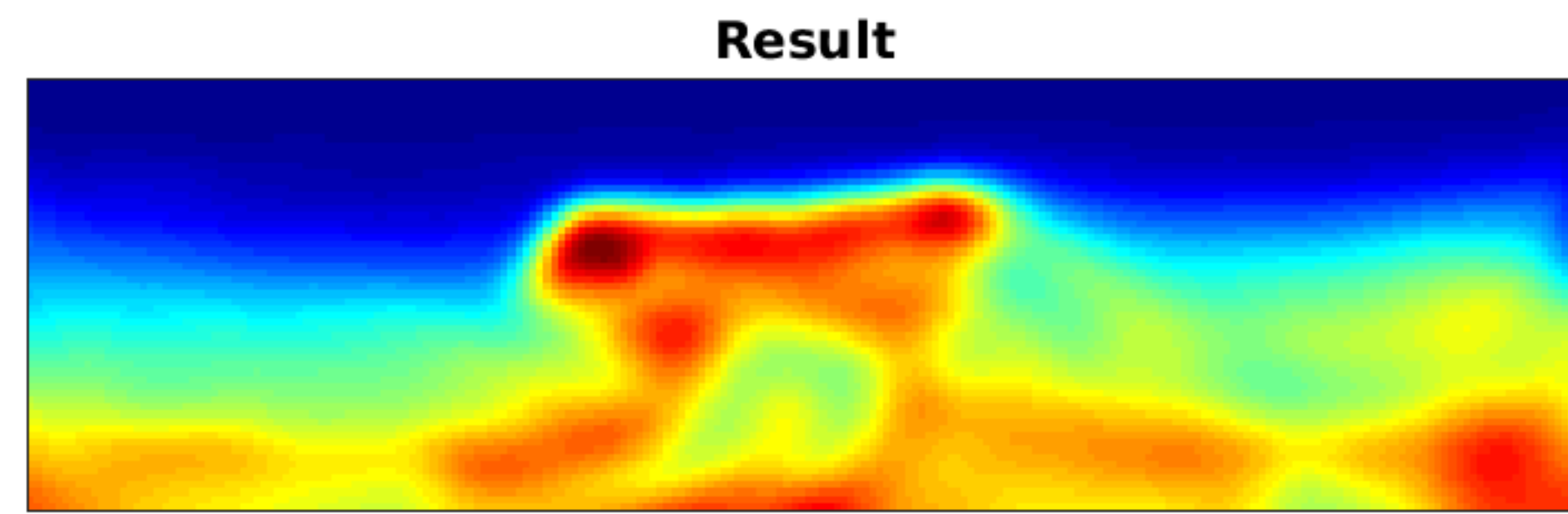
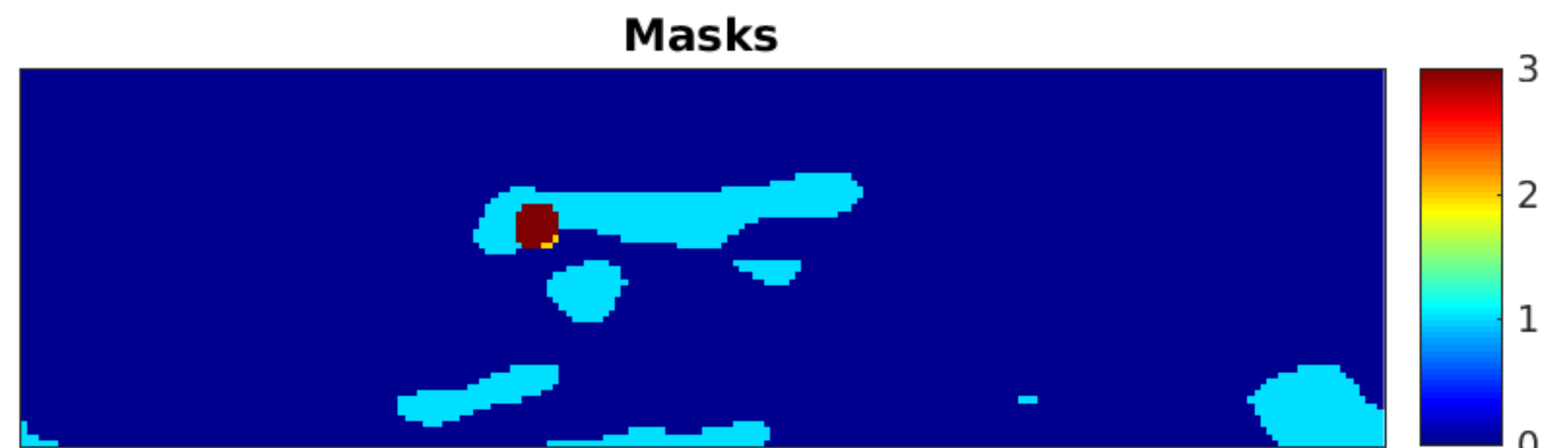
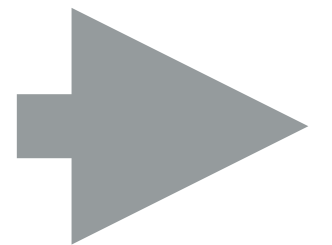
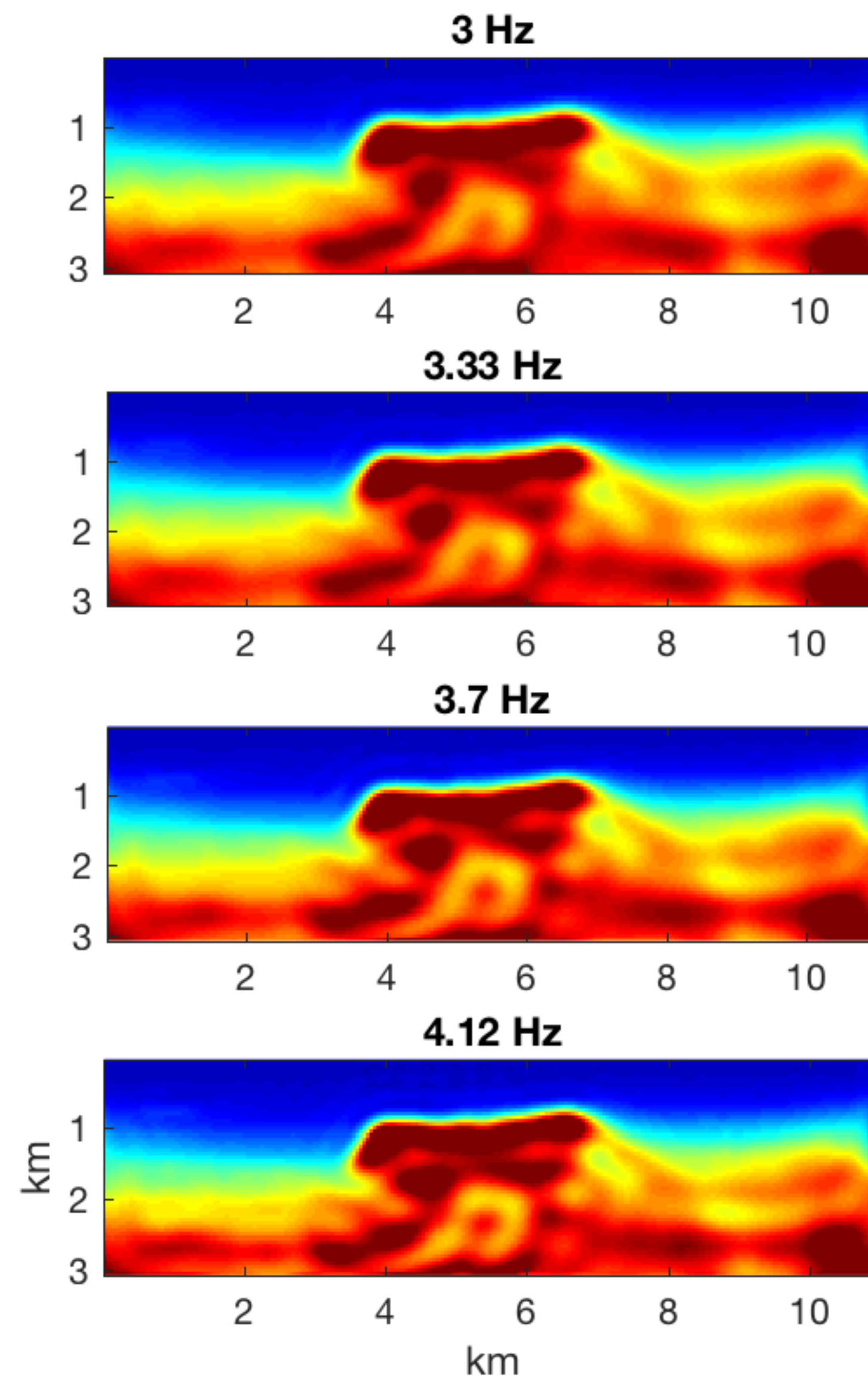
Max = 0.22

Mean = 0.0033

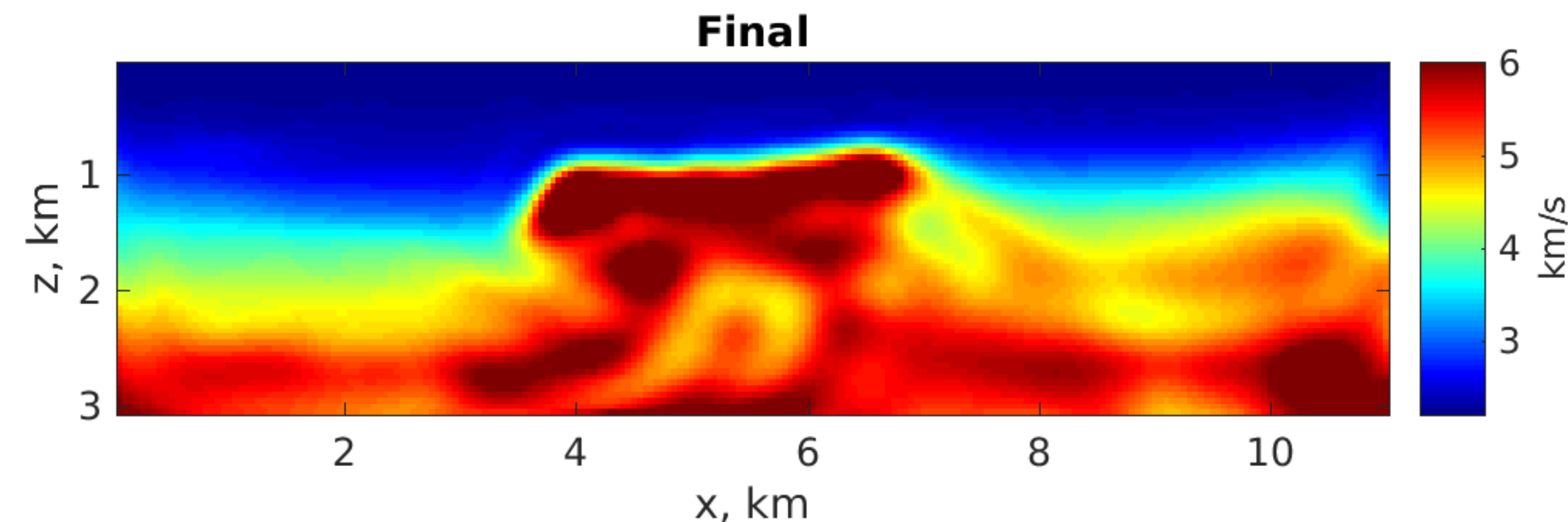
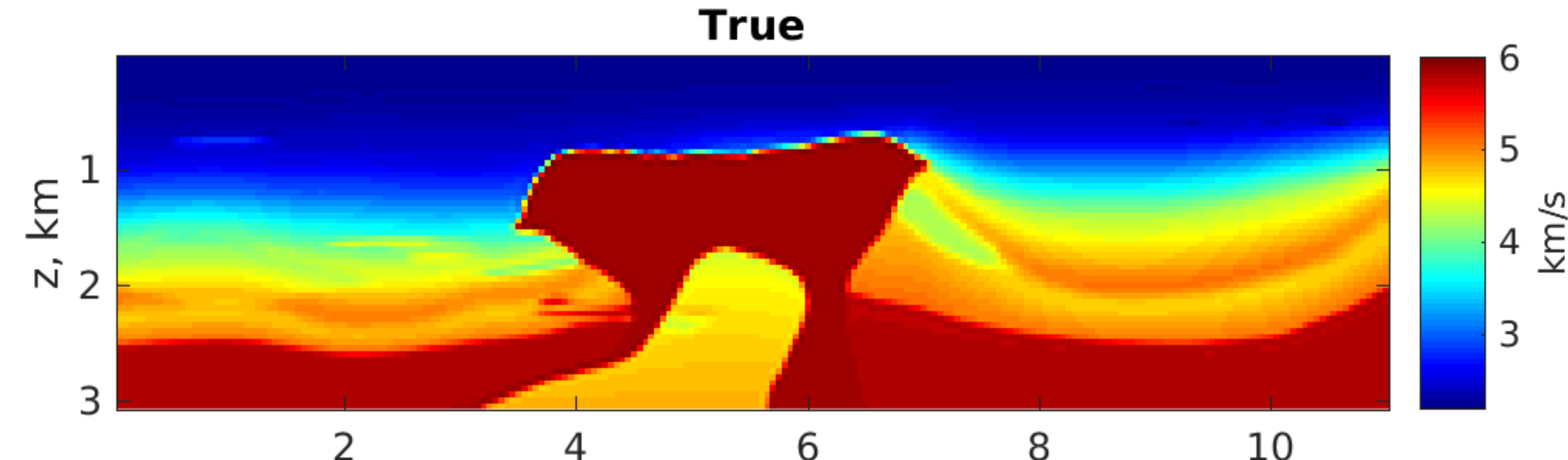
Input



Input

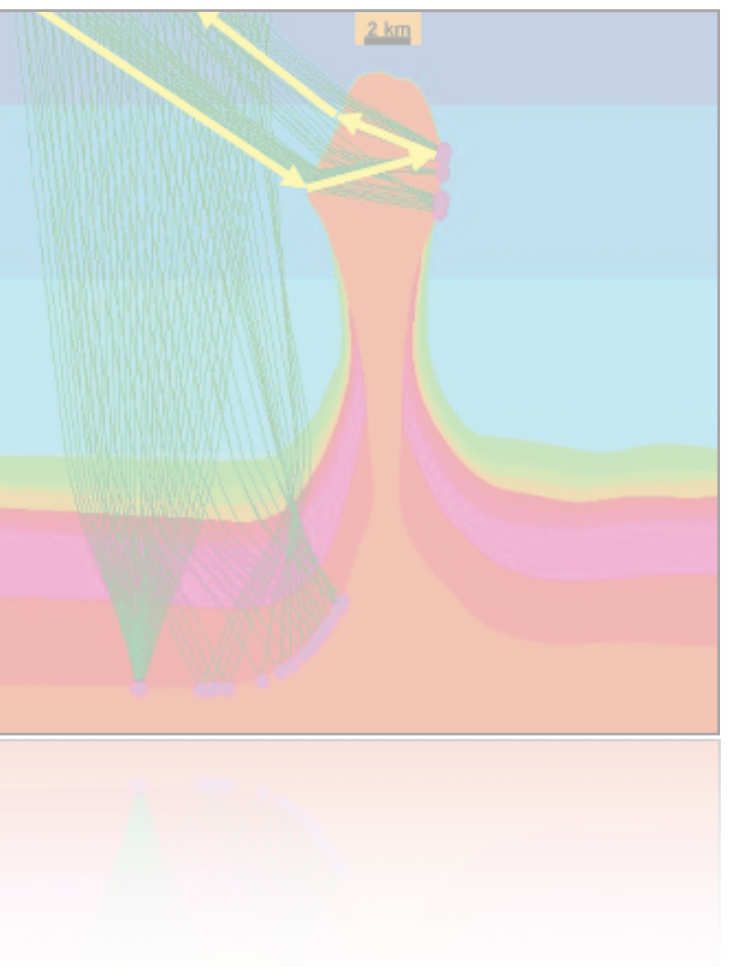


“Flooded” model



Outline

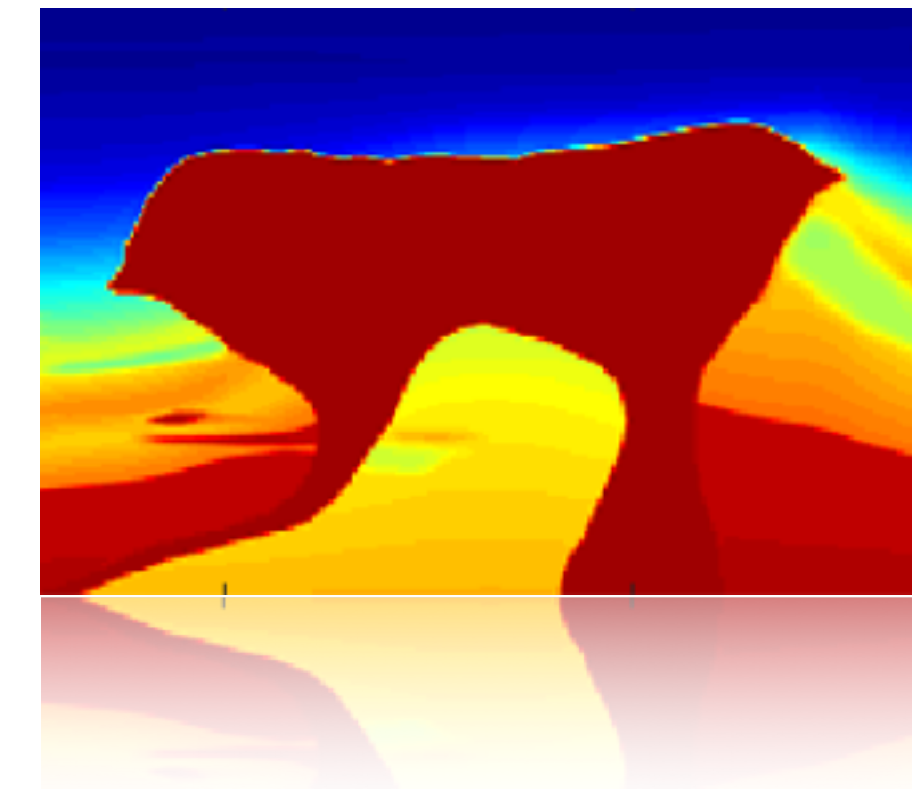
Motivation



Salt flooding technique



BP2004 model results

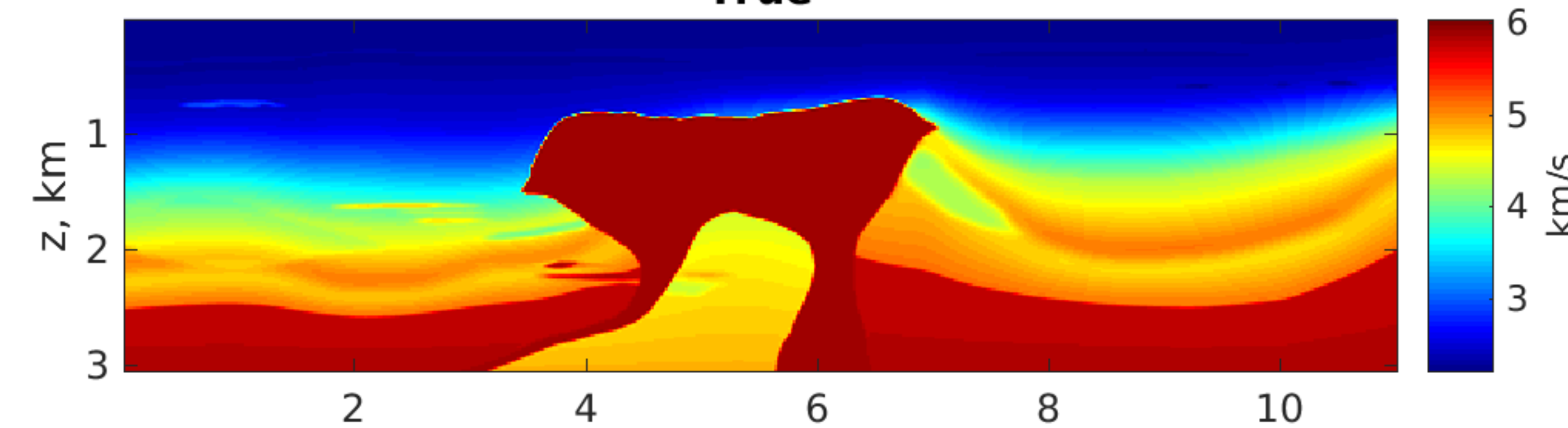


Central part of BP 2004

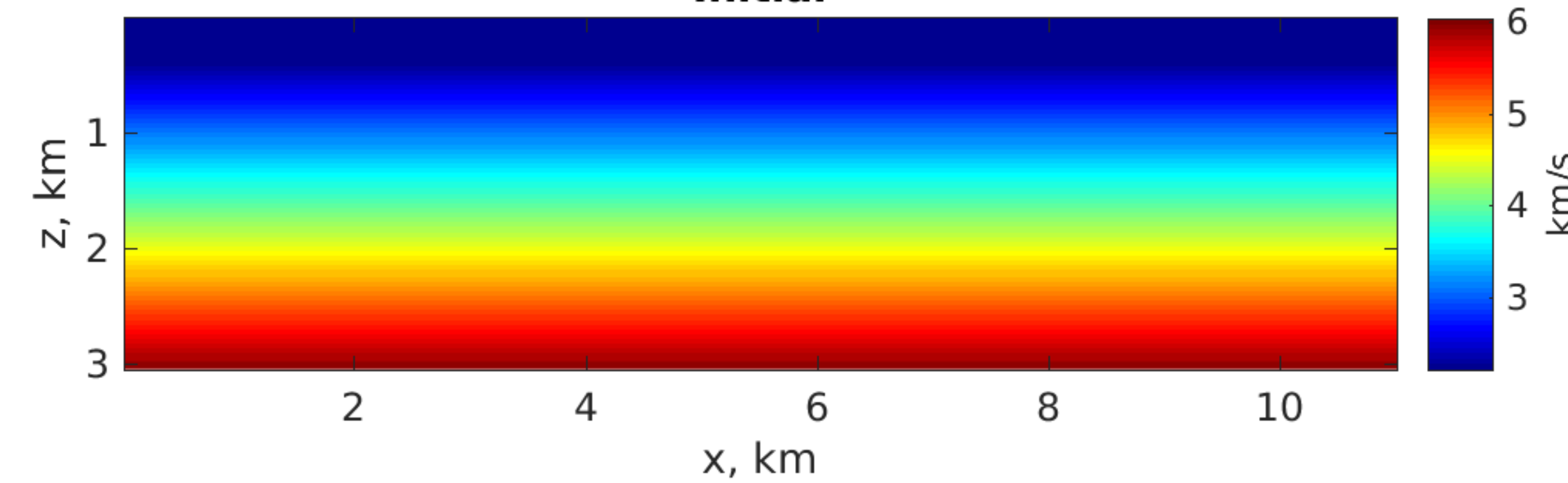
frequency range 3 -11 Hz

Initial

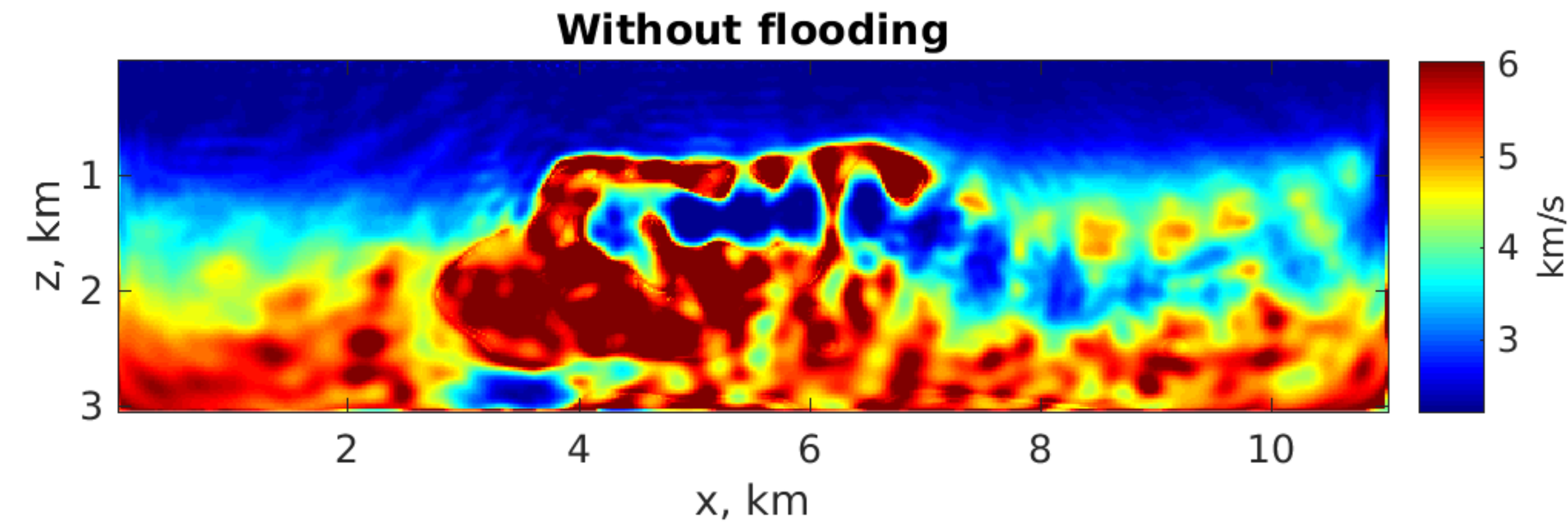
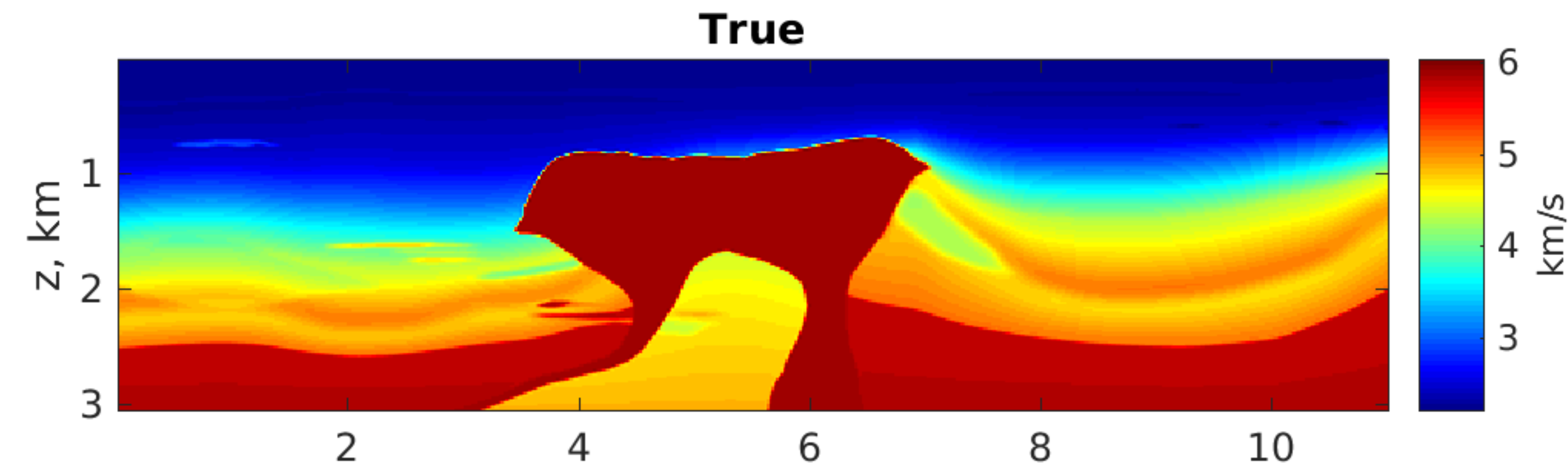
True



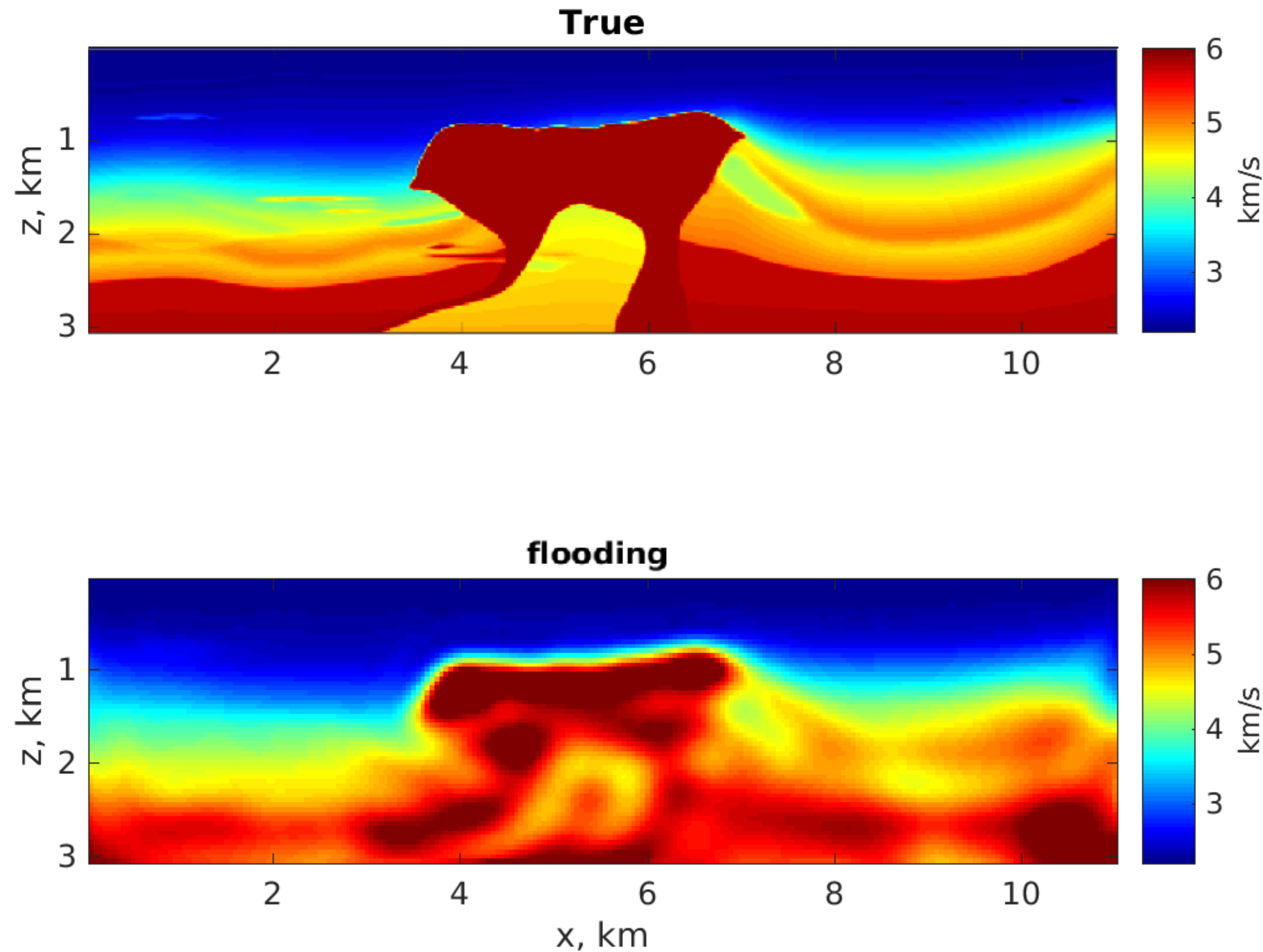
Initial



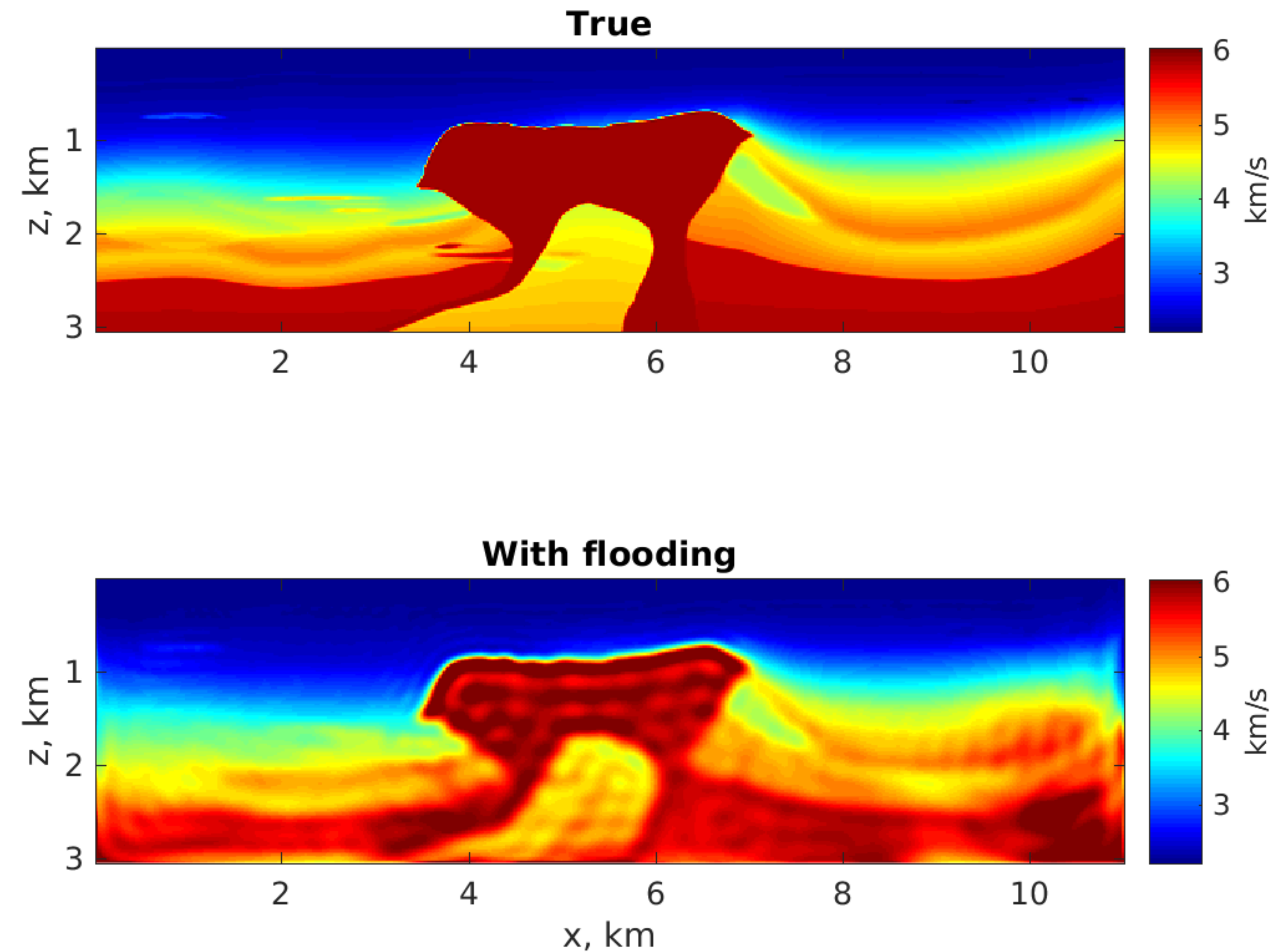
FWI without flooding



Flooding result



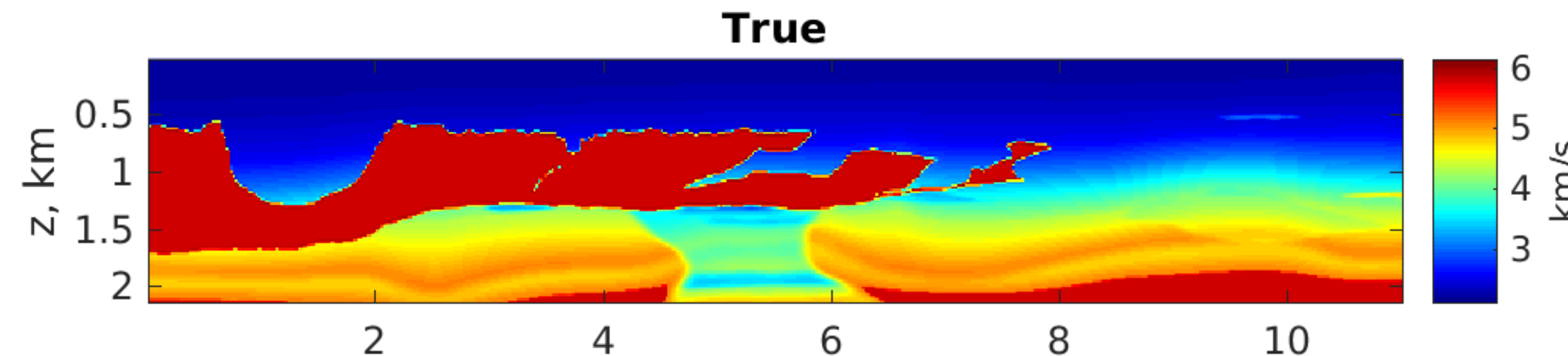
FWI with flooding



Left part of BP 2004

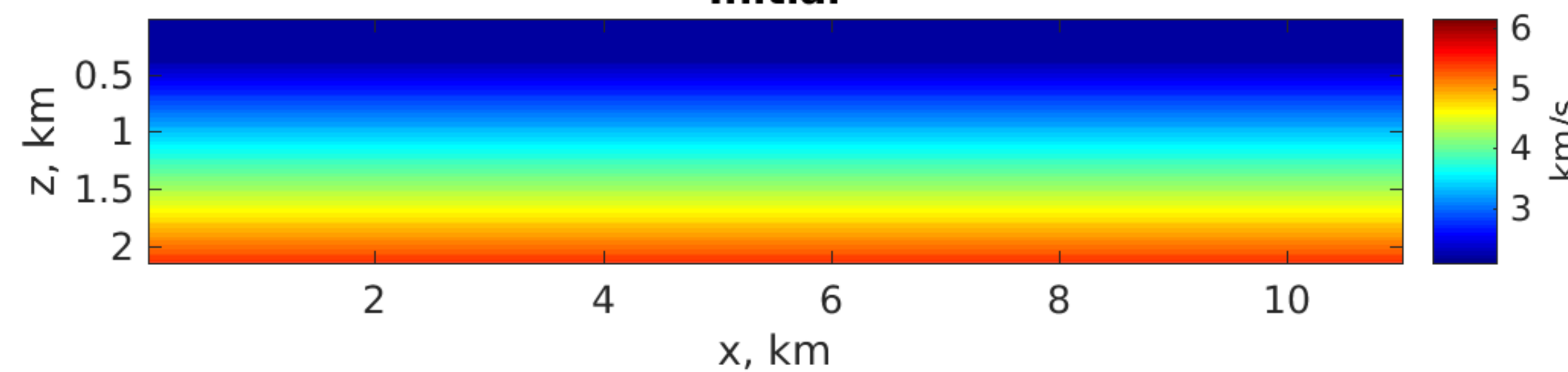
frequency range 4 -11 Hz

Initial

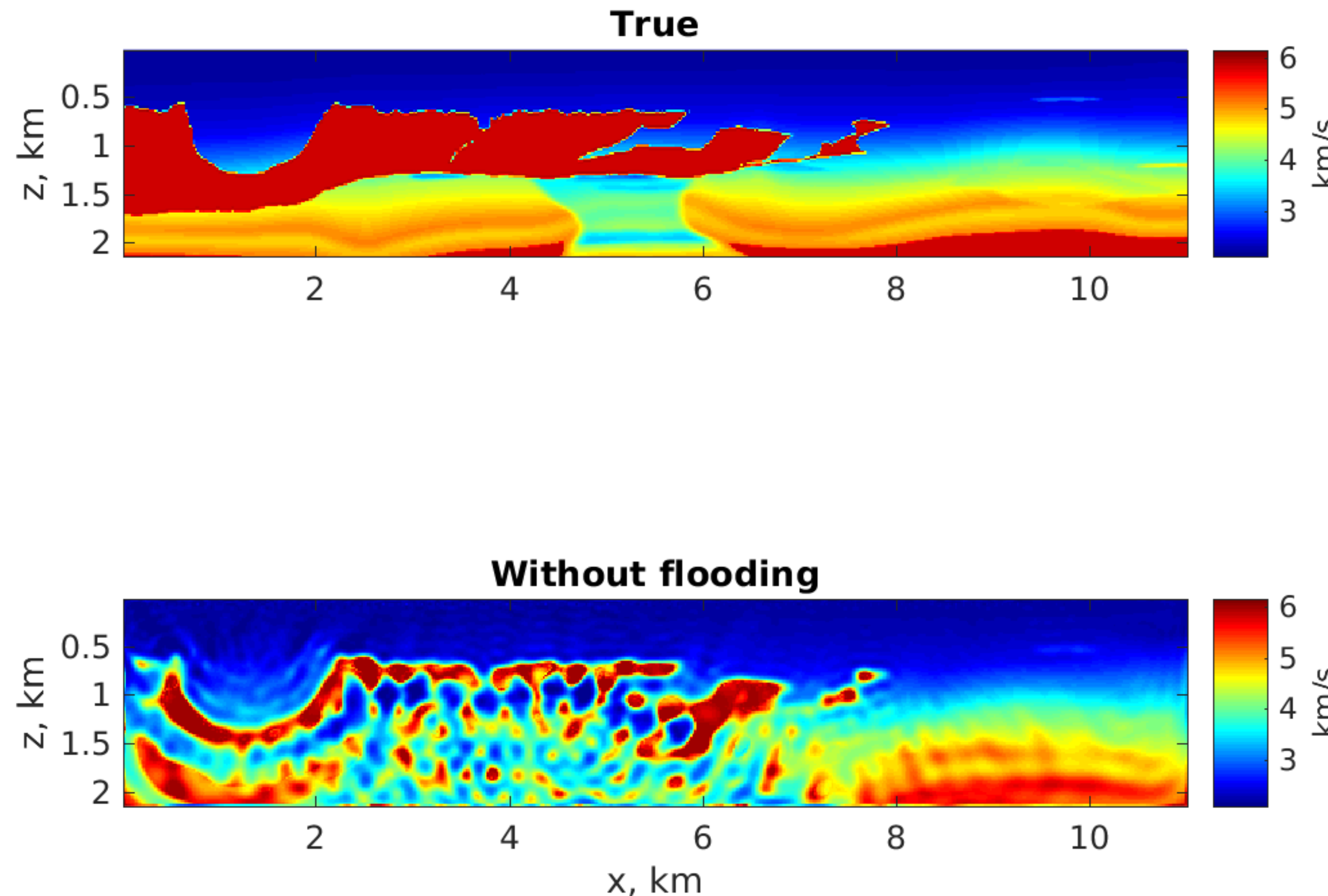


Size: 107×550 , $dx = 20$ m

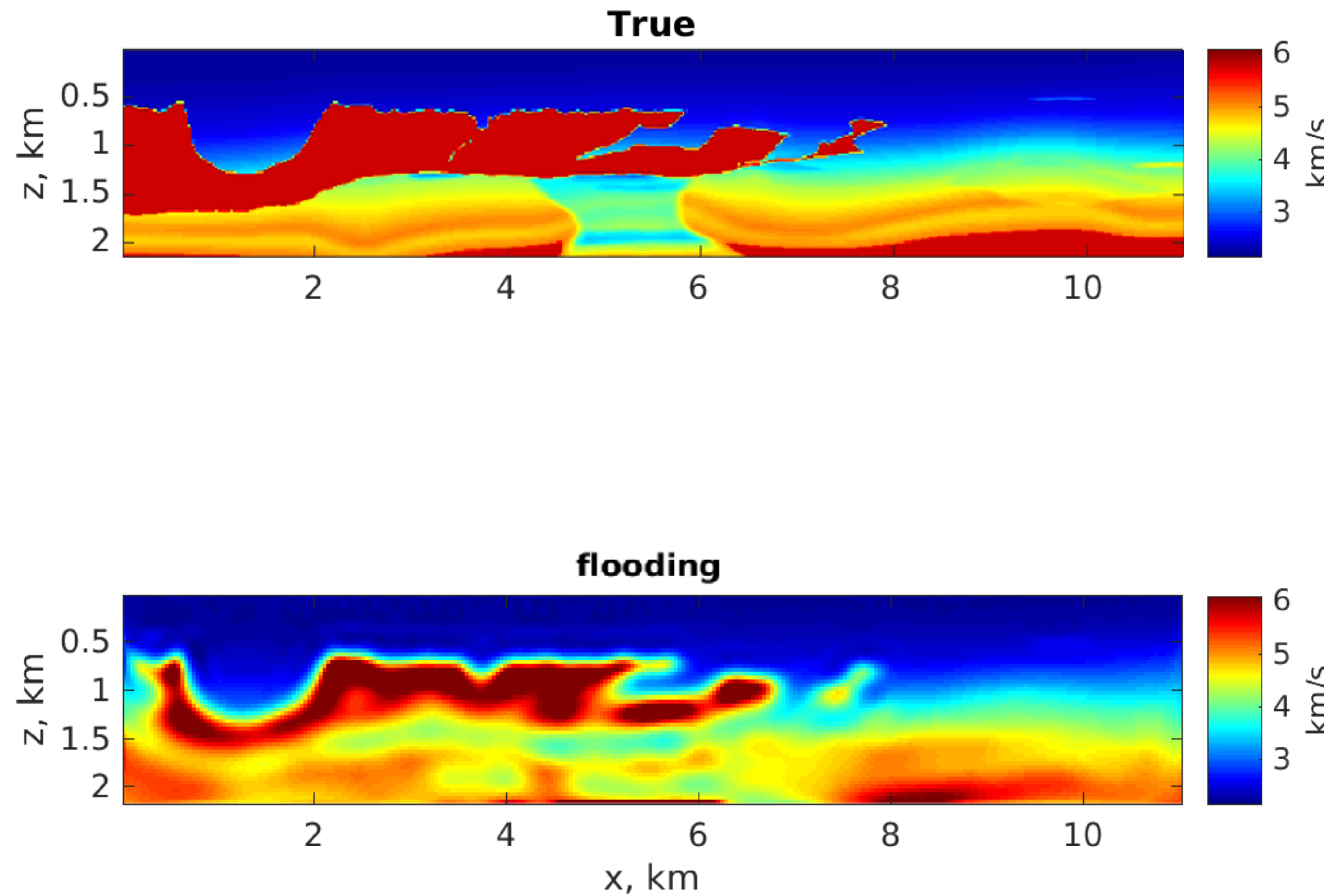
Initial



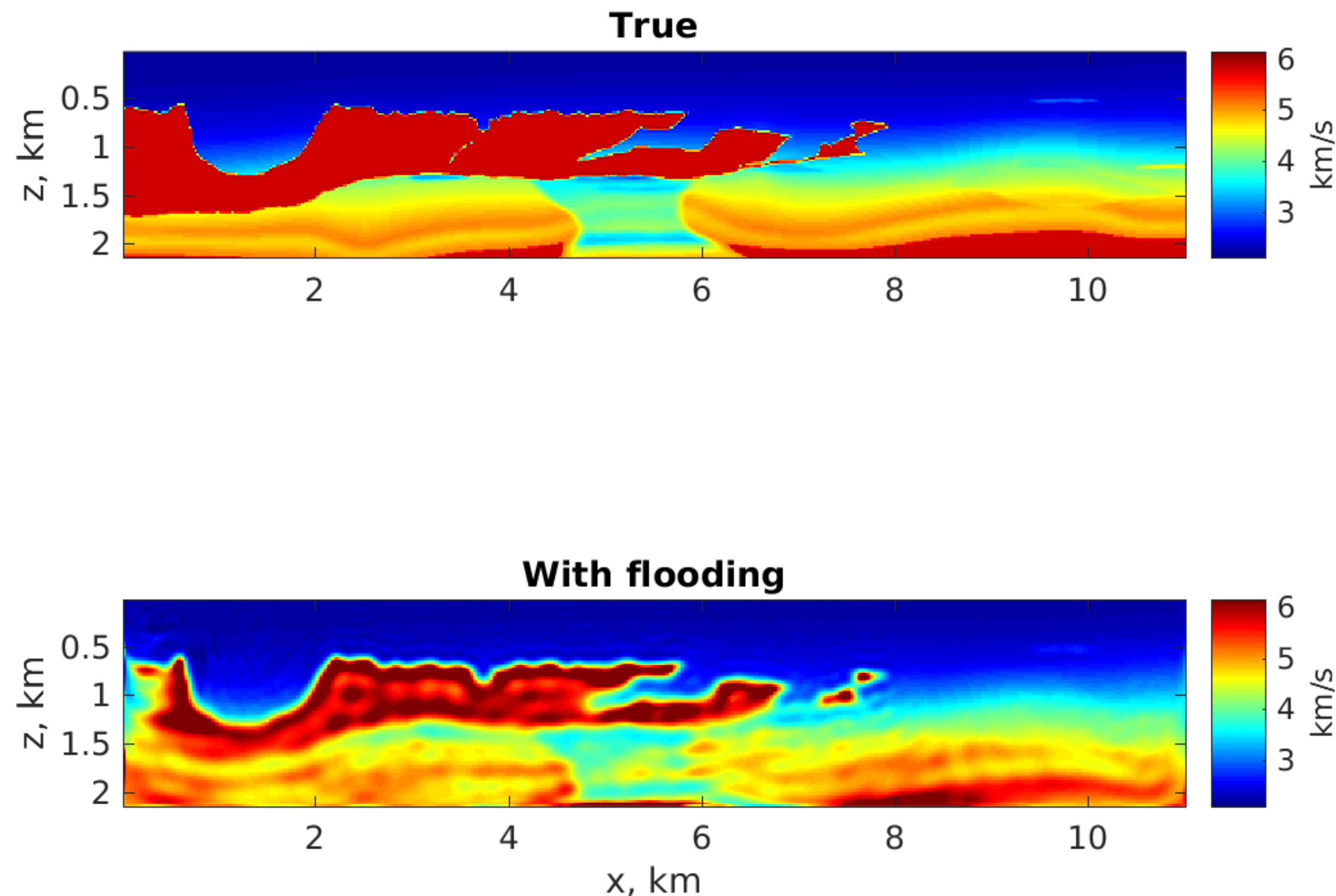
FWI without flooding



Flooding result



FWI with flooding



Conclusions

- Updates at different frequencies can be analyzed to improve FWI
- Variance-based salt flooding
 - Gives good initial model
 - Easy to embed into an existing FWI
 - Independent on forward solver
 - Low computational costs
- Limitations
 - Shifted artifacts
 - Initial variance threshold

Acknowledgements

- Seismic Modeling and Inversion Group
- Seismic Wave Analysis Group
- KAUST
- Tristan van Leeuwen (Utrecht University)
- Veronica Tremblay (KAUST)

Conclusions

- Updates at different frequencies can be analyzed to improve FWI
- Variance-based salt flooding
 - Gives good initial model
 - Easy to embed into an existing FWI
 - Independent on forward solver
 - Low computational costs
- Requirements
 - Shifted artifacts
 - Initial variance threshold

Bibliography

Jones, Ian F., and Ian Davison. "Seismic imaging in and around salt bodies." *Interpretation* 2.4 (2014): SL1-SL20.

Quincy Zhang, Itze Chang, and Li Li (2009) Salt interpretation for depth imaging – where geology is working in the geophysical world. SEG Technical Program Expanded Abstracts 2009: pp. 3660-3664.

Esser, Ernie, et al. "Constrained waveform inversion for automatic salt flooding." *The Leading Edge* 35.3 (2016): 235-239.

Tariq Alkhalifah (2016). "Full-model wavenumber inversion: An emphasis on the appropriate wavenumber continuation." *GEOPHYSICS*, 81(3), R89-R98.

Nick McArnie (2013), PES GB, London, Frequency Decomposition and colour blending of seismic data - "More than an image to me"